DENDRONIZED POLYMERS AND SURFACES FOR BIOLOGICAL APPLICATIONS

DENDRONIZED POLYMERS AND SURFACES: STRATEGIES TOWARD NOVEL THERAPEUTICS AND BIOMATERIALS

By

SOUMYA RAHIMA BENHABBOUR

M.Sc. (University of Minnesota, Duluth) 2001

B.S.E. (Algerian Petroleum Institute, IAP) 1997

A Thesis

Submitted to the School of Graduate Studies

In Partial Fulfillment of the Requirements

for the Degree of

Doctor of Philosophy

in

Chemistry

McMaster University

DOCTOR OF PHILOSOPHY (2008)
(Chemistry)

McMASTER UNIVERSITY
Hamilton, Ontario

TITLE: Dendronized Polymers and Surfaces: Strategies Toward Novel Therapeutics and Biomaterials

Author: Soumya Rahima Benhabbour, M.Sc. (University of Minnesota, Duluth)

Supervisor: Professor Alex Adronov

Number of Pages: xviii, 188

Abstract

Combining linear polymers and dendrimers provides numerous advantages such as increased solubility, biodegradability and a large number of functionalizable peripheral moieties. In this work, novel carborane-containing dendronized polymers were designed as potential candidates for Boron Neutron Capture Therapy (BNCT). These polymers were successfully synthesized using two different approaches. The resulting carborane-functionalized polymers were dendronized using a divergent approach to introduce aliphatic polyester dendrons of generation 1-4 grafted from the polymer backbone. Both approaches produced water-soluble dendronized polymers with high molecular weights.

The synthetic approach developed in the first part of this work was also applied in the functionalization of poly(ethylene glycol) (PEG)-grafted gold surfaces with hydrophilic dendrons. In this project, the effect of surface dendronization on protein adsorption was investigated. Contrary to our expectation, protein resistance was found to decrease when the surfaces were covalently functionalized with the hydrophilic dendrons despite their improved hydrophilicity. It was postulated that several factors could be responsible for the increased protein adsorption to the dendronized surfaces, including increased surface area, the introduction of hydrogen-bond donor groups, and a decrease in the mobility of the surface-grafted polymers as a result of inter- and intra-molecular hydrogen bonding between the dendrons. To circumvent these confounding phenomena, while maintaining surface hydrophilicity, we have chosen to covalently attach PEG mono-methyl ether (PEG-OMe) chains of various molecular weight to the peripheral hydroxyl groups of first to fourth generation dendronized surfaces. Results showed that

protein adsorption was reduced when dendronized surfaces were grafted with PEG-OMe chains. The hydroxyl-terminated G1-G4 dendronized surfaces and PEG-grafted dendronized surfaces were also investigated for cell adhesion and proliferation. These studies showed that little or no cell adhesion occurred on PEG-grafted gold surfaces. However, greater cell affinity for the dendronized surfaces was observed. When dendronized surfaces were coupled with PEG-OMe chains, cell adhesion was significantly diminished.

Acknowledgments

First and foremost I would like to thank my supervisor Dr. Alex Adronov for his generous support, tremendous encouragement, and continuous guidance and advice throughout my Ph.D work. His admirable scientific drive and dynamic and kind personality have been a great inspiration for success and hard work, and I consider myself very privileged to have had the chance to learn from his invaluable experience. The past five years have been a great learning journey and an amazing experience, mainly due to the research and lab group I have been part of.

Special thanks to my committee members, Drs. Michael Brook and Heather Sheardown, for their continuous interest and helpful comments and input to the present work. Dr. Brook, for challenging me in all areas of chemistry and pushing me to think beyond my limits. Dr. Sheardown, for all the helpful discussions and for giving me the opportunity to carry out all the biological work in her labs and providing me with the help and guidance to complete this work. Thank you!

To all members of the Adronov group, past and present, who have contributed to this work in some form, I thank you. I would like to thank my friends in the lab, Greg, Gregor, Patigul, and Christa. All of you have made my time at McMaster extremely enjoyable and full of great memories, and I wish you all the most success and happiness in the future.

From an administrative standpoint, I would like to thank all the chemistry office staff, past and present: Carol Dada, Josie Petrie, Lynda Fraser, Barbra DeJean, Tammy

Feher, and Sheila Marston have been of great help and made time here a lot easier by always offering help and advice when needed.

Special thanks to Matthew Parrott for being my second family and best friend and for all his help and support. His presence in my life has brought me tremendous joy, and over the past three years, he has shown me nothing but love and friendship and I could not thank him enough for that. Sharing this experience with him and being part of the highs and lows of the graduate student life together has been one of the most life fulfilling experiences, and I could not have asked for a better person to share it with. I look forward to many more years and wonderful experiences to share with you and I cannot wait for an exciting future ahead of us.

To my wonderful parents and two sisters whose continuous support and unconditional love has been the pillar and driving force for me to always give my best and continue forward. Without them I would never have been able to sustain the distance and tough decisions that came along in the past few years. I consider myself extremely fortunate to have the best and most open and understanding parents in the world, and the two best sisters who are also my best friends. They are the most important people in my life and I could never thank them enough for what they have offered me in my life. This thesis is dedicated to them with all my love and much appreciation for their presence in my life and to the memory of my grandmother who passed away in 2007.

Table of Contents

Page

List of Figures and Schemes

List of Figures **Page**

List of Schemes **Page**

Chapter 1: Overview of the Biological Applications of Dendronized Polymers and Surfaces

Abstract

The use of synthetic polymers in the biomedical field has gained tremendous ground in the past few decades due to their numerous advantages over natural polymers. The synthetic flexibility with which they are made enables the introduction of functional groups that allow fine-tuning of their properties such as, degradation rate, biocompatibility, biodistribution and many more. Dendronized polymers are a new class of polymeric drug conjugates with a unique cylindrical shape and characteristic properties different from their individual dendrimer and linear polymer analogues. These macromolecules have been investigated for numerous applications including, catalysis, light harvesting, energy transfer, active therapeutics, drug delivery and many more. Among the various dendrons synthesized to date, aliphatic polyesters are biodegradable polymers and have been widely investigated for biological applications. These moieties have been particularly applied in the synthesis of dendrimers, dendronized polymers, and recently dendronized surfaces.

1.1. Introduction

1.1.1. Dendrimers

Examples of dendritic structure on our planet are innumerable and range from snow flakes and lightning patterns to biological systems such as plant/animal vasculatures, neurons, and tree branching/root systems.[1] Although the concept of dendritic architectures was originally introduced many decades earlier by Flory,[2-4] it was not until the late 1970s that the first synthesis of such dendritic molecules was reported by Buhleier *et al.*, who applied the concept of repetitive growth with branching to low molecular weight amines.[5] This work was paralleled by the independent development of the divergent synthesis of "true dendrimers" by the group of D. A. Tomalia, then located at Dow Chemical Co.[6] The first report using the term "dendrimer" and describing a detailed preparation of poly(amidoamine) (PAMAM) dendrimers was presented by Tomalia at the 1st International Polymer Conference, Society of Polymer Science, Japan (SPSJ) in 1984. This work was then published in 1985 and was followed by the synthesis of "arborol" systems by Newkome *et al.* in the same year.[7] Both of these dendritic structures were constructed divergently, starting from a multifunctional core molecule and growing outward to the periphery. In 1990, Fréchet introduced the convergent approach in the synthesis of poly(ether) dendrimers.[8,9] In this approach, the synthesis starts at what eventually becomes the periphery, and is elaborated inward to the core to afford outstanding control over growth, structure, and functionality.[1]

In contrast to the ever-increasing number of peripheral coupling steps required in the divergent synthesis of dendrimers (Figure 1.1.A), the convergent growth, with its

constant number of reactions per growth, allows for a significant reduction in the amount of reagents used and intermediate purification steps required at each step of growth (Figure 1.1.B).

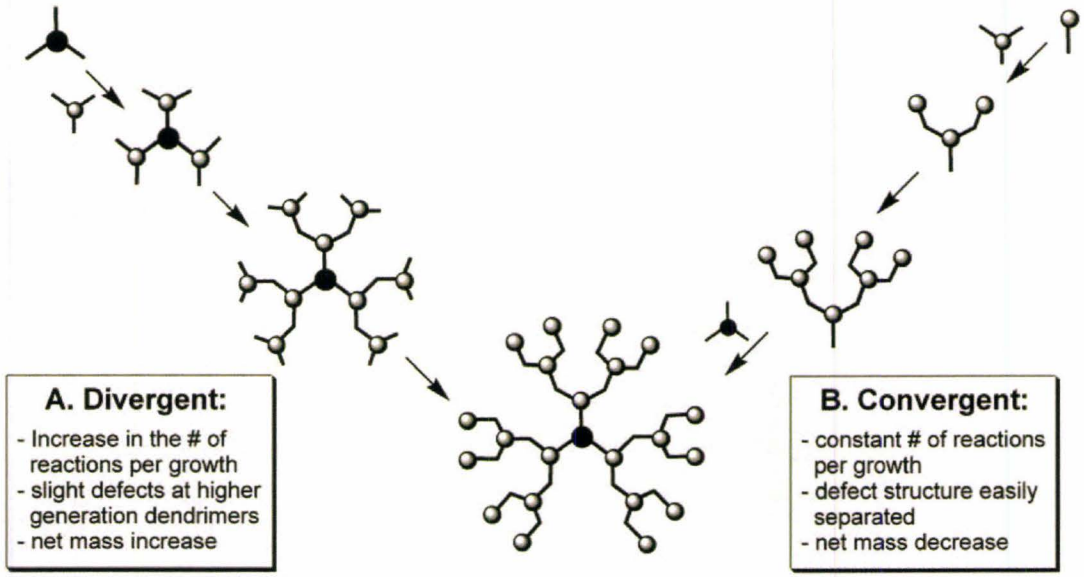

Figure 1.1. Representation of dendrimer synthesis by the divergent and convergent methods.

Although the iterative syntheses of both linear and branched small molecules and even macromolecules, such as linear oligopeptides and branched poly(lysine), were not new, Tomalia's dendrimers had evidently something special to offer. These well-defined highly branched structures offer many unique properties such as low viscosity[10] and thermal properties[11] that are significantly different from linear polymers, and which fascinate and challenge researchers in a number of disciplines. This has led to the

growing interest in dendrimers, and their numerous applications in a wide range of areas including catalysis, light harvesting, molecular encapsulation, and biomedecine.[12-18] One of the most valued properties of dendritic architectures is the large number of functionalizable groups that offer the ability to tailor their chemical and physical properties to suit a specific application. In contrast to linear polymers in which the influence of the end groups on their physical and chemical properties is negligible, in dendrimers the situation is quite different. The fraction of end groups is significantly large at high generations, and therefore, the nature of the peripheral groups strongly influences the properties of a dendrimer.[19] These intrinsic properties of dendrimers make them potential multivalent molecules that can be used as scaffolds for the preparation of new polymeric systems for drug delivery and targeting applications.[20-24] The commercial availability of dendritic systems is, however, limited with currently PAMAM and poly(propyleneimine) (PPI) as the only commercially available dendrimers. The polycationic nature of these systems renders them toxic in cells and animals, limiting their direct use in biomedical applications.[25-27] As a result, the search for new dendritic systems for biomedical applications continues to be of considerable interest.

In the later 1990s, A. Hult and H. Ihre developed new dendritic architectures based on the 2,2-bis(hydroxymethyl) propanoic acid (bis-MPA) monomer, which exhibits unique advantages over PAMAM, PPI, and poly(aryl ether) dendrimers.[19] This polyester system is water soluble in the neutral state, which avoids the necessity to functionalize it with solubilizing groups. In addition, even though polyester bonds are in most cases susceptible towards hydrolysis, a feature generally exploited for biodegradable systems,

the sterically hindered neopentyl ester bond of the bis-MPA monomer makes the backbone more stable towards both nucleophilic attack and acid-catalyzed hydrolysis. These advantages paralleled with their biocompatibility and low toxicity make them attractive scaffolds for the preparation of drug carriers. The Fréchet group has explored the use of polyester dendritic molecules as model systems designed to meet the properties needed for their intended application as drug carriers, including water solubility, nontoxicity, and stability of the polymeric backbone.[28] Other potential applications of the polyester dendrimers include their use as scaffolds for boron delivery to target malignant cells and their potential use as boron neutron capture (BNCT) therapy agents. This work has been explored in our group by M. C. Parrott *et al.* who developed a series of highly boron-loaded polyester dendrimers as potential BNCT agents.[29] Although these molecules exhibited a high boron content and excellent aqueous solubility, their major limitation was the tedious, multi-step synthesis required to reach molecular weights exceeding the renal cut off known to be in the range of 30-50 kDa.[30] More recently, a new class of polymeric drug conjugates combining a linear polymeric backbone with dendritic side chains, also known as a dendronized polymer (Figure 1.2.C), has been explored by an increasing number of researchers. These polymers were first reported in a patent by Tomalia and Kirchhoff in 1987,[31] and it was not until a few years later that the first synthetic approaches to make these "rod-like dendrimers"[31] were reported.[32-35] These macromolecules are unique because of the high degree of control over their size and shape in addition to the large number of functionalizable groups at various locations in the molecules, including chain end, polymer backbone, dendron branch point and

periphery (Figure 1.2.C).[36-38] At higher dendron generations, dendronized polymers exhibit a unique cylindrical shape, which provides them with physical properties that cannot be achieved with either linear polymers or dendrimers. In addition, these cylindrical macromolecules, when appropriately functionalized for biological applications, have been found to have an enhanced blood circulation half-life.[39,40] This prolonged circulation time of high molecular weight dendronized polymers has enabled their passive targeting to tumour tissue by a process known as the enhanced permeability and retention (EPR) effect.[41-43] In this phenomenon, which was described by Maeda and co-workers two decades ago,[44] the irregular in shape and leaky blood vessels in the tumor tissue, and the poorly aligned endothelial cells facilitate transport of macromolecules within tumor tissues. Moreover, the poor lymphatic drainage in tumor tissue help the retention and accumulation of macromolecules in the tumor.[45,46]

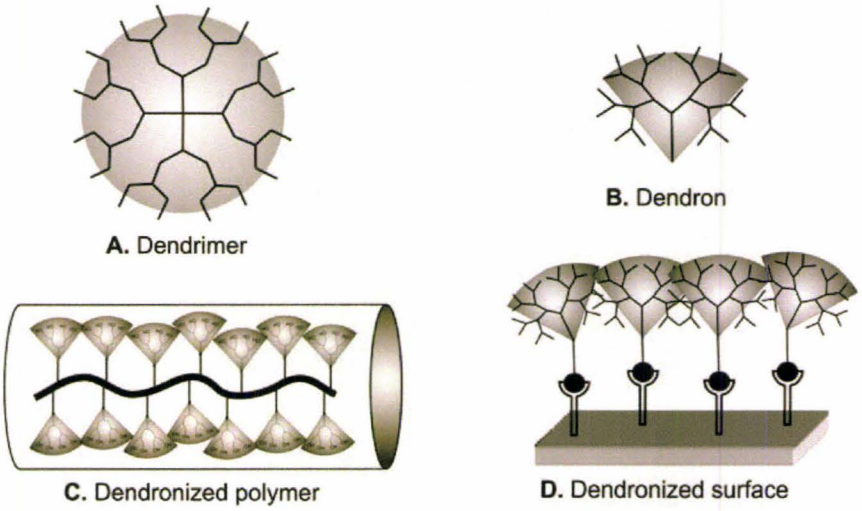

Figure 1.2. Schematic illustration of the various dendritic systems that can be achieved.

1.1.2. Dendronized polymers

1.1.2.1. Synthesis of dendronized polymers

Dendronized polymers are unique in that they combine the ability to achieve high molecular weights, attributed to their polymeric backbone, with the ability to incorporate a large number of functionalizable groups, and a great flexibility to tune their properties due to the presence of tethered dendrons. The main challenges in designing these cylindrically shaped molecules include steric repulsion between dendrons leading to incomplete reactions and uncontrolled polymerizations, autocatalytic degradation of sensitive dendrons, and potential inter and/or intra molecular coupling between dendrons, which can result in a drastic increase of the PDI. Dendronized polymers are made using either of the two principal synthetic approaches known as the "grafting-onto" route and the macromonomer route (Scheme 1.1).[33,47] In the first approach, a premade polymer comprising anchoring groups along its backbone is functionalized with pre-made dendrons. The major limitation of this synthetic approach is the difficulty in achieving complete functionalization of the polymeric backbone at each anchoring point. This is mainly caused by steric hindrance, which becomes a major issue due to the shielding of the anchoring groups on the backbone by dendrons already attached in close proximity, in addition to the possibility of dendron self-shielding of its core group used as the attachment point to the backbone (Scheme 1.1.A). This limitation can be overcome using a large excess of dendron to drive the reaction to completion, however, this large excess may in turn result in purification issues of the final product.[37] Another way to overcome this limitation is by coupling low generation dendrons to the pre-made polymer to avoid

overcrowding of high generation dendrons and achieve greater percentages of functionalization of the pre-made polymer. The dendron growth is then carried out using the divergent dendrimer synthesis (Scheme 1.1.B).[48,49]

Scheme 1.1. The various synthetic routes to dendronized polymers.

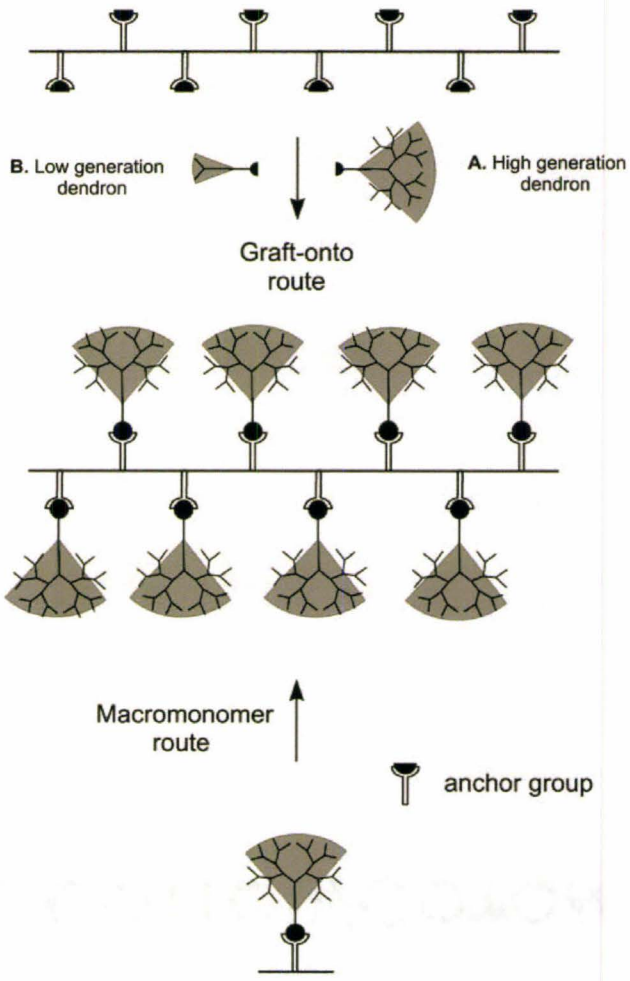

The "grafting-onto" approach offers more synthetic freedom as dendrons can be made by divergent or convergent growth. This approach was recently utilized by Fréchet

and co-workers using commercially available poly(*p*-hydroxystyrene) as a backbone and aliphatic polyester dendrons of up to the fifth generation to generate, for the first time, dendronized polymers with molecular weights exceeding 10^6 Da, and with very narrow PDI (< 1.2).[50] In contrast, the macromonomer approach, in which a dendron-functionalized macromonomer is used to generate the desired dendronized polymer, is considered superior to the "grafting-onto" approach due to complete incorporation of dendrons to every repeat unit of the polymer backbone.[38] However, steric hindrance may become an issue particularly for macromonomers bearing dendrons of generation three or higher, where incoming monomers cannot connect to the chain end due to high steric hindrance. As a consequence, low molecular weight dendronized polymers are usually generated via the macromonomer approach.[33,51] Several polymerization methods have been exploited to make dendronized polymers using the macromonomer approach including radical polymerization,[38,49,51-57] ring-opening metathesis polymerization (ROMP),[58-60] Suzuki polycondensation,[59,61-64] and Heck coupling.[65]

1.1.2.2. Design of dendronized polymers for biological applications

In contrast to dendrimers, very few studies have been reported on the potential use of dendronized polymers for biological applications.[66,67] In these applications, the choice of polymer backbone and dendrons is very important in developing new systems with properties complying with the prerequisites for biomaterials. Among the various dendrimers developed, aliphatic polyester dendrons have very high promise for biological

applications due to their highly hydrophilic nature, biodegradability, and biocompatibility, which make them ideal candidates as biomaterials and drug delivery agents.[40,68]

Recently, Fréchet and co-workers reported the first *in vitro* and *in vivo* studies on hydrophilic dendronized polymers based on the commercially available poly(4-hydroxystyrene) backbone and fourth generation aliphatic polyester dendrons.[40] These studies showed that the dendronized polymers exhibited very low levels of toxicity with cell viability greater than 85% at a concentration of 0.25 mg/mL.[40] The *in vivo* biodistribution studies of these dendronized polymers revealed a positive correlation between polymer size and its blood circulation time, where the highest molecular weight polymer (Mn = 130 kDa) had a half-life of 44 h.[40] Long blood circulation time, known to play an important role in enhanced tumor accumulation, makes the development of dendronized polymers as drug carriers a very promising area of research.

1.1.3. Dendronized Surfaces

Functionalization with dendrons has not been limited to linear polymeric systems. In fact, their application has been recently extended to the functionalization and modification of various solid substrates (i.e., glass, silica, and gold),[69-71] nanoparticles,[72,73] fullerenes, and carbon nanotubes (Figure 1.1.D).[74] Controlling physical and chemical properties of surfaces is of a significant importance to numerous technological and biological applications. The use of self-assembled monolayers (SAMs) on surfaces has been widely studied as model systems for providing fundamental

understanding of surface and interfacial phenomena. To further develop the fundamental understanding of structure-property relationships and achieve control over surface properties by manipulating surface structure, several studies focused on investigating assemblies of more complex molecules on surfaces. Dendritic molecules with their highly branched and well defined structures can form highly ordered SAMs with a large number of functional groups at the periphery, providing the possibility to create unique materials with surface characteristics that can be tuned and controlled at the molecular level. The structural precision of dendritic molecules has motivated numerous studies aimed at various applications including catalysis,[75] surface coatings,[76] chemical sensors,[77] biosensors,[78] and many more.

The first reports on polymers end-grafted to surfaces were published in the late 70s by Alexander and early 80s by de Gennes, which have initiated a great foundation for both academic and industrial researchers.[79,80] Since then, the number of reports on surface-tethered polymers has escalated, describing their synthetic methods, properties, and applications in a wide range of areas including electronics,[81-83] catalysis,[84] and biotechnology.[85-87] The most desirable and widely used technique for the modification of surfaces with macromolecular architectures is the covalent bonding of thin organic layers to the substrate using the two main strategies known as the "grafting-onto" and the "grafting-from" approaches.[88-93] Various synthetic approaches have been employed including plasma polymerization, self-assembled mono- and multi-layers, click chemistry,[94] and a number of techniques combining electropolymerization with radical polymerization that have been exploited using the "grafting-from" techniques. This

approach involves the immobilization of initiators onto the substrate and *in situ* surface polymerization using atom transfer radical polymerization (ATRP),[95,96] ring-opening metathesis (ROMP),[97] or nitroxide-mediate polymerization (NMP)[97] to control the molecular weight and the thickness of the grafted polymer chains. For more details on the synthetic methods of surface-grafted linear polymers, the reader is referred to previous pertinent reviews on this topic.[98,99] In the present report, we choose to focus on branched architectures, and mostly dendritic structures and their applications in surface chemistry. These highly multivalent macromolecules have become attractive alternatives to classical linear polymers in a wide range of research fields due to their well-defined three-dimensional architectures.[100-104] The next few sections will focus on the various synthetic methods used to prepare self-assembled monolayers of dendritic macromolecules on solid substrates.

1.1.3.1. Synthesis of dendronized surfaces

Like dendronized polymers, dendronized surfaces are made using either the "grafting-onto" or "grafting-from" strategies. The limitations associated with the "grafting-onto" approach are similar to those described for dendronized polymers, where the lack of control over the number of dendrons coupled to the surface and steric hindrance, which can lead to low grafting density, are the main issues associated with this approach. The "grafting-from" strategy is based on a step-wise dendron growth and allows larger dendrons to be immobilized on the surface in a more controlled fashion.[105] This strategy is advantageous over the "grafting-onto" approach and allows control over

the size of the grafted dendrons, the density of functional groups at the periphery, and the surface structure.[106] This approach is also more convenient from the synthetic point of view, since dendron growth can be carried out with relatively simple molecules and by iterative immersion and rinse steps. This is in contrast with solution synthesis of dendrons, which involves more tedious deprotection/growth steps and repeated purifications, thereby making it more time and cost effective. Various surfaces including gold,[107-116] mica,[117,118] and silica/silicon substrated,[119,120] have been functionalized with branched macromolecules such as star polymers, hyperbranched polymers, and dendrons.

1.1.3.2. Functionalization of gold surfaces

Since first reported by Nuzzo and Allara,[121-123] self-assembled monolayers (SAMs) prepared by adsorption of molecules bearing thiol groups or disulfides on gold have been tremendously investigated.[124,125] Modified gold surfaces provide a well-defined model system for the control of surface chemistry and properties such as reactivity, specific affinity, hydrophilicity, and biocompatibility, which allow introduction of specific functions to the substrate in numerous applications.[125-136] The majority of the dendrimer-based SAMs reported in the literature are based on poly(amido amine) (PAMAM), poly(benzyl ether), poly(propyleneimine), carbosilane groups, and recently aliphatic polyester dendrons.

1.1.3.3. Grafting of hyperbranched polymers to gold surfaces

Hyperbranched polymers benefit from easier preparation methods when compared to dendrons, however, these polymers lack the structural uniformity and the synthetic control that dendrons have. Although used in a number of applications, very few examples of hyperbranched polymers grafted onto gold surfaces have been reported in the literature. Haag and co-workers were the first to report the synthesis of a gold surface grafted with a series of hyperbranched polymers based on polyglycerol (PG) moieties (Figure 1.3.2).[112] The synthesis of the PG derivatives bearing a dithiolane ring, suitable for the formation of stable SAMs on gold,[137-140] was carried out via a partial esterification of the hydroxyl groups of a pre-made PG substrate with thioctic acid (Scheme 1.2).[112] The PG precursors were obtained by DCC-mediated coupling using various core initiators. The SAMs of PG derivatives on gold were subsequently formed by chemisorption of the gold substrates in a solution containing the corresponding disulfide derivatives of the various PGs (Scheme 1.2).[112]

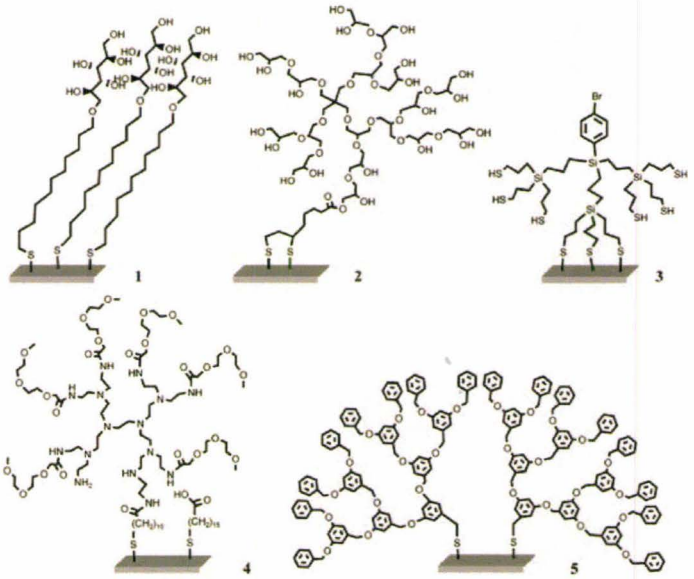

Figure 1.3. Highly hydrophilic linear, branched, and dendritic aliphatic polyethers and other dendritic structures grafted to gold surfaces.

Scheme 1.2. Synthesis of self-assembled monolayers of hyperbranched polyglycerols on gold surfaces.[112]

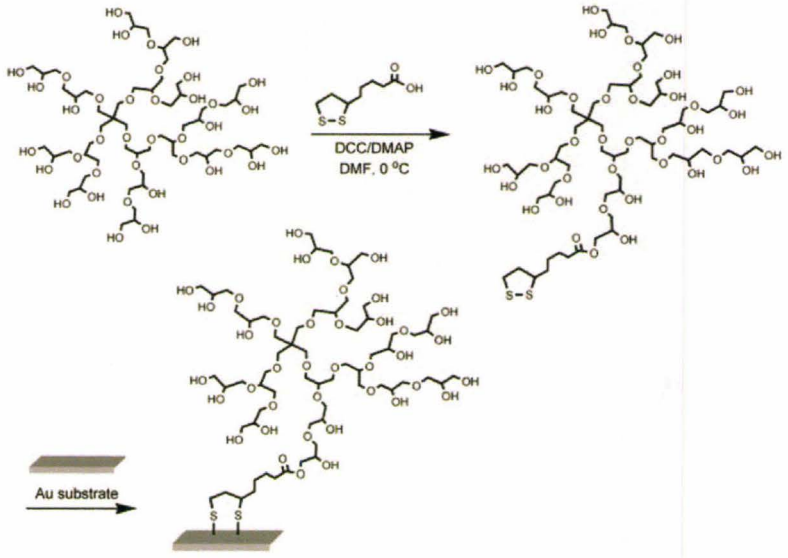

1.1.3.4. Grafting of dendrons to gold surfaces

1.1.3.4.1. Poly(amidoamine) (PAMAM) dendrons

Poly(amidoamine) (PAMAM), a commercially available dendron, has been the most extensively studied among the various dendrons made to date. Numerous studies have been reported on SAMs of PAMAM dendrons on gold surfaces for a wide range of applications including catalysis,[84] sensor devices,[141,142] nanoelectronics[82,83,143] and most commonly for biological applications. Crooks and co-workers were among the first to report the synthesis of thiol-functionalized G4 PAMAM dendrimers and formation of stable SAMs on flat Au surfaces and Au nanoparticles for use in sensing devices and catalysis.[106,110,111,113,114,144-146] Other methods for grafting PAMAM dendrimers on gold substrates include the preparation of amine or carboxylic acid functionalized SAMs on gold surfaces and subsequent coupling with carboxyl-terminated or amine-terminated PAMAM dendrimers, respectively (Scheme 1.3).

Scheme 1.3. Synthesis of PAMAM self-assembled monolayers on pre-functionalized gold surfaces.[113]

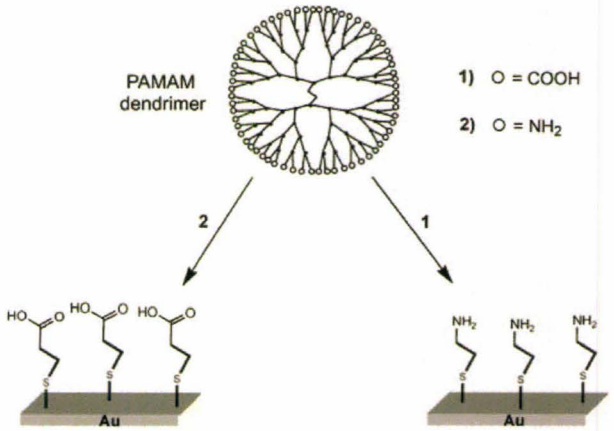

Chemisorption of gold substrates with solutions of PAMAM thiol dendrons to covalently tether dendrons directly onto the gold substrates via a Au-S bond has also been used to generate SAMs of PAMAM dendrons with a high density of functionalizable groups that can be used in various coupling reactions. Yu and co-workers explored PAMAM-thiol dendrons as a novel route to develop bioreactive gold surfaces for biochip applications.[147,148] This was one of the first reports investigating the direct immobilization of dendron thiols on a gold surface without the use of extra spacer monolayers on gold. (Scheme 1.4).[131]

Scheme 1.4. Synthesis of PAMAM-thiol dendrons and their direct immobilization on gold surfaces.[148]

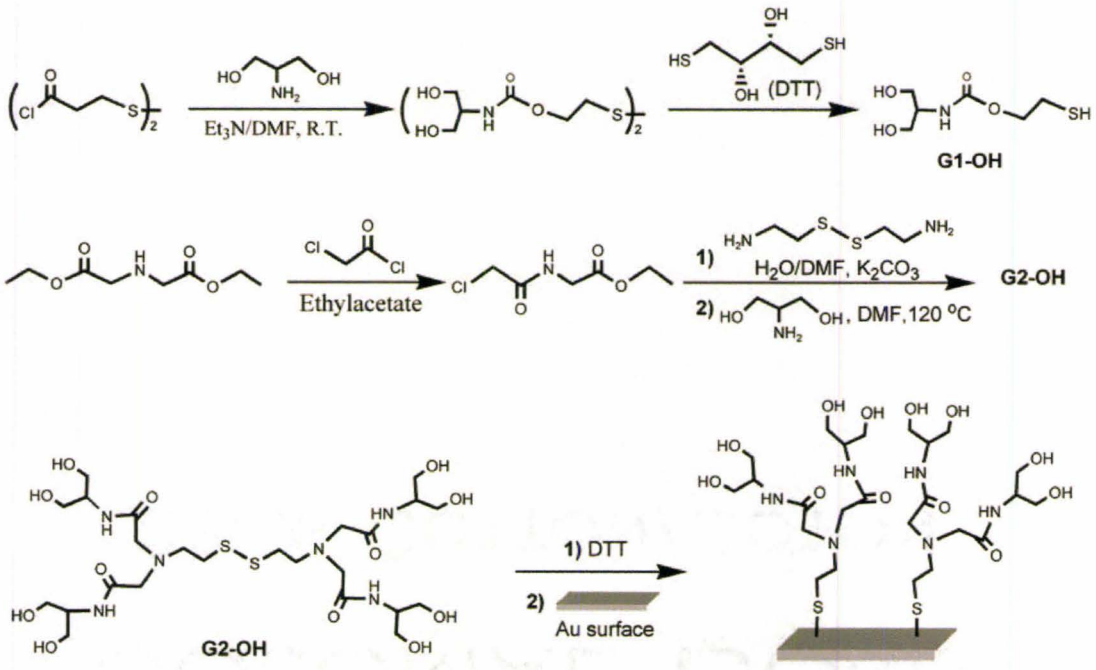

1.1.3.4.2. Polyether dendrons

Self assembled monolayers of polyether dendrons, also referred to as the Fréchet type dendrons,[149] have been studied extensively for various applications such as lithography, energy transfer, and light harvesting.[150-154] The most commonly studied polyether dendrons are the poly(aryl ether) dendrons. Dong *et al.* prepared a series of SAMs of poly(aryl ether) dendrons on gold substrates by introducing a thiol group at the dendron focal point.[155] Using the convergent route, several polyether dendron thiols of various generations were synthesized, resulting in well-defined dendritic structures prior to their chemisorption on gold substrates (Figure 1.4).[155-160] These systems were found to exhibit specific patterns on the surfaces which were closely related to the size of the dendrons, making them extremely useful in the development of patterned surfaces in a designed and controlled way, which is highly recommended in numerous applications.[156]

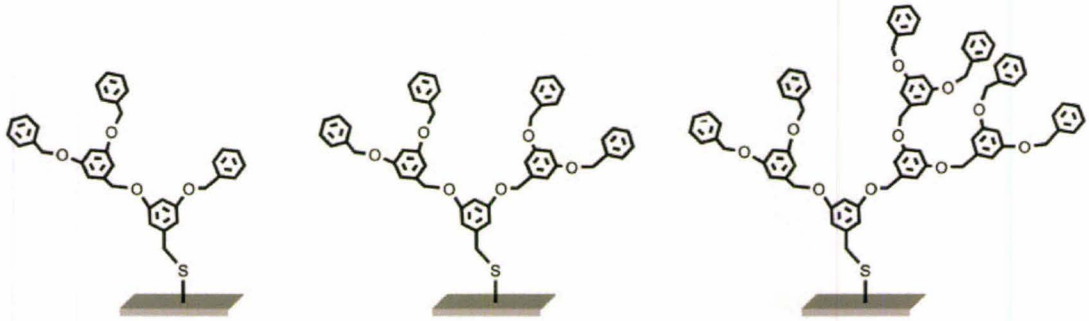

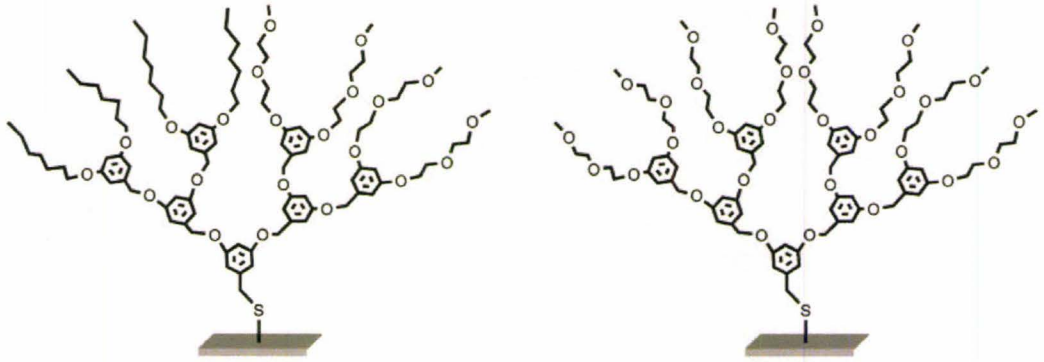

Figure 1.4. Monolayers of various symmetric and asymmetric poly(aryl ether) dendrons on gold surfaces.[155]

1.1.3.4.3. Organosilane dendrons

Unlike PAMAM and polyether dendrons, the use of organosilane dendrons as SAMs on gold substrates has only been explored recently when Xiao *et al.* reported the first organosilane-based SAMs on mica.[161,162] Since then, very few examples have been reported on the grafting of organosilane dendrons to solid substrates and to gold surfaces in particular.[130] Cai and co-workers investigated the synthesis of G0 and G1 alkylsilane

dendrons bearing multiple thiol groups at the periphery and bromophenyl groups at the core (Figure 1.3.3).[130] The presence of multiple thiol groups allowed a way to control the spacing between the focal reactive groups in the monolayers, while the bromophenyl groups were exploited for anchoring conjugated molecules onto the SAMs using the Heck reaction.[163] The organosilane dendrons were grafted to the gold substrates using the Au-S chemistry by chemisorbing the gold substrates in solutions containing the thiolated dendrons.[130]

1.1.3.4.4. Aliphatic polyester dendrons

Contrary to PAMAM and PPI dendrimers, which exhibit significant toxicity due to the presence of multiple cationic amine groups at their peripheries,[164,165] aliphatic polyester dendrons are neutral, biocompatible and biodegradable molecules and are, therefore, very promising candidates for biological applications.[166-168] In addition to their aforementioned advantages, the polyester dendrons are highly soluble in water, contrary to the poly(aryl ether) dendrimers developed by Fréchet and Hawker,[149] which necessitate incorporation of a large number of solubilizing groups at their periphery to overcome their poor solubility for drug delivery applications.[169,170] A new class of polyester dendrons based on the 2,2-bis(hydroxymethyl) propionic acid (bis-MPA) monomer, originally developed by H. Ihre and A. Hult,[171-173] was recently explored by Fréchet and co-workers as a new candidate for the development of anticancer drug delivery systems.[174,175] Various other polyester dendrimers, incorporating monomers such as glycerol,[167,168] succinic acid,[166] phenylalanine and lactic acid,[166] have also been developed

and explored for potential use in biological and tissue engineering applications. Although the interest in polyester dendrimers has increased tremendously in the past few years, very few examples of the preparation of SAMs based on these dendrimers on surfaces have been reported in the literature.[115,116] The first example describing the grafting of aliphatic polyester dendrons on gold surfaces was reported recently by Malmström and co-workers.[115] A series of disulfide polyester dendrons of generation 1 to 3 were synthesized using the convergent route followed by subsequent chemisorption of gold substrates with solutions containing the dendrons to generate the monolayers (Scheme 1.5). This approach allowed control over the chemistry and characterization of the dendritic structures prior to the formation of SAMs onto the gold substrates. However, at higher generations, this technique can suffer from steric crowding, which can lead to non-homogenous or incomplete surface coverage.

Scheme 1.5. Synthesis of gold-grafted aliphatic polyester dendrons.[115]

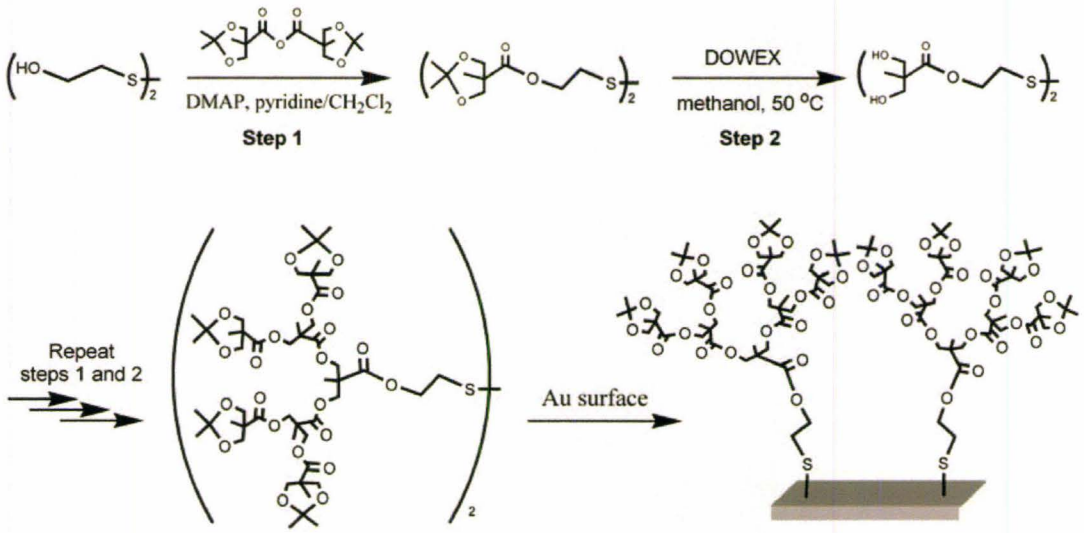

1.1.3.5. Grafting of dendrons to other surfaces

1.1.3.5.1. Grafting of dendrons to silicon-containing substrates

Various dendrons have been grafted to silicon surfaces such as silicon dioxide and PDMS, and investigated for numerous uses including organic coatings,[176,177] development of protein microarrays,[178] chemical sensors, and lithography.[124,179,180] The preparation of SAMs of dendrons on silicon surfaces has been done using various synthetic approaches. For example, Engström and co-workers have examined the formation of first generation PAMAM dendrons on silicon dioxide surfaces and subsequent dendron growth to higher generations using the divergent approach.[181] The first step of this synthesis involved a silanization reaction using alkyl silanes to form amine-terminated SAMs on silicon dioxide substrates. Subsequent reaction of the terminal amine groups of the SAMs with methyl acrylate formed the first generation dendrons which served as the anchor from which higher generations were divergently synthesized (Scheme 1.6).[181]

Scheme 1.6. Preparation of a G1 PAMAM dendron monolayer on a silicon surface.[181]

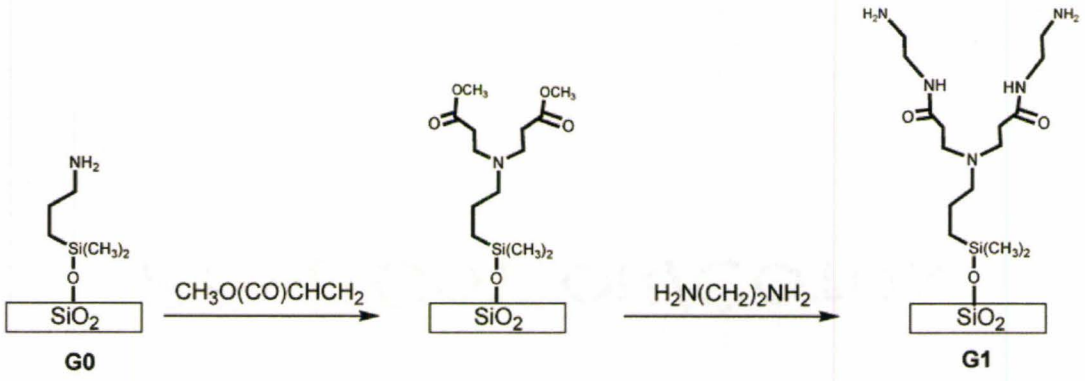

In a separate report, Archer and co-workers have outlined the synthesis of SAMs of carbosilane dendrons on silicon wafers using the divergent dendron growth.[176] The SAMs were formed by immersing clean silicon substrates into solutions of alkytrichlorosilanes followed by reaction of the terminal double bonds of the SAMs with dichloromethylsilane in the presence of a platinum catalyst. The resulting dichlorosilane groups were subsequently reacted with vinylmagnesium bromide to produce the first generation of grafted carbosilane dendrons. Higher generation dendrons were obtained by iterating the above procedure (Scheme 1.7).[176]

Scheme 1.7. Synthesis of self-assembled monolayers of carbosilane dendrons on silicon wafers using the divergent dendron growth.[176]

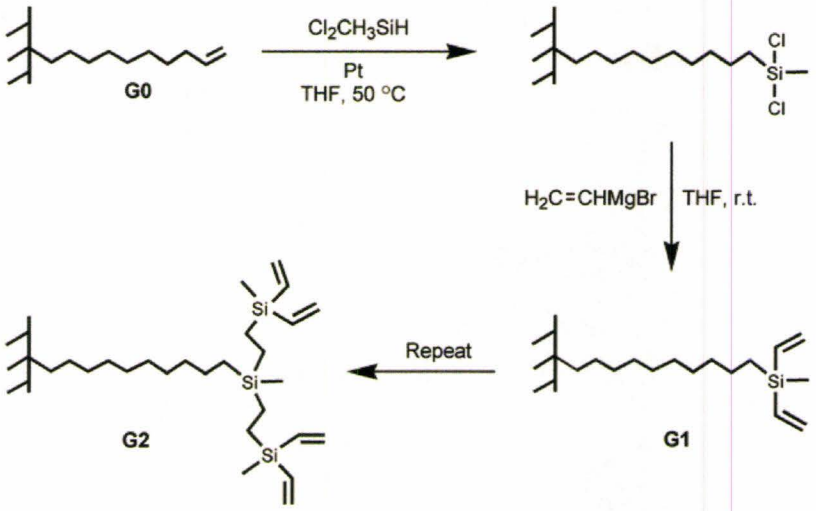

More recently, Pollock *et al.* described the synthesis of immobilized PAMAM dendrons onto surface-modified silicon wafers using the "grafting-from" strategy.[182] The

first step of this synthesis involved coating the silicon substrates with a thin film of a poly(acrylic acid) (PAA), which was introduced using the plasma polymerization technique. The resulting PAA film was subsequently treated with poly(ethyleneimine) (PEI) to generate an amine surface suitable for PAMAM dendron synthesis (Scheme 1.8).[182]

Scheme 1.8. Synthesis of immobilized PAMAM dendrons onto surface-modified silicon wafers using the "grafting-from" strategy.[182]

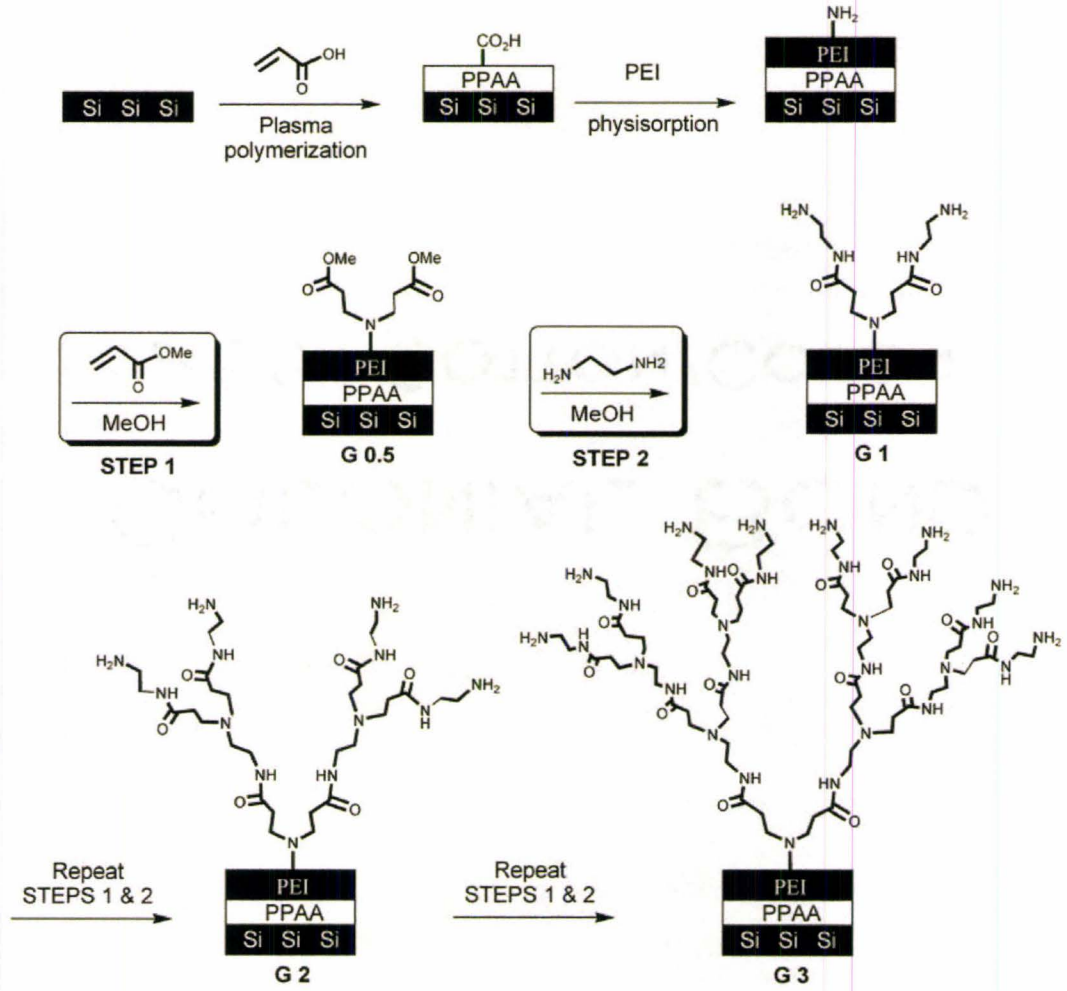

Other examples were reported by Ajikumar *et al.*[178] and Cha *et al.*[183] who grafted the commercially available PAMAM dendrimers to silicon and PDMS surfaces respectively. In the study by Ajikumar *et al.*, carboxyl-terminated PAMAM dendrimers were grafted to an amino silylated silicon wafer via an esterification reaction of the EDC/NHS activated dendrimers (Scheme 1.9).[178]

Scheme 1.9. Coupling of PAMAM dendrimers to amino silylated silicon surfaces using EDC/NHS.[178]

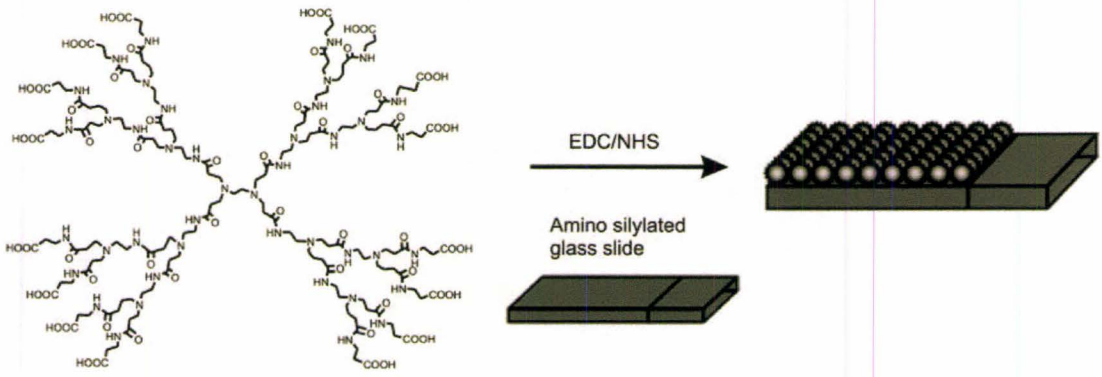

Cha *et al.* used a different approach where monolayers of PAMAM dendrimers were formed on plasma-treated PDMS surfaces using two synthetic routes. In the first route, solutions of PAMAM dendrimers were cast onto air-plasma-treated PDMS surfaces forming a dendrimer monolayer via hydrogen and ionic bonds between the dendrimers and the functional groups on the oxidized surface (Scheme 1.10).[183] In the second approach, the PDMS surfaces were treated with maleic anhydride (MAH) plasma to generate succinic anhydride groups on the surface. Subsequent reaction between the

amines of the PAMAM dendrimers and succinic anhydride groups resulted in the formation of SAMs of dendrimers on the PDMS surfaces (Scheme 1.10).[183]

Other examples include grafting of various hyperbranched polyesters to silicon substrates via solution adsorption or spin-coating techniques.[177,184] The aforementioned systems have potential for numerous applications including surface catalysis, also referred to as lab on a chip technology, bio-sensing and protein binding surfaces, and continue to be the focus of many researchers in the area of surface chemistry.

Scheme 1.10. Formation of PAMAM self-assembled monolayers on plasma-treated PDMS surfaces.[183]

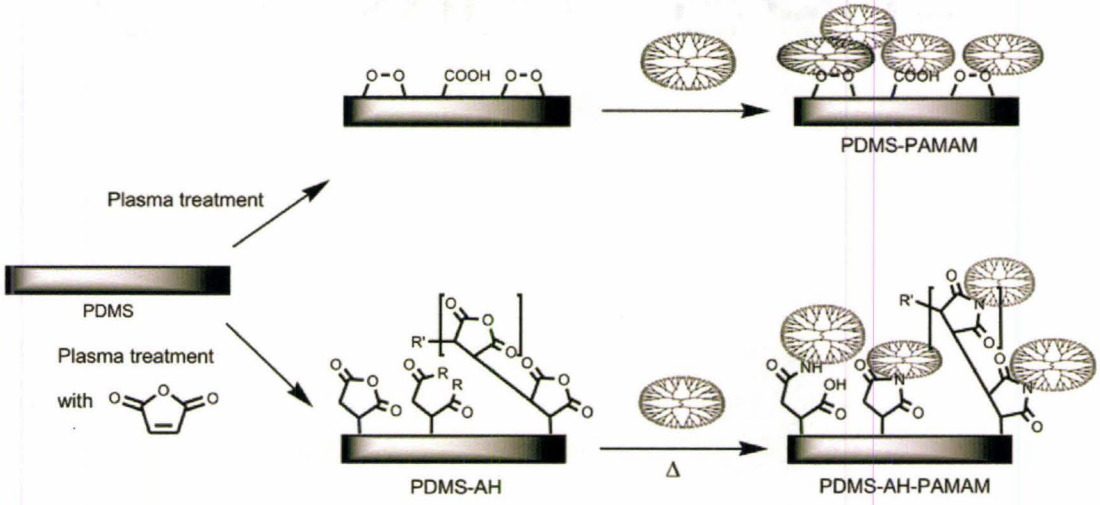

1.1.3.6. Biological Applications of dendronized surfaces

1.1.3.6.1. Surfaces grafted with PAMAM dendrons

One of the major applications of PAMAM-grafted gold surfaces is in the biotechnological field. These dendrons have proved very effective as bridging molecules between gold surfaces and biological macromolecules such as peptides, proteins, antibodies, and DNA strands. [78,109,185] However, despite their broad range of applications, modification of the peripheral amine groups of these dendrimers with neutral or anionic moieties is generally needed to avoid toxicity and liver accumulation associated with their polycationic nature.[164,165] SAMs of PAMAM dendrimers and dendrons on gold substrates have been studied as novel bio-fouling resistant systems. However, results demonstrated that PAMAM dendrimers were susceptible to non-specific protein adsorption which has been attributed to the positively charged terminal amines under physiological conditions of pH 7.4, thereby limiting their versatility as biomolecular interfaces.[144,186,187] To overcome this limitation, and taking advantage of their multivalency, the peripheral amine groups on the PAMAM dendrons have been derivatized with biocompatible moieties such as poly(ethylene glycol) (PEG) and oligo(ethylene glycol) (OEG), which are well-known biomaterials to reduce non-specific protein adsorption.[188-194] Yam *et al.* prepared a series of OEG-modified PAMAM films on SAMs of 11-mercaptoundecanoic acid on gold surfaces (Scheme 1.11). They found that these surfaces resisted approximately 95% of fibrinogen adsorption on the surfaces (Figure 1.5).[145]

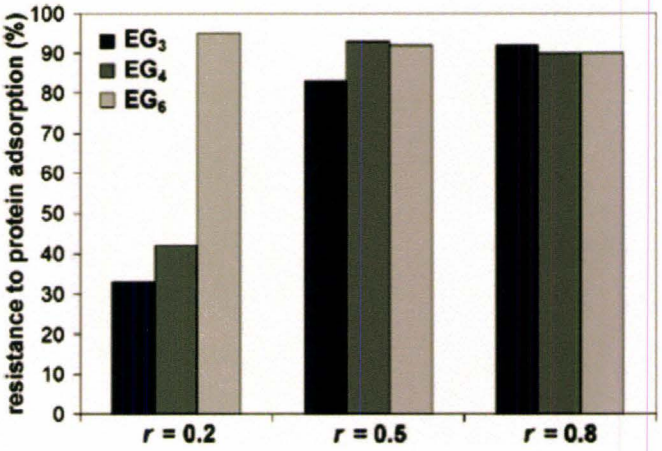

Figure 1.5. Resistance to protein adsorption (%) of films derived from EG_n-PAMAM prepared at various chain densities on SAMs of 11-mercaptoundecanoic acid on gold. r = fraction (density) of EG_n-biotin attached to PAMAM with respect to the total number of surface NH_2 groups.[145]

Similar results were reported by Kim and co-workers, showing a significant reduction in the adsorption of serum proteins on OEG-PAMAM films formed on gold surfaces compared to their PAMAM film analogues.[144] These results were attributed to the high surface coverage with OEG chains imparted by the multivalent PAMAM dendrimers (Figure 1.6).

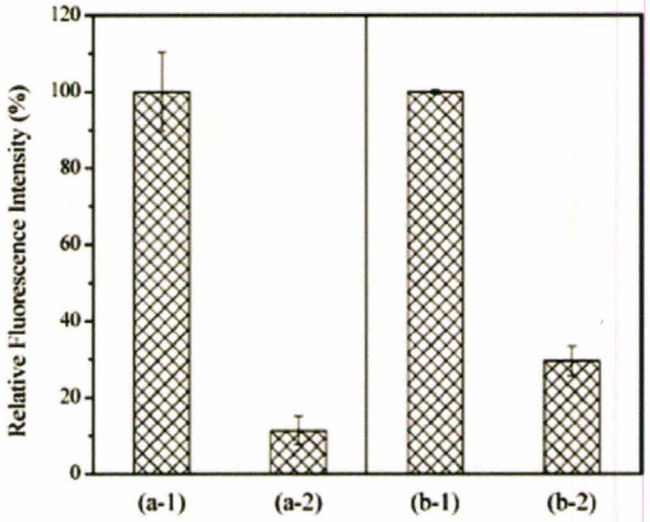

Figure 1.6. Non-specific binding of bovine serum albumin (BSA, 1 mg/mL in PBS) over the PAMAM dendrimer (a-1) and EO_3-dendrimer layers (a-2); non-specific adsorption of serum proteins (1 mg/mL in PBS) over the PAMAM dendrimer (b-1) and EO_3-dendrimer layers (b-2).[144]

1.1.3.6.2. Surfaces grafted with polyether dendrons

Fréchet and co-workers have explored the use of poly(aryl ether) dendrimers for drug delivery applications, however, their highly hydrophobic nature combined with a backbone that is inherently resistant to degradation renders them less suitable for such applications.[195] Haag and co-workers reported the first study investigating SAMs of dendritic polyglycerols (PG) on gold substrates and their potential application in developing novel low-fouling surfaces.[112]

Scheme 1.11. Preparation of films derived from EG_n-PAMAM on 11-mercaptoundecanoic acid SAMs on gold substrates.[145]

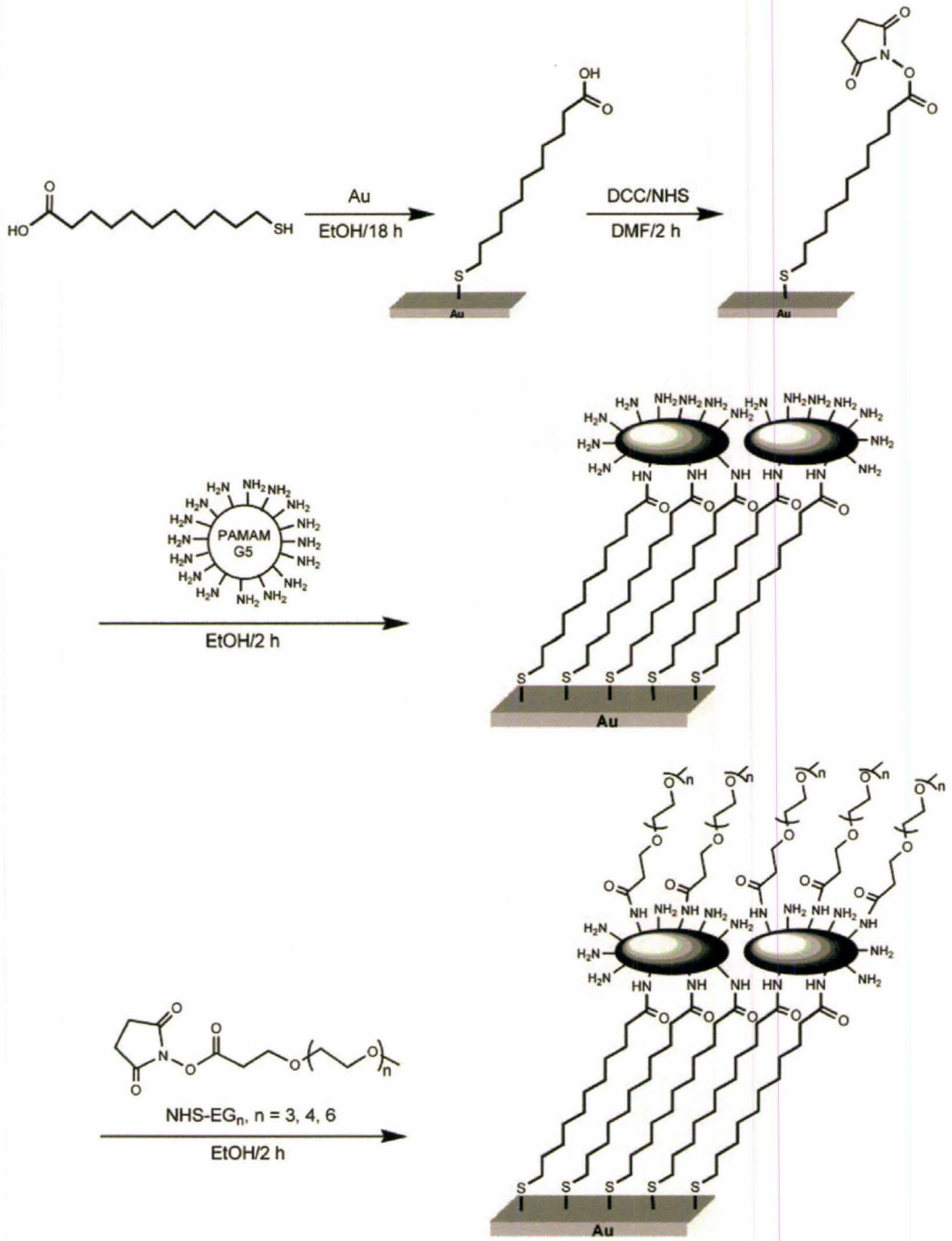

This study was based on previously reported criteria to achieve good protein resistance, and on a structural analysis of previous examples including the use of a branched PEG-grafted poly(ethylenimine) (Figure 1.3.3),[196] and biopolymers presenting sugar derivatives such as Dextran,[197-199] and manitol (Figure 1.3.1),[200] which have been shown to be highly resistant to non-specific protein adsorption. By analogy to the manitol SAMs prepared by Mrksich and co-workers and despite the presence of a high number of hydrogen-bond donors, which is against a criterion formulated by Whitesides and co-workers,[201] the hydrophilic PG-Thioctic acid derivatives proved to be very highly resistant to protein adsorption.[112] Protein adsorption to various PG-grafted gold surfaces was measured using surface plasmon resonance (SPR). Results showed that protein resistance using fibrinogen was observed only with SAMs of PGs covalently attached to the gold substrates, whereas strong fibrinogen adsorption was observed with the physically adsorbed PGs (Figure 1.7.a). Additionally, SAMs formed by PG derivatives on gold were far more efficient as protein resistant surfaces compared to SAMs consisting of the linear hexadecanethiol (HDT) (Figure 1.7.b). Structural relationship of the various PG SAMs on protein resistance was also investigated in this study, and results revealed that PGs with higher degree of branching were more inert to protein adsorption. These PG monolayers exhibited protein resistance that was on par with PEG SAMs, and significantly more effective than dextran-coated surfaces, which are commonly used as a low-fouling biomaterial.[112]

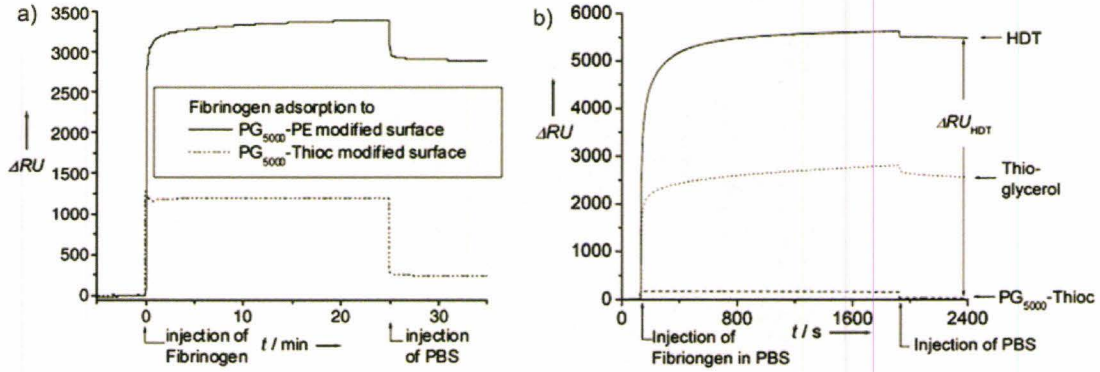

Figure 1.7. SPR sensograms comparing a) covalently versus physically formed SAMs of PGs on gold; b) Linear HDT versus dendritic PG SAMs on gold.[112]

The goal of this thesis work was to develop new dendronized systems for boron delivery and protein resistance based on the aliphatic polyester dendrons, and investigate their potential towards developing novel therapeutics and biomaterials. First, the application of the polyester dendrons to develop novel carborane-containing dendronized polymers is described. These highly boron-containing macromolecules serve as model systems and potential candidates for boron neutron capture therapy (BNCT). The use of polyester dendrons to functionalize gold substrates is then discussed, and their study as model systems towards protein resistance and cell adhesion and proliferation is described in detail. The following chapters demonstrate the potential use of dendritic polyester systems in the biological field. This work addresses important issues in the development of novel pharmaceuticals and biomaterials and emphasizes the role of dendritic macromolecules in achieving the desired properties for specific applications.

1.1.4. References

(1) Tomalia, D. A.; Frechet, J. M. J. *J Polym Sci Pol Chem* **2001**, *40*, 2719-2728.
(2) Flory, P. J. *J Am Chem Soc* **1941**, *63*, 3083.
(3) Flory, P. J. *J Am Chem Soc* **1941**, *63*, 3091.
(4) Flory, P. J. *J Am Chem Soc* **1942**, *64*, 132.
(5) Buhleier, E.; Wehner, W.; Vogtle, F. *Synthesis* **1978**, 155.
(6) Tomalia, D. A.; Baker, H.; Dewald, J.; Hall, M.; Kallos, G.; Martin, S.; Roeck, J.; Ryder, J.; Smith, P. *Polym J* **1985**, *17*, 117-132.
(7) Newkome, G. R.; Yao, Z.-q.; Baker, G. R.; Gupta, V. K. J. *Org. Chem.* **1985**, *50*, 2003.
(8) Hawker, C. J.; Frechet, J. M. J. *J Am Chem Soc* **1990**, *112*, 7638-7647.
(9) Hawker, C.; Frechet, J. M. J. *J Chem Soc Chem Comm* **1990**, 1010-1013.
(10) Mourey, T.; Turner, S. R.; Rubenstein, M.; Frechet, J. M. J.; Hawker, C.; Wooley, K. L. *Macromolecules* **1992**, *25*, 2401.
(11) Wooley, K. L.; Hawker, C.; Pochan, C. J.; Frechet, J. M. J. *Macromolecules* **1993**, *26*, 1514.
(12) Stiriba, S.-E. *Angew. Chem. Int. Ed. Engl.* **2002**, *41*, 1329-1334.
(13) Patri, A. K. *Curr. Opin. Chem. Biol.* **2002**, *6*, 466-471.
(14) Aulenta, F. *Eur. Polym. J.* **2003**, *39*, 1741-1771.
(15) Boas, U.; Heegaard, P. M. H. *Chem. Soc. Rev.* **2004**, *33*, 43-63.
(16) Gillies, E. R.; Frechet, J. M. J. *Drug Discovery Today* **2005**, *10*, 35-43.
(17) Hawker, C.; Frechet, J. M. J. *Journal of Chemical Society, Perkin Translations* **1992**, *1*, 2459-2469.
(18) Jansen, J. F. G. A.; de Brabander-Van der Berg, E. M. M.; Meijer, E. W. *Science* **1994**, *266*, 1226-1229.
(19) Ihre, H. R.; Anders, H. *Macromolecules* **1998**, *31*, 4061-4068.
(20) Esfand, R.; Tomalia, D. A. *Drug Discov Today* **2001**, *6*, 427-436.
(21) Liu, M. J.; Frechet, J. M. J. *Pharm. Sci. Technol.* **1999**, *2*, 393-401.
(22) Liu, M. J.; Kono, K.; Frechet, J. M. J. *J Polym Sci Pol Chem* **1999**, *37*, 3492-3503.
(23) Liu, M. J.; Kono, K.; Frechet, J. M. J. *J Control Release* **2000**, *65*, 121-131.
(24) Kono, K.; Liu, M. J.; Frechet, J. M. J. *Bioconjugate Chem* **1999**, *10*, 1115-1121.
(25) Duncan, R.; Malik, N. *Proc. Int. Symp. Control. Release Bioact. Mater.* **1996**, *23*, 105-106.
(26) Malik, N.; Wiwattanapatapee, R.; Klopsch, R.; Lorenz, K.; Frey, H.; Weener, J. W.; Meijer, E. W.; Paulus, W.; Duncan, R. *J Control Release* **2000**, *65*, 133-148.
(27) Supattapone, S.; Wille, H.; Uyechi, L.; Safar, J.; Scott, M. R. *J. Virol* **2001**, *75*, 3453-3461.
(28) Ihre, H. R.; De Jesus, O. L. P.; Szoka, F. C.; Frechet, J. M. J. *Bioconjugate Chem* **2002**, *13*, 443-452.
(29) Parrott, M. C.; Marchington, E. B.; Valliant, J. F.; Adronov, A. *Journal of the American Chemical Society* **2005**, *127*, 12081-12089.
(30) Haag, R.; Kratz, F. *Angew. Chem. Int. Ed.* **2006**, *45*, 1198-1215.

(31) Tomalia, D. A.; Kirchholff, P. M. *Eur. Pat. Appl. 234408* **Sep 2, 1987**.
(32) Hawker, C. J.; Frechet, J. M. J. *Polymer* **1992**, *33*, 1507-1511.
(33) Percec, V.; Heck, J.; Tomazos, D.; Falkenberg, F.; Blackwell, H.; Ungar, G. *J. Chem. Soc. Perkin Trans.* **1993**, 2799-2811.
(34) Freudenberger, R.; Claussen, W.; Schluter, A. D.; Wallmeier, H. *Polymer* **1994**, *35*, 4496-4501.
(35) Yin, R.; Zhu, Y.; Tomalia, D. A.; Ibuki, H. *J. Am. Chem. Soc.* **1998**, *120*, 2678-2679.
(36) Schluter, A. D. *Top. Curr. Chem.* **1998**, *197*, 165-191.
(37) Schluter, A. D.; Rabe, J. P. *Angew. Chem. Int. Ed. Engl.* **2000**, *39*, 864-883.
(38) Zhang, A.; Shu, L.; Bo, Z.; Schluter, A. D. *Macromol. Chem. Phys.* **2003**, *204*, 328-339.
(39) Nishikawa, M.; Takakura, Y.; Hashida, M. *Adv. Drug Deliv. Rev.* **1996**, *21*, 135-155.
(40) Lee, C. C.; Yoshida, M.; Frechet, J. M. J.; Dy, E. E.; Szoka, F. C. *Bioconjugate Chemistry* **2005**, *16*, 535-541.
(41) Jain, R. K. *Cancer Research* **1987**, *47*, 3039-3051.
(42) Maeda, H.; Wu, J.; Sawa, T.; Matsumura, Y.; Hori, K. *J. Control. Release* **2000**, *65*, 271-284.
(43) Haag, R.; Kratz, F. *Angew. Chem. Int. Ed. Engl.* **2006**, *45*, 1198-1215.
(44) Matsumura, Y.; Maeda, H. *Cancer Res* **1986**, *46*, 6387-6392.
(45) Duncan, R.; Sat, Y. N. *Ann Oncol* **1998**, *9*, 39-39.
(46) Iyer, A. K.; Khaled, G.; Fang, J.; Maeda, H. *Drug Discov Today* **2006**, *11*, 812-818.
(47) Freudenberger, R.; Claussen, W.; Schluter, A. D.; Wallmeier, H. *Polymer* **1994**, *35*, 4496-4501.
(48) Grayson, S. M.; Frechet, J. M. J. *Macromolecules* **2001**, *34*, 6542-6544.
(49) Malkoch, M.; Carlmark, A.; Woldergiorgis, A.; Hult, A.; Malmstrom, E. *Macromolecules* **2004**, *37*, 322-329.
(50) Yoshida, M.; Fresco, Z. M.; Ohnishi, S.; Frechet, J. M. J. *Macromolecules* **2005**, *38*, 334-344.
(51) Carlmark, A.; Malmstrom, E. *Macromolecules* **2004**, *37*, 7491-7496.
(52) Draheim, G.; Ritter, H. *Macromol. Chem. Phys.* **1995**, *196*, 2211-2222.
(53) Percec, V.; Ahn, C. H.; Ungar, G.; Yeardley, D. J. P.; Moller, M.; Sheiko, S. S. *Nature* **1998**, *398*, 161-164.
(54) Chen, Y. M.; Chen, C. F.; Liu, W. H.; Xi, F. *Macromol. Rapid Commun.* **1996**, *17*, 401-407.
(55) Neubert, I.; Schluter, A. D. *Acta Polym.* **1996**, *47*, 455-459.
(56) Shu, L.; Schluter, A. D. *Macromol. Chem. Phys.* **2000**, *201*, 239-245.
(57) Cheng, C. X.; Tang, R. P.; Zhao, F. X. *J. Appl. Polym. Sci.* **2004**, *91*, 2733-2737.
(58) Percec, V.; Schluter, A. D.; Ronda, J. C.; Johansson, G.; Ungar, G.; Zhou, J. P. *Macromolecules* **1996**, *29*, 1464-1472.
(59) Percec, V.; Schluter, A. D. *Macromolecules* **1997**, *30*, 5783-5790.

(60) Prokhorova, S. A.; Sheiko, S. S.; Mourran, A.; Azumi, R.; Beginn, U.; Zipp, G.; Ahn, C. H.; Holerca, M. N.; Percec, V.; Moller, M. *Langmuir* **2000**, *16*, 6862-6867.
(61) Schluter, A. D.; Wegner, G. *Acta Polym.* **1993**, *44*, 59-69.
(62) Claussen, W.; Schulte, N.; Schluter, A. D. *Macromol. Rapid Commun.* **1995**, *16*, 89-94.
(63) Karakaya, B.; Claussen, W.; Gessler, K.; Saenger, W.; Schluter, A. D. *J. Am. Chem. Soc.* **1997**, *119*, 3296-3301.
(64) Bo, Z.; Rabe, J. P.; Schluter, A. D. *Angew. Chem. Int. Ed. Engl.* **1999**, *38*, 2370-2372.
(65) Bao, Z.; Amundson, K. R.; Lovinger, A. J. *Macromolecules* **1998**, *31*, 8647-8649.
(66) Gossl, I.; Shu, L. J.; Schluter, A. D.; Rabe, J. P. *J. Am. Chem. Soc.* **2002**, *124*, 6860-6865.
(67) Ghosh, S. *Biomacromolecules* **2004**, *5*, 1602-1605.
(68) Lee, C. C.; Grayson, S. M.; Frechet, J. M. J. *J. Polym. Sci., Part A: Polym. Chem.* **2004**, *42*, 3563-3578.
(69) Dong, B.; Huo, F. W.; Zhang, L.; Yang, X. Y.; Wang, Z. Q.; Zhang, X.; Gong, S. Y.; Li, J. H. *Chem-Eur J* **2003**, *9*, 2331-2336.
(70) Cha, B. J.; Kang, Y. S.; Won, J. *Macromolecules* **2001**, *34*, 6631-6636.
(71) Sharma, M.; Dube, A.; Engstrom, J. R. *J Am Chem Soc* **2007**, *129*, 15022-15033.
(72) Crooks, R. M.; Zhao, M.; S., L.; Chechik, V.; Lee, K. Y. *Acc. Chem. Res.* **2001**, *34*, 181-190.
(73) Chechik, V.; Crooks, R. M. *Langmuir* **1999**, *15*, 6364-6369.
(74) Woo, S.; Lee, Y.; Sunkara, V.; Cheedarala, R. K.; Shin, H. S.; Choi, H. C.; Park, J. W. *Langmuir* **2007**, *23*, 11373-11376.
(75) Zhao, M. Q.; Crooks, R. M. *Angew Chem Int Edit* **1999**, *38*, 364-366.
(76) Zhang, Q.; Archer, L. A. *Langmuir* **2006**, *22*, 717-722.
(77) Ulman, A. *Adv Mater* **1990**, *2*, 573-582.
(78) Svobodova, L.; Snejdarkova, M.; Hianik, T. *Anal Bioanal Chem* **2002**, *373*, 735-741.
(79) Alexander, S. *Journal of Physics* **1977**, *38*, 983.
(80) de Gennes, P. G. *Macromolecules* **1980**, *13*, 1069.
(81) Klein, J.; Kumacheva, E.; Mahalu, D.; Perahia, D.; Fetters, L. J. *Nature* **1994**, *370*, 634.
(82) Osifchin, R. G.; Andres, R. P.; Henderson, J. I.; Kubiak, C. P.; Dominey, R., N. *Nanotechnology* **1996**, *7*, 412.
(83) Sato, T.; Ahmed, H.; Brown, D.; Johnson, B. F. G. *J. Appl. Phys.* **1997**, *82*, 696.
(84) Zhao, M.; Crooks, R. M. *Angew. Chem. Int. Ed. Engl.* **1999**, *38*, 364.
(85) de la Fuente, J.; Barrientos, A. G.; Rojas, T. C.; Canada, J.; Fernandez, A.; Penades, S. *Angew. Chem. Int. Ed. Engl.* **2001**, *40*, 2257.
(86) Cao, Y.-W.; Jin, R.; Mirkin, C. A. *J. Am. Chem. Soc.* **2001**, *123*, 7961.
(87) Li, Z.; Jin, R.; Mirkin, C. A.; Letsinger, R. L. *Nucleic Acids Research* **2002**, *30*, 1558.
(88) Pyun, J.; Matyajaszewki, K. *Chem. Mater.* **2001**, *13*, 3436.

(89) Wuelfing, W. P.; Gross, S. M.; Miles, D. T.; Murray, R. W. *J. Am. Chem. Soc.* **1998**, *120*, 12696.
(90) Teranishi, T.; Hosoe, M.; Miyake, M. *Adv. Mater.* **1997**, *9*, 65.
(91) Jordan, R.; West, N.; Ulman, A.; Chou, Y. M.; Nyuken, O. *Macromolecules* **2001**, *34*, 1606.
(92) Lowe, A. B.; Sumerlin, B. S.; Donovan, M. S.; McCormick, C. L. *J. Am. Chem. Soc.* **2002**, *124*, 11562.
(93) Corbierre, M. K.; Cameron, N. S.; Sutton, M.; Mochrie, S. G. J.; Lurio, L. B.; Ruhm, A.; Lenox, R. B. *J. Am. Chem. Soc.* **2001**, *123*, 10411.
(94) Ostaci, R.-V.; Damiron, D.; Capponi, S.; Vignaud, G.; Leger, L.; Grohens, Y.; Drockenmuller, E. *Langmuir* **2007**.
(95) Matrab, T.; Chancolon, J.; Mayne L'hermite, M.; Rouzaud, J. N.; Deniau, G.; Boudou, J. P.; Chehimi, M. M.; Delamar, M. *Colloids Surf.* **2006**, *287*, 217-221.
(96) Zhang, H.; Shouro, D.; Itoh, K.; Takata, T.; Jiang, Y. *Journal of Applied Polymer Science* **2008**, *108*, 351-357.
(97) Voccia, S.; Gabriel, S.; Serwas, H.; Jerome, R.; Jerome, C. *Prog. Org. Coat.* **2006**, *55*, 175-181.
(98) Zhao, B.; Brittain, W. J. *Prog. Polym. Sci.* **2000**, *25*, 677-710.
(99) Currie, E. P. K.; Norde, W.; Cohen Stuart, M. A. *Advances in Colloid and Interface Science* **2003**, *100*, 205-265.
(100) Tomalia, D. A.; Baker, H.; Dewald, M.; Hall, G.; Kallos, S.; Roeck, M. J.; Ryder, J.; Smith, P. *Polym. J.* **1985**, *17*, 117.
(101) Tully, D. C.; Frechet, J. M. J. *Chem. Comm.* **2001**, *14*, 1229-1239.
(102) Stiriba, S.; Frey, H.; Haag, R. *Angew. Chem. Int. Ed. Engl.* **2002**, *41*, 1329-1334.
(103) Svenson, S.; Tomalia, D. A. *Adv. Drug Deliv. Rev.* **2005**, *57*, 2106-2129.
(104) Crooks, R. M.; Wells, M. *J. Am. Chem. Soc.* **1996**, *118*, 3988-3989.
(105) Bourque, S. C.; Alper, H.; Manzer, L. E.; Arya, P. *J. Am. Chem. Soc.* **2000**, *122*, 956-957.
(106) Wanunu, M.; Vaskevich, A.; Shanzer, A.; Rubinstein, I. *J. Am. Chem. Soc.* **2006**, *128*, 8341-8349.
(107) Wells, M.; Crooks, R. M. *J. Am. Chem. Soc.* **1996**, *118*, 3988.
(108) Tokuhisa, H.; Zhao, M.; Baker, L. A.; Phan, V. T.; Dermody, D. L.; Garcia, M. E.; Peez, R. F.; Crooks, R. M.; Mayer, T. M. *J. Am. Chem. Soc.* **1998**, *120*, 4492.
(109) Mark, S. S.; Sandhyarani, N.; Zhu, C.; Campagnolo, C.; Batt, C. A. *Langmuir* **2004**, *20*, 6075.
(110) Chechik, V.; Crooks, R. M. *Langmuir* **1999**, *15*, 6364-6369.
(111) Hong, M. Y.; Yoon, H. C.; Kim, H. S. *Langmuir* **2003**, *19*, 416.
(112) Siegers, C.; Biesalski, M.; Haag, R. *Chem. Eur. J.* **2004**, *10*, 2831-2838.
(113) Manriquez, J.; Juaristi, E.; Munoz-Muniz, O.; Godinez, L. A. *Langmuir* **2003**, *19*, 7315-7323.
(114) Chapman, R. C.; Ostuni, E.; Liang, M. N.; Meluleni, G.; Kim, E.; Yan, L.; Pier, G.; Warren, H. S.; Whitesides, G. M. *Langmuir* **2001**, *17*, 1225-1233.
(115) Ostmark, E.; Macakova, L.; Auletta, T.; Malkoch, M.; Malmstrom, E.; Blomberg, E. *Langmuir* **2005**, *21*, 4512-4519.

(116) Benhabbour, S. R.; Liu, L.; Sheardwon, H.; Adronov, A. *Macromolecules* **2008**, *41*, 2567-2576.
(117) bielinska, A. N.; Kukowska-Latallo, J. F.; Johnson, J.; Tomalia, D. A.; Baker Jr., J. R. *Nucleic Acids Research* **1996**, *24*, 2176.
(118) Pericet-Camara, R.; Papastavrous, G.; Borkovec, M. *Langmuir* **2004**, *20*, 3264.
(119) Bar, G.; Rubin, S.; Cutts, R. W.; Taylor, T. N.; Zawodzinski, T. A. *Langmuir* **1996**, *12*, 1172.
(120) Baker, L. A.; Zamborini, F. P.; Sun, L.; Crooks, R. M. *Anal. Chem.* **1999**, *71*, 4403.
(121) Nuzzo, R. G.; Allara, D. L. *J. Am. Chem. Soc.* **1983**, *105*, 4481.
(122) Nuzzo, R. G.; Zegarski, B. R.; Dubois, L. H. *J. Am. Chem. Soc.* **1987**, *109*, 733.
(123) Nuzzo, R. G.; Fusco, F. A.; Allara, D. L. *J. Am. Chem. Soc.* **1987**, *109*, 2358.
(124) Ulman, A. *Chem. Rev.* **1996**, *96*, 1533.
(125) Zhong, C.-J.; Porter, M. D. *Anal. Chem.* **1995**, *9A*, 67.
(126) Chidsey, C. E. D.; Murray, R. W. *Science* **1986**, *231*, 25.
(127) Ulman, A. *Adv. Mater.* **1990**, *2*, 573.
(128) Thomas, R. C.; Kim, T.; Crooks, R. M.; Houston, J. E.; Mikhalske, T. A. *J. Am. Chem. Soc.* **1995**, *117*, 3830.
(129) Sullivan, T. P.; Huck, W. T. S. *J. Org. Chem.* **2003**, *17*.
(130) Yam, C. M.; Cho, J.; Cai, C. *Langmuir* **2003**, *12*, 6862-6868.
(131) Flink, S.; Boukamp, B. A.; van der Berg, A.; van Beggel, F. C. J. M.; Reinhoudt, D. N. *J. Am. Chem. Soc.* **1998**, *120*, 4652.
(132) Rojas, M. T.; Kaifer, A. E. *J. Am. Chem. Soc.* **1995**, *117*, 5883.
(133) Almirall, E.; Fragoso, A.; Cao, R. *Electrochem. Commun.* **1999**, *1*, 10.
(134) Ledesma-Garcia, J.; Manriquez, J.; Gutierrez-Granados, S.; Godinez, L. A. *Electroanalysis* **2003**, *15*, 659.
(135) Maye, M. M.; Lou, Y.; Zhong, C. *Langmuir* **2000**, *16*, 7520.
(136) Feldheim, D. L.; Keating, C. D. *Chem. Soc. Rev.* **1998**, *27*, 1.
(137) Wang, Y.; Kaifer, A. E. *J. Phys. Chem. B* **1998**, *102*, 9922-9927.
(138) Madoz, J.; Kuznetzov, B. A.; Medrano, F. J.; Garcia, J. L.; Fernandez, V. M. *J. Am. Chem. Soc.* **1997**, *119*, 1043-1051.
(139) Dong, Y.; Abaci, S.; Shannon, C. *Langmuir* **2003**, *19*, 8922-8926.
(140) Duan, C.; Meyerhoff, M. E. *Mikrochim. Acta.* **1995**, *117*, 195-206.
(141) Elghanian, R.; Storhoff, J. J.; Mucic, R. C.; Letsinger, R. L.; Mirkin, C. A. *Science* **1997**, *277*, 1078.
(142) Sastry, M.; Lala, N.; Patil, V.; Chavan, S. P.; Chittiboyina, A. G. *Langmuir* **1998**, *14*, 4138.
(143) Snow, A. W.; Wohltjen, H. *Chem. Mater.* **1998**, *10*, 947.
(144) Hong, M. Y.; Kim, Y.-J.; Lee, J. W.; Kim, K.; Lee, J.-H.; Yoo, J.-S.; Bae, S.-H.; Choi, B.-S.; Kim, H. S. *Journal of Colloid and Interface Science* **2004**, *274*, 41-48.
(145) Yam, C. M.; Deluge, M.; Tang, D.; Kumar, A.; Cai, C. *Journal of Colloid and Interface Science* **2006**, *296*, 118-130.

(146) Kwon, S. H.; Hong, B. J.; Park, H. Y.; Knoll, W.; Park, J. W. *Journal of Colloid and Interface Science* **2007**, *308*, 325-331.
(147) Yang, M.; Tsang, E. M. W.; Wang, Y. A.; Peng, X.; Yu, H.-Z. *Langmuir* **2005**, *21*, 1858-1865.
(148) Wang, Y.; Li, J.; Chen, H.; Peng, X. *J. Am. Chem. Soc.* **2002**, *124*, 2293-2298.
(149) Hawker, C. J.; Frechet, J. M. J. *J. Am. Chem. Soc.* **1990**, *112*, 7638-7647.
(150) Gilat, S. L.; Adronov, A.; Frechet, J. M. J. *J. Org. Chem.* **1999**, *64*, 7474-7484.
(151) Lee, L. F.; Adronov, A.; Schaller, R. D.; Frechet, J. M. J.; Saykally, R. J. *J. Am. Chem. Soc.* **2003**, *125*, 536-540.
(152) Christoffels, L. A. J.; Adronov, A.; Frechet, J. M. J. *Angew. Chem. Int. Ed. Engl.* **2000**, *112*, 2247-2251.
(153) Tully, D. C.; Wilder, K.; Frechet, J. M. J.; Trimble, A. R.; Quate, C. F. *Adv. Mater.* **1999**, *11*, 314-318.
(154) Tully, D. C.; Trimble, A. R.; Frechet, J. M. J.; Wilder, K.; Quate, C. F. *Chem. Mater.* **1999**, *11*, 2892-2898.
(155) Dong, B.; Huo, F.; Zhang, L.; yang, X.; Wang, Z.; Zhang, X.; Gong, S.; Li, J. *Chem. Eur. J.* **2003**, *9*, 2331-2336.
(156) Zhang, L.; Huo, F.; Wang, Z.; Wu, L.; Zhang, X. *Langmuir* **2000**, *16*, 3813-3817.
(157) Bo, Z.; Zhang, L.; Zhao, B.; Zhang, X.; Shen, J.; Hoppener, S.; Chi, L.; Fuchs, H. *Chem. Lett.* **1998**, *27*, 1197.
(158) Zhang, L.; Zou, B.; Dong, B.; Huo, F. W.; Zhang, X.; Chi, L. F.; Jiang, L. *Chem. Comm.* **2001**, 1906.
(159) Zhang, L.; Huo, F. W.; Wang, Z. Q.; Wu, L. X.; Zhang, X.; Hoppener, S.; Chi, L. F.; Fuchs, H.; Zhao, J. W.; Niu, L.; Dong, S. J. *Langmuir* **2000**, *16*, 3813.
(160) Gorman, C. B.; Miller, R. L.; Chen, K.-Y.; Bishop, A. R.; Haasch, R. T.; Nuzzo, R. G. *Langmuir* **1998**, *14*, 3312-3319.
(161) Xiao, Z. D.; Cai, C. Z.; Deng, X. B. *Chem. Comm.* **2001**, 1442-1443.
(162) Xiao, Z. D.; Cai, C.; Mayeux, A.; Milenkovic, A. *Langmuir* **2002**, *18*, 7728-7739.
(163) Littke, A. F.; Fu, G. C. *J. Am. Chem. Soc.* **2001**, *123*, 6989.
(164) Jevpraesesphant, R. *J. Pharm.* **2003**, *252*, 263-266.
(165) Malik, N. *J. Control. Release* **2000**, *65*, 133-148.
(166) Grinstaff, M. W. *Chemistry* **2002**, *8*, 2838-2846.
(167) Boysen, M. M. K. *Eur. J. Org. Chem.* **2003**, 4376-4386.
(168) Frey, H.; Haag, R. *J. Biotechnol.* **2002**, *90*, 257-267.
(169) Liu, M. *J. Control. Release* **2000**, *65*, 121-131.
(170) Liu, M. *J. Polym. Sci., Part A: Polym. Chem.* **1999**, *37*, 3492-3503.
(171) Ihre, H.; Soderlind, E.; Hult, A. *Abstr Pap Am Chem S* **1995**, *210*, 187-Pmse.
(172) Ihre, H.; Hult, A.; Frechet, J. M. J.; Gitsov, I. *Macromolecules* **1998**, *31*, 4061-4068.
(173) Ihre, H.; De Jesus, O. L. P.; Frechet, J. M. J. *J Am Chem Soc* **2001**, *123*, 5908-5917.
(174) Ihre, H. *Bioconjugate Chemistry* **2002**, *13*, 433-452.
(175) De Jesus, P. O. L. *Bioconjugate Chemistry* **2002**, *13*, 453-461.
(176) Zhang, Q.; Archer, L. A. *Langmuir* **2006**, *22*, 717-722.

(177) Sidorenko, A.; Zhai, X. W.; Simon, F.; Pleul, D.; Tsukruk, V. V. *Macromolecules* **2002**, *35*, 5131-5139.
(178) Ajikumar, P. K.; Ng, J. K.; Tang, Y. C.; Lee, J. Y.; Stephanopoulos, G.; Too, H.-P. *Langmuir* **2007**, *23*, 5670-5677.
(179) Schreiber, F. *Prog. Surf. Sci.* **2000**, *65*, 151.
(180) Tsukruk, V. V. *Adv. Mater.* **2001**, *13*, 95.
(181) Sharma, M.; Dube, A.; Engstrom, J. R. *J. Am. Chem. Soc.* **2007**, *129*, 15022-15033.
(182) Pollock, N.; Fowler, G.; Twyman, L. J.; McArthur, S. L. *Chem. Comm.* **2007**, 2482-2484.
(183) Cha, B. J.; Kang, Y. S.; Won, J. *Macromolecules* **2001**, *34*, 6631-6636.
(184) Sidorenko, A.; Zhai, X. W.; Peleshanko, S.; Greco, A.; Shevchenko, A.; Tsukruk, V. V. *Langmuir* **2001**, *17*, 5924.
(185) Degenhart, G. H.; Dordi, B.; Schonherr, H.; Vancso, C. J. *Langmuir* **2004**, *20*, 6216-6224.
(186) Zheng, J.; Li, J.; Chen, S.; Jiang, S. *Langmuir* **2004**, *20*, 8931.
(187) Vanderah, D. J.; La, H.; Naff, J.; Silin, V.; Rubinson, K. A. *J. Am. Chem. Soc.* **2004**, *126*, 13639.
(188) Lee, S. W.; Laibinis, P. E. *Biomaterials* **1998**, *19*, 1669.
(189) Prime, K. L.; Whitesides, G. M. *J. Am. Chem. Soc.* **1993**, *115*, 10714.
(190) Jeon, S. I.; Lee, J.-H.; Andrade, J. D.; de Gennes, P. G. *Journal of Colloid and Interface Science* **1991**, *6*, 91.
(191) Harder, P.; Grunze, M.; Dahint, R.; Whitesides, G. M.; Laibinis, P. E. *J. Phys. Chem. B* **1998**, *102*, 426.
(192) Perstin, A. J.; Grunze, M.; Garbuzova, I. A. *J. Phys. Chem. B* **1998**, *102*, 4918.
(193) McPherson, T.; Kidane, A.; Szleifer, I.; Park, K. *Langmuir* **1998**, *14*, 176.
(194) Zhu, B.; Eurell, T.; Gunawan, R.; Leckband, D. *J. Biomed. Mater. Res.* **2001**, *56*, 406.
(195) Kono, K.; Liu, M.; Frechet, J. M. J. *Bioconjugate Chemistry* **1999**, *10*, 1115-1121.
(196) Andrade, J. D.; Hlady, V. *Adv. Polym. Sci.* **1986**, *79*, 1-63.
(197) Osterberg, E.; Bergstrom, K.; Holmberg, K.; Riggs, J. A.; Alstine, J. M. V.; Schuman, T. P.; Burns, N. L.; Harris, J. M. *Colloids Surf.* **1993**, *77*, 159-169.
(198) Osterberg, E.; Bergstrom, K.; Holmberg, K.; Schuman, T. P.; Riggs, J. A.; Burns, N. L.; Alstine, J. M. V.; Harris, J. M. *J. Biomed. Mater. Res.* **1995**, *29*, 741-747.
(199) Holland, N. B.; Qiu, Y.; Ruegsegger, M.; Marchant, R. E. *Nature* **1998**, *392*, 799-801.
(200) Luk, Y.-Y.; Kato, M.; Mrksich, M. *Langmuir* **2000**, *16*, 9604-9608.
(201) Chapman, R. G.; Ostuni, E.; Takayama, S.; Holmlin, R. E.; Yan, L.; Whitesides, G. M. *Journal of the American Chemical Society* **2000**, *122*, 8303-8304.

Chapter 2: Synthesis and Properties of Carborane-Containing Dendronized Polymers

Abstract

Carborane-containing dendronized polymers were successfully synthesized using two different approaches up to the fourth generation. Nitroxide-mediated polymerization (NMP) was effective for the polymerization of carborane-functionalized styrenic monomers, leading to well-defined polymers with high boron content and narrow molecular weight distributions (PDI < 1.1). The resulting carborane-functionalized polymers could then be dendronized using a divergent approach to introduce aliphatic polyester dendrons of generation 1 to 4 grafted from the polymer backbone. This first approach afforded a maximum degree of dendronization of 70%. To increase the degree of dendronization, a first-generation macromonomer was polymerized using NMP to yield a fully functionalized first-generation dendronized polymer. This material was also dendronized up to the fourth generation. Both approaches produced water-soluble dendronized polymers (1 mg/mL in pure water) with high molecular weights (in excess of 70 kDa). It was found that the solubility of the polymer produced from the second approach, where dendronization occurred at every monomer unit, exceeded that of the first approach. This chapter has been reproduced in part with permission from *Macromolecules* **2007**, 5678–5688. Copyright 2007 American Chemical Society.

2.1. Introduction

Carborane-containing macromolecules have attracted attention due to the unique properties of the icosahedral boron-rich carborane clusters. As a result of their high thermodynamic stability, these compounds have been postulated as potential flame retardant materials.[1] In Addition, the extremely high neutron capture cross section of ^{10}B atoms, the highest of all light elements,[2] not only makes them ideal for radiation shielding coatings,[3] but also enables their use in medicinal applications.[4] Specifically, one type of chemotherapy, dubbed Boron Neutron Capture Therapy (BNCT), is an extensively studied experimental approach for tumor treatment,[5] and has been the focus of extensive research since first proposed by Locher and coworkers in 1936.[4] This method relies on the cytotoxic effect produced as a result of the nuclear reaction between ^{10}B and thermal neutrons.[2] In this binary procedure, upon irradiation of ^{10}B nuclei with thermal neutrons, a radiation dose composed of high linear energy transfer (LET) lithium ions and alpha particles (^{7}Li and α) is produced and has a penetration path length of about 10 μm in biological tissues, which is approximately equivalent to one cell diameter.[6] Therefore, it is theoretically possible to destroy cancer cells without affecting adjacent healthy cells if a significantly high ^{10}B concentration is selectively accumulated within a tumor. However, one of the main challenges to BNCT therapy has been achieving the selective delivery of high ^{10}B concentrations to cancer cells, where a minimum of 10^9 ^{10}B atoms per cell, or approximately 30 μg ^{10}B per gram of tumor tissue, is needed.[7,8]

To address this issue, carborane cages have received significant attention due to their boron-rich nature, high stability, charge neutrality, and ease of chemical

modification.[9] Unfortunately, the lipophilic nature of carboranes prohibits their direct intravenous delivery to target tissues. To overcome this difficulty, conjugation of carborane cages with various hydrophilic biological molecules, including sugars,[10] nucleic acids,[10] liposomes[11], and DNA binding units such as trimethoxy indole (TMI)[12] has been investigated, but very limited success has been achieved. Recently the incorporation of carborane cages within dendrimers has begun to attract attention. In the early 1990's, Newkome and co-workers synthesized a completely water soluble hydrocarbon dendrimer internally functionalized with multiple carborane cages.[13] Subsequently, Qualmann *et al.* also reported a water soluble poly(lysine) dendrimer functionalized with carborane units, where the carboranes were introduced at the dendrimer periphery.[14] In addition, other carborane containing dendritic structures have been reported, [15-17] but none of these have simultaneously exhibited water solubility, biocompatibility, biodegradability, and low toxicity, which are key properties required for BNCT.

In our group, we have recently extended this approach to the incorporation of carborane cages within aliphatic polyester dendrimers to produce water soluble conjugates using the divergent dendrimer growth approach.[18-20] These carborane-functionalized aliphatic polyester dendrimers were prepared up to the fifth generation and, due to their numerous peripheral hydroxyl groups, they exhibited water solubility. Additionally, based on previous studies, it is known that the aliphatic polyester dendrimer structure is non-toxic and biocompatible.[21] However, the tedious step-wise synthesis of these macromolecules limited the achievable molecular weights (MWs) to approximately

20 kDa, which is well below the MW cutoff for renal filtration, known to be in the range of 30-50 kDa.[22] To overcome this limitation, we decided to investigate the synthesis of a similar class of branched macromolecules that can reach MWs greater than 50 kDa using an easier synthetic approach. This can be achieved by combining a classic polymerization method with the divergent dendrimer synthesis to make carborane containing dendronized polymers, as depicted in Figure 2.1.

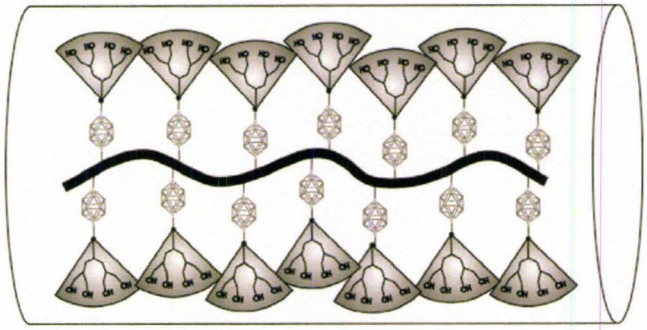

Figure 2.1. Schematic representation of carborane-loaded dendronized polymer.

Dendronized polymers[23] represent an interesting new class of macromolecules that have a unique cylindrical shape and can exhibit a large number of functionalizable groups at their periphery.[24] The growth of aliphatic polyester dendrons from linear polymer backbones to produce water soluble dendronized polymers has recently been reported.[24-27]

Here, we present the synthesis and characterization of carborane-containing dendronized polymers based on the same aliphatic polyester dendritic units, as a new addition to the family of macromolecules with promising properties for BNCT

applications. As far as the authors know, this is the first report on carborane-containing dendronized polymers, combining high MW (> 50 kDa), water solubility, high boron content, and a low polydispersity index (PDI).

2.2. Results and Discussion

2.2.1. Synthesis and polymerization of carborane-functionalized monomers

The preparation of dendronized polymers can be carried out in a number of ways, including (a) polymerization of dendron-functionalized macromonomers, (b) grafting of dendrons to a linear polymer backbone or (c) the divergent dendronization of appropriately functionalized linear polymers. We initially chose to use a combination of methods (a) and (c), where a low-generation dendritic monomer is first polymerized and then dendronized to higher generations. To accomplish this, we treated *p*-carborane with two equiv. of *n*-butyllithium (*n*-BuLi) in THF, followed by treatment with two equiv. of trimethylene oxide to give *p*-dihydroxypropyl carborane (**2.1**) in 90% yield after acidic work-up and crystallization of the crude product from chloroform (Scheme 2.1).[20] The resulting diol (**2.1**) was treated with one equiv. of the highly reactive benzylidene-protected anhydride of bis-MPA (**2.2**), which was synthesized in two steps following a literature procedure.[28] The resulting mono-functionalized hydroxyl carborane (**2.3**) was isolated in 50% yield after purification by column chromatography. Further treatment of (**2.3**) with one equiv. of acryloyl chloride gave the [G1]-(Bn) acrylate monomer (**2.4**) in 98% yield after purification by column chromatography (Scheme 2.1).

Scheme 2.1. Synthesis of [G1]-(Bn)-dendronized acrylate polymer, DMAP = 4-dimethylaminopyridine

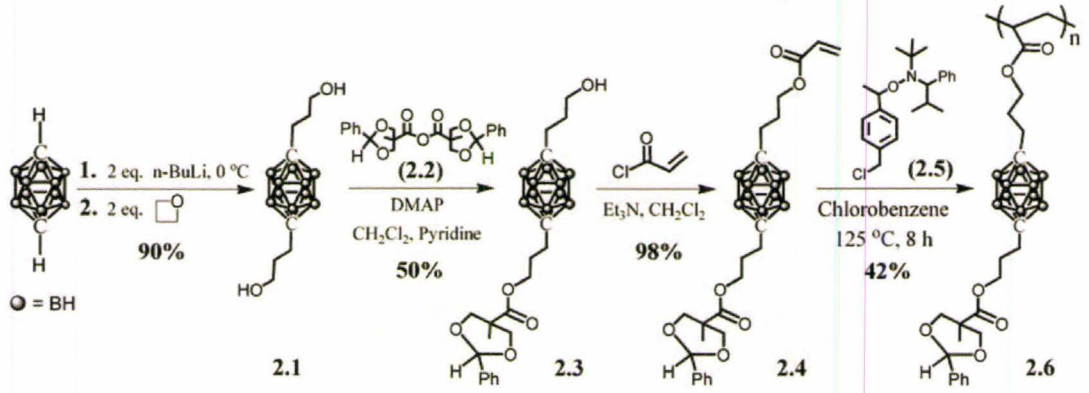

With monomer (**2.4**) in hand, polymerization was attempted using the nitroxide-mediated polymerization (NMP) strategy. This was done by heating the universal alkoxyamine initiator (**2.5**), initially reported by Hawker and coworkers,[29] to 125°C in the presence of monomer **2.4**, using chlorobenzene as the solvent. Unfortunately, the polymers obtained using this methodology were bimodal in nature, with size exclusion chromatography (SEC) data indicating the presence of high MW (M_w > 280 kDa) main peaks and low MW (M_w < 7 kDa) shoulders. Attempts to optimize the polymerization conditions by varying the reaction time and monomer concentration all failed to give a well-defined polymer with low PDI (Table 2.1).

Table 2.1. Results from polymerization of monomer **2.4** by nitroxide-mediated polymerization (NMP) using various conditions.

Monomer: Initiator Ratio	[Monomer] (M)	Reaction time (h)	Temperature* (°C)	Polymer nature	M_w† (g/mol)	Polydispersity index (PDI)
40:1	0.4	1	125	Broad	27,000	2.4
40:1	0.4	8	125	Broad	28,000	2.0
40:1	0.4	12	125	Multimodal	54,000	3.4
40:1	0.9	1	125	Multimodal	14,000	1.4
40:1	0.9	8	125	Multimodal	45,000	2.6
40:1	1.5	1	125	Broad	54,000	1.6
40:1	1.5	8	125	Broad	280,000	2.5

* All polymerizations were conducted in chlorobenzene.
† Weight average molecular weight (M_w) from size exclusion chromatography (SEC) using polystyrene standards.

Having been unsuccessful in the production of well-defined polymers from the acrylate monomer **2.4**, we turned our attention to the preparation of an analogous styrene functionalized *p*-carborane monomer (**2.7**) (Scheme 2.2). From previous studies, we have already shown that NMP of a styrene-functionalized *o*-carborane gave a well defined polymer with PDI < 1.1,[18] and we reasoned that similar results could be obtained with the *p*-carborane analog.

Scheme 2.2 Synthesis of carborane-functionalized styrene monomer, THF = tetrahydrofuran.

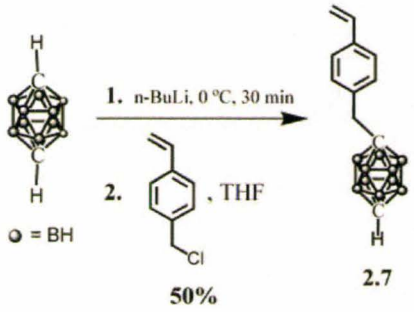

The synthesis of monomer (**2.7**) was again accomplished by deprotonating *p*-carborane with *n*-BuLi (1.0 equiv.) in THF to give a statistical mixture of three components, including a monoanion, a dianion, and the starting material.[20] This mixture was then treated with 1 equiv. of 4-vinylbenzyl chloride to give the *p*-carborane functionalized monomer (**2.7**) in 50% yield after purification by column chromatography using hexanes as the eluent.

Contrary to the results with monomer **2.4**, this styrenic monomer was successfully polymerized by NMP to give a well-defined polymer (**2.9**) that could be subsequently dendronized (Scheme 2.3). The polymerization involved 80 equiv. of monomer (**2.7**) in the presence of 1 equiv. of the alkoxyamine initiator (**2.5**), a catalytic amount of the free nitroxyl radical (**2.8**) (0.05 equiv.), and acetic anhydride (1.8 equiv.). After degassing under N_2 for 1 h, the polymerization was carried out for different time periods at 125°C. We have found that high MWs (> 16 kDa) and low PDIs (< 1.1) were afforded with a monomer concentration of 5.0 M and a polymerization time of 7 h, producing polymers in greater than 90% yield (Table 2.2, bold entry). Other conditions, where the monomer concentration was decreased or the monomer to initiator ratio was varied, resulted in either lower molecular weights or broader molecular weight distributions (Table 2.2). We refer to the polymerization of monomer **2.7** by NMP as *Route A*. After this successful polymerization, dendronization of carborane-loaded poly(styrene) (CPS, **2.9**) to higher generations was achieved using the divergent dendrimer growth, as detailed below.

Scheme 2.3. Synthesis of [G-1]-$(OH)_2$ to [G-4]-$(OH)_{16}$-dendronized polymers.

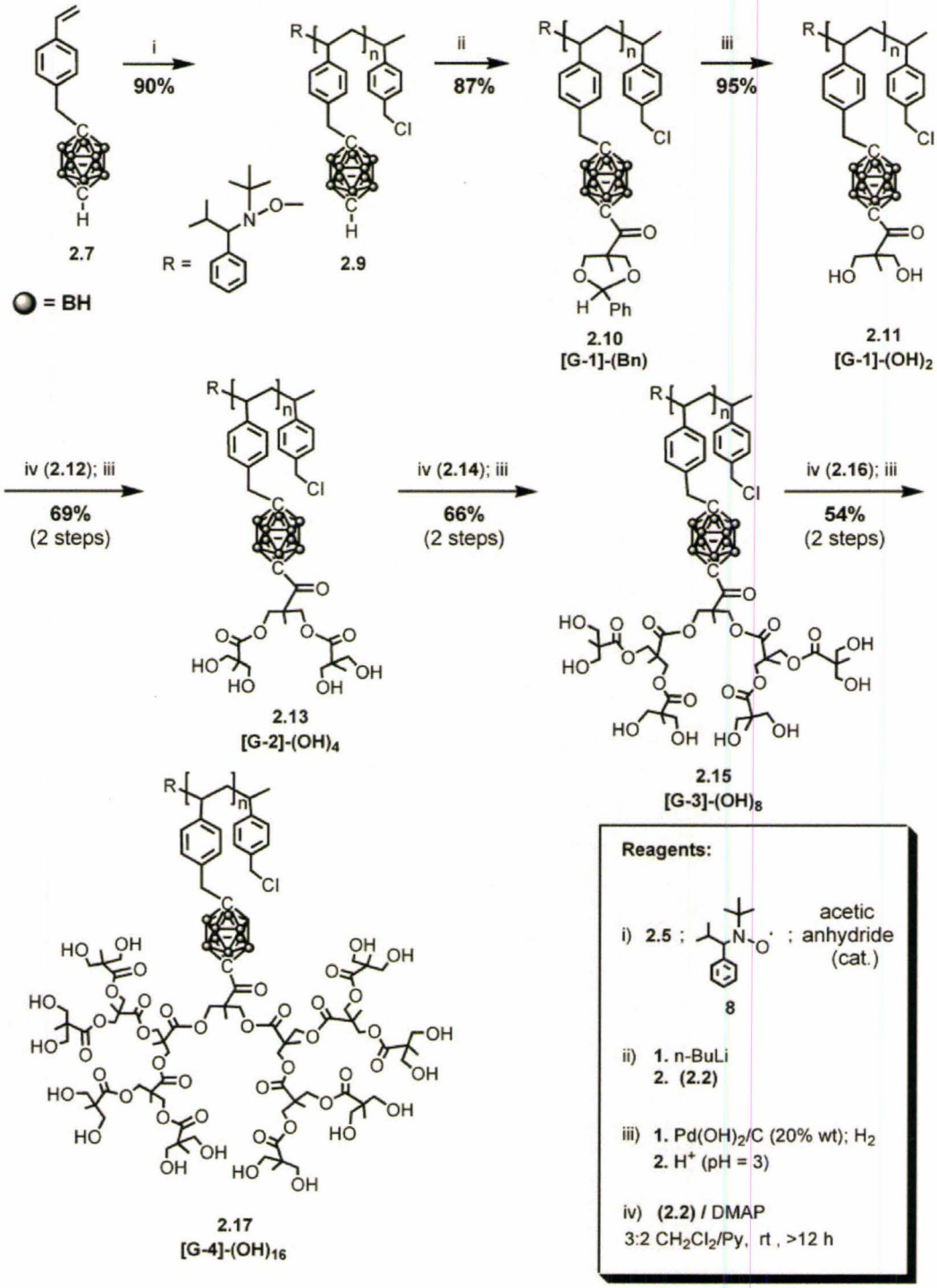

Table 2.2. Results from polymerization of monomer **2.7** by nitroxide-mediated polymerization (NMP) using various conditions.

Monomer: Initiator Ratio	[Mono-mer] (M)	Reaction Time (h)	Tempera-ture* (°C)	Polymer Nature	M_w† (g/mol)	Polydispersity index (PDI)
40:1	1.5	3	125	Monomodal	3,000	1.08
40:1	1.5	5	125	Monomodal	4,500	1.10
40:1	1.5	7	125	Monomodal	6,000	1.12
40:1	1.5	9	125	Monomodal	7,000	1.11
40:1	1.5	24	125	Monomodal	8,500	1.23
100:1	3.8	8	125	Monomodal	16,000	1.25
100:1	3.8	10	125	Broad	17,000	1.30
100:1	3.8	12	125	Broad	21,500	1.45
80:1	3.8	7	125	Monomodal	12,000	1.08
80:1	**5.0**	**7**	**125**	**Monomodal**	**15,000**	**1.10**
80:1	5.0	10	125	Monomodal	16,000	1.25
80:1	5.0	12	125	Broad	22,000	1.40

* All polymerizations were conducted in chlorobenzene.
† Weight average molecular weight (M_w) from size exclusion chromatography (SEC) using polystyrene standards.

2.2.2. Dendronization of the pre-formed linear carborane-functionalized polymer

The [G1]-(Bn) dendronized polymer was prepared utilizing the "grafting from" approach. The carborane loaded polymer (**2.9**) was first treated with a stoichiometric quantity of *n*-BuLi, relative to the number of carborane units in the polymer. The resulting polyanion was subsequently reacted with excess benzylidene-protected anhydride (**2.2**) to afford the [G1]-(Bn) dendronized polymer with approximately 70% functionalization. The key to this dendronization step was optimization of the polymer concentration prior to reaction with *n*-BuLi to give the polyanion. It was found that when the reaction was carried out at polymer concentrations greater than 0.6 mM, the high anion concentration resulted in precipitation of the polymer and a final product having a

bimodal MW distribution. However, at lower concentrations, precipitation of the polyanion was not observed and the isolated product remained well-defined. The degree of dendronization was determined by comparison of the ^{1}H NMR of the polymer prior to and after reaction with anhydride **2.2**. The ratio of the aromatic (styrene) protons (δ = 6.2-6.6 ppm) from the polymer backbone to the aliphatic protons in the benzylidene protecting groups of the dendron (δ = 5.4 ppm), gave the percentage of carborane units functionalized with the [G1]-(Bn) group, which was found to be approximately 70% (Figure 2.2).

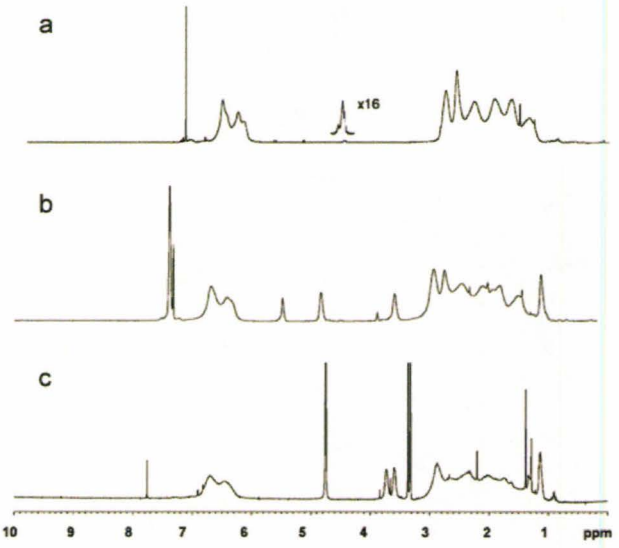

Figure 2.2. ^{1}H NMR of a) polymer **2.9**, b) [G-1]-(Bn)-dendronized polymer **2.10**, c) [G-1]-$(OH)_2$-dendronized polymer **2.11**.

Dendron growth was carried out to the fourth generation using an iterative deprotection and esterification approach. Removal of the benzylidene protecting groups

in the dendronized polymers was carried out using a Pd-catalyzed hydrogenolysis with PdOH/C (20%, wt) in a 1:1 solution of CH_2Cl_2/methanol with typical yields greater than 95%. Although deprotection of low MW dendronized polymers can be achieved in quantitative yields, it was found that this reaction leads to a bimodal MW distribution and significant MW broadening at higher generations. Similar results were reported by Yoshida *et al.* in the divergent synthesis of dendronized poly(hydroxystyrene) with very high MW.[24] It was reported that trans acetalization by-products were responsible for this effect, and they could be removed by carrying out the deprotection under homogenous acid-catalyzed conditions instead of hydrogenolysis. However, several iterations to achieve quantitative yields were required.[24,20] In our study, we found it more efficient to carry out a near quantitative Pd-catalyzed deprotection first, followed by the acid-catalyzed deprotection using H_2SO_4 (2% v/v) in THF/MeOH (4:3 v/v), as this allowed for a total reaction time of less than 24 h. This treatment was followed by neutralization of the excess acid with ammonia, and the products were isolated in nearly quantitative yields after several washings with THF/MeOH (9:1) to remove all the ammonium sulfate salt that was generated. The deprotection reaction was followed by NMR (^1H, ^{13}C, 600 MHz) and SEC analysis to verify the completion of the reaction. This was indicated by the absence of proton signals from the benzylidene protecting group in the ^1H NMR, as well as the absence of any high MW shoulder in the SEC analysis, which is a result of intermolecular coupling of polymer chains.

Achieving complete deprotection is a key step to the successful synthesis of well-defined high generation dendronized polymers. This is clearly shown in Figure2.3, which

depicts the major difference between the dendronized polymers obtained following an incomplete deprotection using hydrogenolysis alone, and the polymers obtained when the deprotection was driven to completion using the acid-catalyzed conditions described above. In the former case, SEC analysis indicated that, beyond the second generation, significant shoulders at high MW (corresponding to double, triple, and quadruple the MWs of the major peak) were formed (Figure 2.3.a). However, as illustrated in Figure 2.3b, the polymers obtained following complete deprotection using the acid-catalyzed second step were well-defined, with no presence of shoulders at higher MWs. These results confirm that the origin of the aforementioned by-products was the incomplete removal of benzylidene groups prior to dendron growth.

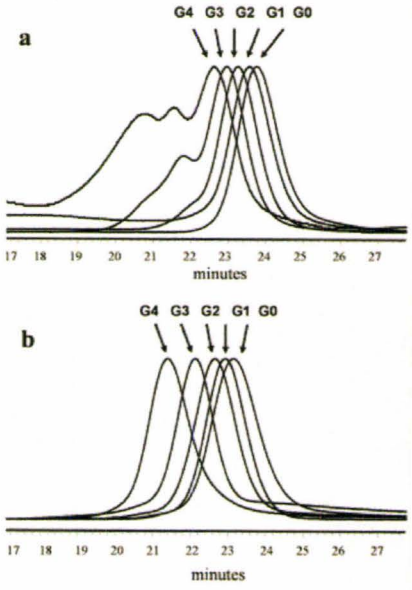

Figure 2.3. Size exclusion chromatography (SEC) analysis of [G0] – [G4]-benzylidene protected polymers having performed generation growth after Pd-catalyzed deprotection only (a), and Pd-catalyzed deprotection followed by acid-catalyzed deprotection (b).

2.2.3. Molecular weight determination by SEC

In this study, SEC was used to evaluate the molecular weight of the carborane containing dendronized polymers. The observed weight average molecular weight (M_w, PS standard) and PDIs obtained by SEC are summarized in Table 2.3. The underestimation of the M_w by SEC, leading to a large discrepancy between the theoretical MW values and SEC derived values, is caused by the significant difference in the hydrodynamic radii of the dendronized polymers, with their compact rod-like architecture, as compared to the linear poly(styrene) (PS) standards used to calibrate the instrument. As has been previously observed, this effect becomes more pronounced for the higher generation dendronized polymers, where the observed MWs were significantly lower than the theoretical values (Table 2.3).[24] These results show the limitations of SEC for the characterization of these materials, requiring the utilization of NMR analysis to obtain a more accurate estimation of the MW. The MW evaluation from ^{1}H NMR was achieved by comparing the integration of the two chloromethyl protons (δ = 4.5 ppm), initially part of the alkoxyamine initiator (**2.5**), to the aromatic proton signals (δ = 6.0 – 6.8 ppm) originating from the polymer backbone, or to the proton signal of the benzylidene protecting group (δ = 5.4 ppm). The MWs estimated by NMR analysis were found to be in good agreement with the theoretical MWs (Table 2.3).

Table 2.3. Comparison of molecular weights (MWs) determined by size exclusion chromatography (SEC) to the theoretical and NMR calculated MWs.

Compound	Theoretical MW*	SEC (THF)† M_w	PDI	NMR Calc. MW
CPS (**2.9**)	21,000	15,000	1.06	21,000
[G1]-(Bn)-CPS (**2.10**)	37,000	18,000	1.15	32,000
[G1]-$(OH)_2$-CPS (**2.11**)	27,000	13,000	1.09	29,000
[G2]-$(Bn)_2$-CPS (**2.12**)	49,000	20,000	1.14	54,000
[G2]-$(OH)_4$-CPS (**2.13**)	40,000	16,000	1.18	33,000
[G3]-$(Bn)_4$-CPS (**2.14**)	84,000	23,000	1.15	92,000
[G3]-$(OH)_8$-CPS (**2.15**)	65,000	19,000	1.15	74,000
[G4]-$(Bn)_8$-CPS (**2.16**)	153,000	30,000	1.18	164,000
[G4]-$(OH)_{16}$-CPS (**2.17**)	115,000	25,000	1.16	114,000

* Based on the SEC data of (**2.9**)
† Relative to polystyrene standards, THF = tetrahydrofuran.

2.2.4. Water solubility and boron content

The main goal of the present work was to synthesize water soluble carborane-functionalized dendronized polymers with high boron content as potential candidates for BNCT. At low generations (G1-G2), the dendronized polymers were insoluble in water. This lack of water solubility is mainly caused by the highly lipophilic carborane cages and polymer backbone. This effect can be overcome by introducing a large number of hydrophilic groups around each carborane cage to impart an overall water solubility. It was found that solubility in water, at a concentration of 0.5 mg/mL, was achieved at the third generation, with 8 hydroxyl groups per carborane cage. Dendronization to the fourth generation, where 16 hydroxyl groups were appended to each carborane cage, resulted in a solubility of 1 mg/mL in water. This was consistent with our previously reported results on carborane loaded dendrimers, where water solubility (1 mg/mL) was achieved with the

same carborane:OH-group ratio of 1:16.[20] At the fourth generation, the deprotected dendronized polymer ([G4]-$(OH)_{16}$-CPS) had a boron content of 12%, and a MW exceeding 100 kDa, as determined from ^{1}H NMR data.

This approach, although successful in making high MW carborane-containing polymers, was still limited by the incomplete functionalization of the pre-made polymer with the [G1]-(Bn) dendron, which left some of the carborane cages unfunctionalized. In order to solve this issue, a different route to making a fully functionalized carborane containing polymer was adopted. This was accomplished by first synthesizing a G1-dendron-containing macromonomer, and then polymerizing it by NMP to obtain a polymer having the [G1]-(Bn) dendron at every repeat unit. This approach is termed *Route B*. Dendronization of the fully [G1]-(Bn)-functionalized polymer was carried out using the same iterative deprotection and coupling steps described previously in *Route A*.[24,25] Preparation of the [G1]-(Bn)-macromonomer (**2.18**) was accomplished by treating monomer (**2.7**) with 1 equiv. of *n*-BuLi in THF to deprotonate the remaining acidic proton on the carbon vertex (Scheme 2.4). This was followed by reaction of the resulting carbanion with the benzylidene protected anhydride (**2.2**) to yield macromonomer (**2.18**) in nearly quantitative yield after purification by column chromatography using CH_2Cl_2/hexanes (1:1) as the eluent.

Scheme 2.4. Synthesis of [G1]-(Bn) macromonomer.

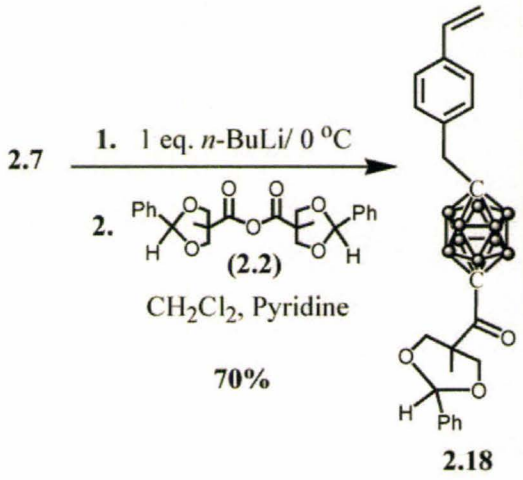

2.2.5. Polymerization of carborane-containing macromonomer

Polymerization of macromonomer **2.18** (80 equiv.) by NMP in the presence of 1 equiv. of the alkoxyamine initiator (**2.5**), catalytic amounts of the free nitroxide radical (**2.8**) (0.05 equiv.), and acetic anhydride (1.8 equiv.), resulted in the formation of well defined, low PDI (< 1.1) polymers having high MWs (> 10 kDa). Best results were achieved with a macromonomer concentration in the range of 0.5-0.7 M and a polymerization time of 7 h. This carborane loaded linear polymer was subsequently dendronized up to the fourth generation using the iterative deprotection and coupling approach described above.

2.2.6. Molecular weight determination

The MWs of the dendronized polymers prepared by *Route B* were determined by SEC and ^{1}H NMR (Table 2.4 and Figure 2.4). Similarly to the previous samples, the

measured SEC values grossly underestimated the polymer MWs, again due to the difference in hydrodynamic volume between the dendronized polymers and the linear PS standards used to calibrate the instrument. Fortunately, ^{1}H NMR measurements, based on the relative integration of the ^{1}H signal corresponding to the two chloromethyl protons (δ = 4.5 ppm), originally part of the alkoxyamine initiator (**2.5**), to the ^{1}H signal corresponding to the benzylidene protecting group proton (δ = 5.4 ppm) again provided closer agreement with the theoretical values (Table 2.4). It should be noted that, due to its lack of solubility in THF, the [G4]-$(OH)_{16}$-CPS could not be characterized by SEC.

Table 2.4. Comparison of molecular weights (MWs) determined by size exclusion chromatography (SEC) to the theoretical and NMR calculated MWs.

Compound	Theoretical MW*	SEC (THF)†		NMR
		M_w	PDI	Calc. MW
[G1]-(Bn)-CPS (**2.19**)	21,000	13,000	1.07	21,000
[G1]-$(OH)_2$-CPS (**2.20**)	17,000	9,500	1.10	17,000
[G2]-$(Bn)_2$-CPS (**2.21**)	35,000	16,000	1.10	36,000
[G2]-$(OH)_4$-CPS (**2.22**)	27,000	13,500	1.20	28,000
[G3]-$(Bn)_4$-CPS (**2.23**)	64,000	20,000	1.18	61,000
[G3]-$(OH)_8$-CPS (**2.24**)	48,000	17,000	1.23	46,000
[G4]-$(Bn)_8$-CPS (**2.25**)	122,000	29,000	1.23	101,000
[G4]-$(OH)_{16}$-CPS (**2.26**)	90,000	N/A	N/A	75,000

* Based on the SEC data of (**2.19**)

† Relative to polystyrene standards, THF = tetrahydrofurane.

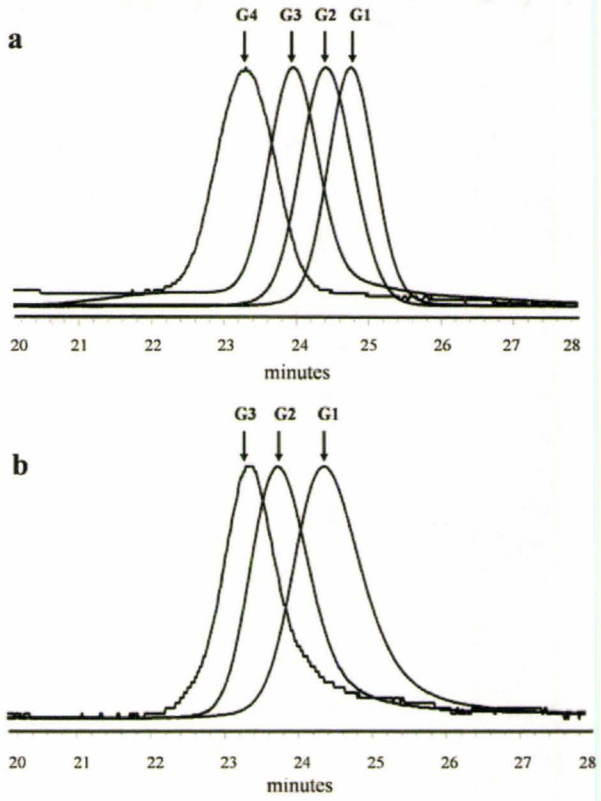

Figure 2.4. Size exclusion chromatography (SEC) analysis of the benzylidene protected G1-G4 series (top), and the deprotected G1-G3 series (bottom) of dendronized polymers.

2.2.7. Water solubility and boron content

The aqueous solubility of the series of polymers prepared by *Route B* was evaluated and compared to the polymer series from *Route A*. It was found that higher solubilities occurred with the polymers synthesized via *Route B* (Table 2.5). Here, a solubility of 1 mg/mL was achieved with the third generation dendronized polymer ([G3]-$(OH)_8$-CPS, **2.24**), and higher concentrations (> 1 mg/mL) were achieved at the fourth generation ([G4]-$(OH)_{16}$-CPS, **2.26**). These results show that when the carborane-loaded

polymer is functionalized with dendrons at each repeat unit, the water solubility is enhanced. The boron content of the fourth generation deprotected dendronized polymer [G4]-$(OH)_{16}$-CPS, prepared using *Route B*, was estimated from ^{1}H NMR to be approximately 8%.

Table 2.5. Solubility in water.

Dendron Generation	**Route A** (mg/mL)	**Route B** (mg/mL)
1	0	0
2	0	0.5
3	0.5	> 1.0
4	> 1.0	> 2.0

2.3. Conclusions

High molecular-weight carborane-containing dendronized polymers were successfully prepared up to the fourth generation by two different approaches. Using the first approach (*Route A*) we were able to achieve approximately 70% functionalization of the carborane-loaded polymer with the first generation dendrons. In the second approach (*Route B*), a fully functionalized dendronized polymer was synthesized by introducing the dendron unit within a macromonomer, followed by polymerization using NMP. Both sets of dendronized polymers were characterized by NMR (^{1}H and ^{13}C) and SEC. It was found that SEC data underestimated polymer MWs, but ^{1}H NMR data closely matched theoretical values. The resulting polymers, having MWs in excess of 50 kDa exhibited water solubility when the OH:carborane ratio exceeded 8:1. Additionally, the fully

dendronized polymers, prepared by *Route B*, exhibited greater solubility than those prepared by *Route A*. However, higher boron content is achieved via *Route A*, where dendronization does not occur at every carborane unit. To our knowledge, this is the first report of the synthesis of well-defined carborane-containing dendronized polymers that exhibit high MW and aqueous solubility. Due to these characteristics, the synthesized polymers may serve as potential agents for BNCT applications, which will be the focus of our future studies.

2.4. Experimental Section

2.4.1. Materials

4-Vinylbenzyl chloride (≥90%), 4-(dimethylamino)pyridine (DMAP, 99%), 2,2-bis(hydroxymethyl) propionic acid (bis-MPA, 98%), benzaldehyde dimethyl acetal (99%), *p*-toluene sulfonic acid-monohydride (*p*-TSAOH, 98%), and n-butyl lithium (2.5M), and palladium hydroxide (20 wt.% Pd/C) were purchased from Sigma-Aldrich. Benzylidene-2,2-bis(oxymethyl)propionic acid and its anhydride were prepared following literature procedures.[30] Dichloromethane (DCM) was distilled under nitrogen from calcium hydride immediately prior to use. Tetrahydrofuran (THF) was passed through two columns of activated molecular sieves using a solvent drying system supplied by MBraun, immediately prior to use. All other reagents were commercially obtained and used without further purification.

2.4.2. Characterization

NMR spectra were measured on Bruker DRX 500 MHz and Avance 600 MHz spectrometers. ^{1}H spectra were recorded at 600 MHz, ^{11}B spectra were recorded at 190 MHz, and ^{13}C NMR spectra were recorded at 150 MHz in $CDCl_3$ or methanol-d_4. The non-deuterated solvent signal was used as the internal standard for both ^{1}H and ^{13}C spectra. Where aliphatic ^{1}H NMR signals from the dendrimer overlap with signals form the B-H in the carborane cage or with the broad polymer signals, an accurate integration could not be assigned. In these cases, theoretical values are provided in parentheses { }. High Resolution Mass spectrometry using Electrospray Ionization (HRMS (EI+)) was conducted for the synthesized monomers on a Micromass Quattro Ultima Triple Quadrupole mass spectrometer using positive ion mode. Elemental analyses were also conducted for the synthesized monomers using a Thermo Flash EA1112 elemental analyzer equipped with a CHN reactor and O reactor. The samples were weighed out on a Mettler-Toledo MX5 balance prior to elemental analysis. Polymer molecular weight and polydispersity index (PDI) were estimated by size exclusion chromatography (SEC) using a Waters 2695 Separations Module equipped with a Waters 2414 refractive index detector and four Polymer Labs PLgel individual pore size columns, with 5 μm bead size and pore sizes of 100 Å, 500 Å, 10^3 Å, and 10^5 Å, kept at 40°C. Polystyrene standards were used for calibration, and tetrahydrofuran (THF) was used as the eluent at a flow rate of 1.0 mL/min.

2.4.3. General procedure for polymer synthesis using nitroxide-mediated polymerization (NMP)

A flame-dried round-bottom flask was charged with *p*-carborane styrene monomer (**2.7**) (1.03 g, 3.95 $\times 10^{-3}$ mol) in chlorobenzene (1.2 mL) under argon. Alkoxyamine initiator (**2.5**) (0.018 g, 4.8 $\times 10^{-5}$ mol), along with catalytic amounts of the free nitroxide radical (**2.8**) (0.3 mL of a 9 mM solution in chlorobenzene, 2.4 $\times 10^{-6}$ mol), and acetic anhydride (8.2 μL, 8.6 $\times 10^{-5}$ mol) were added to the flask charged with monomer **2.7**. The solution was degassed under N_2 for 1 h and heated to 125 °C for 7 h. The polymer was precipitated from methanol as a white solid and recovered by filtration through a glass fritted funnel. The collected solid was dried in a vacuum oven overnight to give **2.9** as a white powder: 0.9 g (90%). ^{1}H NMR (500 MHz, $CDCl_3$): δ (ppm) = 1.2-1.5 (br, ~364 H, $-CH_2CHPh$), 2.1-2.5 (br, ~274 H, $-CHCH_2$), 2.5-2.7 (br, ~228 H, $-CH_2C(BH)_{10}$), 2.7-2.9 (br, ~180 H, $-CH(BH)_{10}$), 4.5 (m, 2 H, $-CH_2PhCl$), 6.3-6.6 (br, ~ 320 H, –Ph). ^{13}C NMR (125 MHz, $CDCl_3$): δ (ppm) = 40.2 ($-CH_2CHPh$), 44.6 ($-CH_2CHPh$) , 58.3 ($-CH_2C(BH)_{10}$), 127.4 ($-CH{=}CCHCH_2$), 129.3 ($-CH{=}CCH_2C(BH)_{10}$), 134.03 ($-CCHCH_2$ and $-CCH_2C(BH)_{10}$). SEC (THF eluent), $M_w = 1.5 \times 10^4$ Da, PDI = 1.06.

2.4.4. General procedure for dendronization of pre-made carborane-loaded polymer

In a flame-dried round-bottom flask, under argon atmosphere, [G0]-polymer (**2.9**) (0.506 g, 3.37 $\times 10^{-5}$ mol) was introduced as a solution in THF (52 mL). The solution was cooled to 0 °C, followed by a slow addition of *n*-BuLi (0.9 mL, 2.2 $\times 10^{-3}$ mol) via a syringe. After 30 min at 0 °C, the solution was warmed up to room temperature, the

benzylidene-protected anhydride (**2.2**) (1.2 g, 2.8 $\times 10^{-3}$ mol) was added, and the reaction mixture was stirred for an extra 8 h at room temperature. The polymer was precipitated from methanol and recovered by filtration through a glass fritted funnel. After drying in a vacuum oven overnight, the [G1]-(Bn)-dendronized polymer (**2.10**) was obtained as a white powder (0.6 g, 87% yield, and ~70% functionalization). ^{1}H NMR (500 MHz, $CDCl_3$): δ (ppm) = 0.8-1.0 (br, ~176 H, $-CH_3C$), 2.5-2.7 (br, ~344 H, $-CH_2CH$), 2.7-3.0 (br, ~385 H, $-CH_2C(BH)_{10}$), 3.5 (br, ~108 H, $-CH_2OCHPh$), 4.4 (m, 2 H, $-CH_2PhCl$), 4.7 (br, ~92 H, $-CH_2OCHPh$), 5.4 (br, ~54 H, $-CHO_2Ph$), 6.1-6.8 (br, ~320 H, $-PhCH_2C(BH)_{10}$), 7.3 (br, ~245 H, $-PhCHO_2$). ^{13}C NMR (125 MHz, $CDCl_3$): δ (ppm) = 17.5 ($-CH_3C$), 40.2 ($-CH_2CHPh$), 44.6 ($-CH_2CHPh$), 49.7 ($-CH_2C(BH)_{10}$), 73.5 ($-CH_2OCHPh$), 81.8 ($-CH_2CHPh$), 84.7 ($-CCH_3$), 102.2 ($-CHO_2Ph$), 126.4 ($-CH{=}CCH_2C(BH)_{10}$ and $-CH{=}CH{-}CCHO_2$), 128.2 ($-CH{=}CH{-}CCH_2C(BH)_{10}$ and $-CH{=}CCHO_2$), 129.0 ($-CH{=}C{-}CH_2C(BH)_{10}$ and $-CH{=}CH{-}CH{=}CCHO_2$), 137.7 ($-CCHCH_2$ and $-CCHO_2$), 193.6 ($-COC(OCH_2)_2CH_3$). SEC (THF eluent), M_w = 1.8 × 10^4 Da, PDI = 1.15.

2.4.5. General procedure for the Pd-catalyzed deprotection of the benzylidene protecting group

A round-bottom flask was charged with the first generation protected carborane polymer, [G1]-(Bn)-CPS (**2.10**) (0.505 g, 2.81 × 10^{-5} mol), and dissolved in a 1:1 mixture of CH_2Cl_2:methanol. Subsequently, PdOH/C (20%) was added, and the flask was evacuated and back-filled with H_2 three times. The flask was fitted with a H_2 filled

balloon and the reaction mixture was stirred vigorously overnight at room temperature. The catalyst was removed by filtration through a plug of celite and washed with methanol. The filtrate was evaporated to dryness on a rotary-evaporator in vacuo, yielding the desired product as a white foam in quantitative yield (0.47g, 99%).

2.4.6. General procedure for acid-catalyzed deprotection of the benzylidene protecting group

Due to the equilibrium between the benzaldehyde, (or benzaldehyde dimethyl acetal) generated as a deprotection byproduct, and the benzylidene protected dendrons, a small percentage (< 10%) of benzylidene groups usually remained after Pd-catalyzed hydrogenolysis. Therefore, the product was subjected to an acid-catalyzed deprotection to achieve complete removal of the benzylidene group. The partially protected polymer, recovered after the Pd-catalyzed hydrogenolysis (**2.10**) (0.47 g, 2.61×10^{-5} mol), was dissolved in THF/methanol (4:3 v/v, 100 mL) and transferred to a round-bottom flask. Concentrated sulfuric acid (2% v/v. pH 3) was added to the flask, and the solution was allowed to stir overnight (8-12 h) at room temperature. The excess sulfuric acid was neutralized with a 7*N* solution of ammonia in methanol, to precipitate ammonium sulfate as a white solid. The precipitate was removed by filtration, and the filtrate was concentrated in vacuo. The viscous liquid was taken up in THF (G1-G2) or in THF/MeOH (9:1) (G3-G4), and filtered to remove any remaining undissolved ammonium sulfate. This was repeated several times until no further salt was observed. Upon

evaporation of solvent, the resulting viscous oil was dried under vacuum to give the deprotected dendronized polymer as a white foam in quantitative yield.

2.4.7. General procedure for the divergent growth of dendrons

A flame-dried round-bottom flask equipped with a magnetic stir bar (under argon atmosphere) was charged with the hydroxyl-terminated dendronized polymer (generation 1-3) in a mixture of CH_2Cl_2/pyridine (3:2). The benzylidene-protected anhydride of bis-MPA (**2.2**) was introduced along with a catalytic amount of 4-dimethylamino pyridine (DMAP) and the solution was stirred for 12-72 h at room temperature. Then, 2 mL of water was added and the reaction was stirred for an extra 18 h to quench the excess unreacted anhydride. The product was isolated by diluting the mixture with CH_2Cl_2 (100 mL) and washing with 1 M $NaHSO_4$ (3 × 100 mL), 10% Na_2CO_3 (3 × 100 mL), and brine (100 mL). The organic layer was dried over anhydrous $MgSO_4$ and filtered through a glass fritted funnel. The filtrate was evaporated to dryness on a rotary-evaporator in vacuo. The polymer was isolated by precipitation from methanol as a white powder in good yields.

2.4.8. Synthesis of compound 2.3

p-Di-hydroxypropyl carborane (**2.1**)[20] (2.05 g, 7.7×10^{-3} mol) was introduced to a flame-dried round-bottom flask, equipped with a magnetic stir bar (under argon atmosphere), and dissolved in CH_2Cl_2:pyridine (5:1, 50 mL). Benzylidene-protected anhydride (**2.2**) (3.32 g, 7.7×10^{-3} mol) was added, along with a catalytic amount of

DMAP (9.40 g, 7.7×10^{-4} mol), and the reaction mixture was stirred overnight at room temperature under argon. The product of the reaction was a statistical mixture of three components, including a mono-ester, a di-ester, and the starting material. The crude product was separated by column chromatography (CH_2Cl_2:EtOAc, 9:1) to give **2.3** as a white powder: 1.78g (50%). ^{1}H NMR (500 MHz, $CDCl_3$): δ (ppm) = 1.02 (s, 3 H, –CH_3C), 1.41 (m, 2 H, –CH_2CH_2OH), 1.55 (m, 2 H, –CH_2CH_2OCO), 1.75 (m, 4 H, –$CH_2(CH_2)_2OCO$ and –$CH_2(CH_2)_2OH$), 3.48 (t, 2 H, J = 6.21, –CH_2OH), 3.65 (d, 2 H, J = 11.37, –CH_2OCHPh), 4.08 (t, 2 H, J = 6.10, –CH_2OCO), 4.60 (d, 2 H, J = 11.38, –CH_2OCHPh), 5.48 (s, 1H, –CHPh), 7.39 (m, 3H, Ph), 7.42 (m, 2H, Ph). ^{13}C NMR (125 MHz, $CDCl_3$): δ (ppm) = 17.81 (–CH_3C), 28.72 (–$CH_2(CH_2)_2OH$ and –$CH_2(CH_2)_2OCO$), 32.47 (–CH_2CH_2OCO), 34.18 (–CH_2CH_2OH), 42.41 (–CCH_3), 61.84 (–CH_2OH), 63.80 (–CH_2OCO), 73.56 (–CH_2OCHPh), 78.22 (–$C(CH_2)_3OH$), 78.86 (–$C(CH_2)_3OCO$), 101.73 (–CHO_2Ph), 126.21 (–CH=C–CHO_2), 128.20 (–C=CH–CH=CH), 128.97 (–CH=$(CH)_2$), 137.78 (CH=C–CHO_2), 173.78 (C–CO_2–$(CH_2)_3$) . Anal. Calc. C 51.70%; H 7.81%. Found: C 51.98%, H 7.69%. HRMS (EI+) m/z calc. for $C_{20}H_{36}B_{10}O_5$ [M+]: 464.6068, found: 464.6105.

2.4.9. [G1]-(Bn)-dendronized acrylate monomer (2.4)

Acryloyl chloride (0.268 mL, 3.30×10^{-3} mol), along with Et_3N (0.920 mL, 6.60×10^{-3} mol) were added to a flame-dried round-bottom flask, charged with compound **2.3** (1.54 g, 3.30×10^{-3} mol) in 10 mL of CH_2Cl_2 under argon. The reaction mixture was stirred for 2 h at room temperature under argon and monitored by TLC. After completion,

the solvent was evaporated in vacuo to give the crude product as a yellow viscous liquid, which was purified by column chromatography (100% DCM) to give the desired acrylate carborane monomer (**2.4**) as a colorless oil: 0.827 g (98%). ^{1}H NMR (200 MHz, $CDCl_3$): δ (ppm) = 1.0 (s, 3 H, $–CH_3C$), 1.5 (m (br), 4 H, $–CH_2(CH_2)_2OCOCH{=}CH_2$ and $–CH_2(CH_2)_2OCOC$), 1.6 (m (br), 4 H, $–CH_2CH_2OCOCH{=}CH_2$ and $–CH_2CH_2OCOC$), 3.6 (d, 2 H, J = 5.54, $–CH_2OCHPh$), 4.0 (m, 4 H, $–CH_2OCOCH{=}CH_2$ and $–CH_2OCOC$), 4.6 (d, 2 H, J = 5.57, $–CH_2OCHPh$), 5.4 (s, 1 H, –CHPh), 5.8 (d, 1 H, J = 5.12, $–CH_2{=}CHCO_2$), 6.1 (dd, 1 H, J = 5.17, $–CH{=}CH_2$), 6.3 (d, 1 H, J = 8.61, $–CH_2{=}CHCO_2$), 7.3 (m, 5 H, –Ph). ^{13}C NMR (50.3 MHz, $CDCl_3$): δ (ppm) = 17.8 (CH_3–C), 28.5 ($–CH_2(CH_2)_2OCOCH{=}CH_2$ and $–CH_2(CH_2)_2OCOC$), 34.0 ($–CH_2CH_2OCOCH{=}CH_2$ and $–CH_2CH_2OCOC$), 42.4 ($–CCH_3$), 63.4 ($–CH_2OCOCH{=}CH_2$), 63.8 ($–CH_2OCOC$), 73.5 ($–CH_2OCHPh$), 101.7 ($–CHO_2Ph$), 125.5 ($–CH{=}CH–CH{=}C–CHO_2$), 126.1 ($–C{=}CH–CH{=}CH$), 128.2 ($–CH{=}C–CHO_2$), 128.9 ($–CH{=}C–CHO_2$), 136.1 ($–CH_2{=}CHCO_2$), 137.7 ($–CH_2{=}CHCO_2$), 167.1 ($–CH_2{=}CHCO_2$), 173.7 ($–CH_3CCO_2(CH_2)_3$). Anal. Calc. C 53.26 %, H 7.38 %. Found: C 53.36 %, H 7.54 %. LRMS (EI+) m/z calc. for $C_{23}H_{38}B_{10}O_6$ [M+]: 518.65, found: 518.72.

2.4.10. [G1]-(Bn)-dendronized acrylate polymer (2.6)

The alkoxyamine initiator (**2.5**) (0.007 g, 1.93×10^{-5} mol), along with catalytic amounts of the free nitroxide radical (**2.8**) (0.1 mL of a 9.08 mM solution in chlorobenzene, 9.6×10^{-7} mol), and acetic anhydride (3.30 μL, 3.5×10^{-5} mol) were added to a flame-dried round-bottom flask charged with macromonomer **2.4** (0.407 g,

7.85×10^{-4} mol) in chlorobenzene (0.4 mL). The solution was degassed under N_2 for 1 h and heated at 125 °C under N_2 for 8 h. The polymer was precipitated from methanol, filtered, and dried in a vacuum oven overnight to give **2.6** as a white powder: 0.17 g (42%). SEC (THF eluent), $M_w = 2.8 \times 10^5$ Da, PDI (broad) = 2.5.

2.4.11. [G0]-styrene monomer (2.7)

p-Carborane (3.02 g, 2.1×10^{-2} mol), dissolved in dry THF (150 mL) was introduced in a flame-dried round-bottom flask (under argon atmosphere) equipped with a magnetic stir bar, and the flask was cooled to 0 °C. To this solution, *n*-BuLi (2.5 M) (1.95 mL, 2.1×10^{-2} mol) was added dropwise, and the solution was stirred for 30 min at 0 °C. The solution was allowed to warm up to room temperature, followed by a very slow addition of 4-vinylbenzyl chloride (2.93 mL, 2.1×10^{-2} mol) via a syringe. The solution was stirred for 8 h at room temperature and was monitored by TLC analysis. The solvent was subsequently removed by rotary-evaporation and the crude product was purified by silica-packed column chromatography in straight hexanes to yield the mono-substituted *p*-carborane monomer (**2.7**) as a white solid (2.70 g, 50%). ^{1}H NMR (500 MHz, $CDCl_3$): δ (ppm) = 2.6 (s, {1 H}, $-CH(BH)_{10}$), 2.9 (s, {2 H}, $-CH_2C(BH)_{10}$), 5.25 (d, 1 H, J = 10.81, $-CH_2$=CHPh), 5.75 (d, 1 H, J = 17.48, $-CH_2$=CHPh), 6.7 (dd, 1 H, J = 17.56, $-CH$=CH_2), 6.9 (d, 2 H, J = 8.11, $-CH$=C–CH=CH_2), 7.3 (d, 2 H, J = 7.95, –CH=C–$CH_2C(BH)_{10}$). ^{13}C NMR (125 MHz, $CDCl_3$): δ (ppm) = 44.5 ($-CH_2C(BH)_{10}$), 58.4 ($-CH_2$=CPh), 113.9 ($-CH_2$=CPh), 126.0 ($-CH$=$CCH_2C(BH)_{10}$), 130.0 (–CH=C–

*C*H=CH_2), 136.3 (–*C*–CH=CH_2). Anal. Calc. C 50.74%; H 7.74%. Found: C 49.95%, H 7.88%. HRMS (EI+) m/z calc. for $C_{11}H_{20}B_{10}$ [M+]: 260.2568, found: 260.2545.

2.4.12. [G1]-$(OH)_2$-CPS (2.11)

Deprotection of **2.10** (0.505 g, 2.81×10^{-5} mol) in 20 mL of (1:1) CH_2Cl_2:methanol was carried out, as described in general procedures, for 12 h at room temperature under H_2 atmosphere, followed by acid-catalyzed deprotection using sulfuric acid in THF/methanol for an extra 12 h at room temperature. For the acid-catalyzed deprotection, to a round bottom flask charged with **2.10** (0.500 g, 2.8×10^{-5} mol) in a solution of THF/methanol (4:3 v/v, 100 mL), concentrated sulfuric acid (2% v/v. pH 3) was added and the solution was stirred overnight at room temperature. The excess sulfuric acid was neutralized with a solution of 7*N* ammonia in methanol, and the resulting ammonium sulfate salt was removed following the same method described in general procedures. Upon evaporation of solvent, the resulting viscous oil was dried under vacuum to give polymer **2.11** as a white foam (0.45 g, 95%). ^{1}H NMR (500 MHz, $CDCl_3$): δ (ppm) = 1.1 (br, ~174 H, –CH_3C), 2.6-2.7 (br, ~433 H, –CH_2CHPh and –CHPhCH_2), 2.7-2.8 (br, ~385 H, –CH_2C$(BH)_{10}$), 3.6 (br, ~115 H, –CH_2OH), 3.96 (br, ~119 H, –CH_2OH), 6.0-6.8 (br, ~320 H, –Ph). ^{13}C NMR (125 MHz, $CDCl_3$): δ (ppm) = 16.1 (–*C*H_3C), 29.7 (–*C*H_2CHPh), 40.1 (–CH_2*C*HPh), 44.5 (–*C*H_2C$(BH)_{10}$), 53.3 (–*C*CH_3), 58.3 (–C*C*H_2OH), 126.3 (–*C*H=CH–$CCH_2(BH)_{10}$), 129.5 (–CH=*C*H–$CCH_2(BH)_{10}$), 134.0 (–CH=CH–*C*$CH_2(BH)_{10}$), 194.1 (–*C*OCCH_3). SEC (THF, eluent), $M_w = 1.3 \times 10^4$ Da, PDI = 1.09.

2.4.13. [G2]-$(Bn)_2$-CPS (2.12)

The coupling was carried out, as described in general procedures, using [G1]-$(OH)_2$-CPS (**2.11**) (0.407 g, 3.13×10^{-5} mol), benzylidene-protected anhydride (**2**) (0.851 g, 1.99×10^{-3} mol), and DMAP (0.25 mL of a 10 mM solution in CH_2Cl_2, 2.5×10^{-6} mol) in a solution of 3:2 CH_2Cl_2/pyridine (25 mL), and stirring for 24 h at room temperature. After quenching, washing, precipitation, and drying, polymer **2.12** was isolated as a white powder (0.6 g, 70%). ^{1}H NMR (500 MHz, $CDCl_3$): δ (ppm) = 0.9 (br, ~403 H, $-CH_3C$, peripheral), 1.2 (br, ~264 H, $-CH_3C$, internal), 2.5-2.7 (br, ~405 H, $-CH_2CH$), 2.7-3.0 (br, ~385 H, $-CH_2C(BH)_{10}$), 3.6 (br, ~264 H, $-CH_2OCHPh$), 4.3 (br, ~116 H, $-CH_2OCHPh$), 4.4 (br, ~136 H, $-CH_2OCHPh$), 4.5 (br, ~242 H, $-CH_2OCHPh$), 5.4 (br, ~120 H, $-CHO_2Ph$), 6.0-6.8 (br, ~320 H, $-PhCH_2C(BH)_{10}$), 7.3 (br, ~190 H, $-PhCHO_2$), 7.4 (br, ~110 H, $-PhCHO_2$). ^{13}C NMR (125 MHz, $CDCl_3$): δ (ppm) = 17.6 ($-CH_3C$, peripheral), 23.46 (CH_3C, internal), 42.5 ($-CH_2CHPh$), 53.9 ($-CH_2CHPh$), 58.3 ($-CH_2C(BH)_{10}$), 64.5 ($-CH_2OCHPh$), 73.3 ($-CH_2OCHPh$), 81.8 ($-CH_2CHPh$), 84.54 ($-CCH_3$), 86.35 ($-CCH_3$), 101.7 ($-CHO_2Ph$) , 126.2 ($-CH{=}CCH_2C(BH)_{10}$ and $-CH{=}CH-CCHO_2$), 128.1 ($-CH{=}CH-CCH_2C(BH)_{10}$ and $-CH{=}CCHO_2$), 128.8 ($-CH{=}C-CH_2C(BH)_{10}$ and $-CH{=}CH-CH{=}CCHO_2$), 129.3 ($-CH{=}C-CH_2C(BH)_{10}$), 134.1 ($-CH{=}CH-CH{=}CCHO_2$), 137.8 ($-CCHCH_2$ and $-CCHO_2$), 172.9 ($-COC(OCH_2)_2CH_3$, internal), 193.7 ($-COC(OCH_2)_2CH_3$, peripheral). SEC (THF, eluent), $M_w = 2.0 \times 10^4$ Da, PDI = 1.14.

2.4.14. [G2]-$(OH)_4$-CPS (2.13)

Deprotection of **2.12** (0.510 g, 2.55×10^{-5} mol) in 20 mL of (1:1) CH_2Cl_2:methanol was carried out, as described in general procedures, using both hydrogenolysis and acid-catalyzed deprotection. The polymer (**2.13**) was recovered as a white foam (0.3 g, 99%). ^{1}H NMR (500 MHz, $CDCl_3$): δ = 1.1 (br, ~430 H, $-CH_3C$), 2.6-2.7 (br, ~392 H, $-CH_2CHPh$ and $-CHPhCH_2$), 2.7-3.0 (br, ~385 H, $-CH_2C(BH)_{10}$), 3.5-3.7 (br, ~502 H, $-CH_2OH$), 4.2-4.3 (br, ~198 H, $-CH_2OH$), 6.0-6.8 (br, ~320 H, –Ph). ^{13}C NMR (125 MHz, $CDCl_3$): δ (ppm) = 16.0 ($-CH_3C$), 17.0 ($-CH_3C$), 29.0 ($-CH_2CHPh$), 40.1 ($-CH_2CHPh$), 44.5 ($-CH_2C(BH)_{10}$), 50.2 ($-CCH_3$), 53.8 ($-CCH_3$), 58.8 ($-CCH_2OH$), 64.4 ($-CCH_2OH$), 126.5 ($-CH{=}CH-CCH_2(BH)_{10}$), 129.3 ($-CH{=}CH-CCH_2(BH)_{10}$), 134.0 ($-CH{=}CH-CCH_2(BH)_{10}$), 175.4 ($-COCCH_3$), 194.1 ($-COCCH_3$). SEC (THF, eluent), $M_w = 1.6 \times 10^4$ Da, PDI = 1.18.

2.4.15. [G3]-$(Bn)_4$-CPS (2.14)

The coupling was carried out as described in general procedures, using [G2]-$(OH)_4$-CPS (**2.13**) (0.208 g, 1.30×10^{-5} mol), benzylidene-protected anhydride (**2.2**) (0.600 g, 1.41×10^{-3} mol), and DMAP (8.2 μL of a solution of 10 mM in CH_2Cl_2, 8.1×10^{-7} mol) in a solution of 3:2 CH_2Cl_2/pyridine (30 mL), and stirring at room temperature for 48 h. upon quenching, washing, precipitation, and drying, polymer **2.14** was isolated as a white powder (0.3 g, 67% yield). ^{1}H NMR (500 MHz, $CDCl_3$): δ (ppm) = 0.9 (br, ~976 H, $-CH_3C$, peripheral), 1.1 (br, ~486 H, $-CH_3C$, internal), 1.5 (br, ~422 H, $-CH_3C$, internal), 2.7-3.0 (br, ~138 H, $-CH_2C(BH)_{10}$), 3.6 (br, ~521 H, $-CH_2OCHPh$), 3.7 (br,

117 H, –CH_2OCHPh), 3.8-4.1 (br, 182 H, –CH_2OCHPh), 4.4 (br, ~501 H, –CH_2OCHPh), 4.6 (br, ~516 H, –CH_2OCHPh), 5.4 (br, ~261 H, –CHO_2Ph), 6.0-6.8 (br, ~320 H, –$PhCH_2C(BH)_{10}$), 7.3 (br, ~1008 H, –$PhCHO_2$), 7.4 (br, ~612 H, –$PhCHO_2$). ^{13}C NMR (125 MHz, $CDCl_3$): δ (ppm) = 16.0 (–CH_3C, peripheral), 17.0 (CH_3C, internal), 19.0 (CH_3C, internal), 29.0 (–CH_2CHPh), 50.8 (–CH_2CHPh), 53.8 (–CH_2CHPh), 58.0 (–$CH_2C(BH)_{10}$), 64.4 (–CH_2OCHPh), 75.0 (–CH_2OCHPh), 101.7 (–CHO_2Ph), 126.0 (–$CH{=}CCH_2C(BH)_{10}$ and –$CH{=}CH{-}CCHO_2$), 128.2 (–$CH{=}CH{-}CCH_2C(BH)_{10}$ and –$CH{=}CCHO_2$), 129.0 (–$CH{=}C{-}CH_2C(BH)_{10}$ and –$CH{=}CH{-}CH{=}CCHO_2$), 134.0 (–$CH{=}CH{-}CH{=}CCHO_2$), 137.8 (–$CCHCH_2$ and –$CCHO_2$), 172.9 (–$COC(OCH_2)_2CH_3$, internal), 193.7 (–$COC(OCH_2)_2CH_3$, peripheral). SEC (THF, eluent), $M_w = 2.3 \times 10^4$ Da, PDI = 1.15.

2.4.16. [G3]-$(OH)_8$-CPS (2.15)

Deprotection of **2.14** (0.210 g, 9.13 x 10^{-6} mol) was carried out, as described in general procedures, using both hydrogenolysis and acid-catalyzed deprotection. For hydrogenolysis, 20 mL of (1:1) CH_2Cl_2:methanol was used with a reaction time of 12 h. After acid-catalyzed deprotection in THF/methanol (4:3 v/v), the polymer (**2.15**) was recovered as a white foam (0.10 g, 99%). ^1H NMR (500 MHz, $CDCl_3$): δ (ppm) = 1.1 (br, ~886 H, –CH_3C), 1.2 (br, ~764 H, –CH_3C), 2.7-2.9 (br, ~325 H, –$CH_2C(BH)_{10}$), 3.6 (br, ~ 1054 H, –CH_2OH), 4.1-4.3 (br, ~500 H, –CH_2OH), 6.0-6.8 (br, ~320 H, –Ph). ^{13}C NMR (125 MHz, $CDCl_3$): δ (ppm) =16.0 (–CH_3C), 17.0 (–CH_3C), 19.0 (–CH_3C), 29.0 (–CH_2CHPh), 50.2 (–$CH_2C(BH)_{10}$), 54.0 (–CCH_3), 58.0 (–CCH_2OH), 64.2 (–CCH_2OH),

75.0 (–CCH_2OH), 126.2 (–CH=CH–$CCH_2(BH)_{10}$), 128.8 (–CH=CH–$CCH_2(BH)_{10}$), 129.3 (–C=CH–CH=$CCH_2(BH)_{10}$), 137.8 (–CH=CH–$CCH_2(BH)_{10}$), 172.9 (–COCCH$_3$), 193.7 (–COCCH$_3$). SEC (THF, eluent), M_w = 1.9 × 10^4 Da, PDI = 1.15.

2.4.17. [G4]-$(Bn)_8$-CPS (2.16)

The coupling was carried out, as described in general procedures, using [G3]-$(OH)_8$-CPS (**2.15**) (0.102 g, 5.37 x10^{-6} mol), benzylidene-protected anhydride (**2.2**) (1.70 g, 3.99 × 10^{-3} mol), and DMAP (8.1 μL of a 10 mM solution in CH_2Cl_2, 8.1 × 10^{-7} mol) in a solution of 3:2 CH_2Cl_2/pyridine (50 mL), and stirring for 72 h at room temperature. Upon quenching, washing, precipitation, and drying, polymer **2.16** was isolated as a white powder (0.16 g, 56% yield). ^{1}H NMR (500 MHz, $CDCl_3$): δ (ppm) = 0.9 (br, ~776 H, –CH_3C, peripheral), 1.1 (br, ~704 H, –CH_3C, internal), 2.7-3.0 (br, ~184 H, –$CH_2C(BH)_{10}$), 3.6 (br, ~800 H, –CH_2OCHPh), 4.3 (br, ~873 H, –CH_2OCHPh), 4.6 (br, ~679 H, –CH_2OCHPh), 5.4 (br, ~464 H, –CHO_2Ph), 6.0-6.8 (br, ~320 H, –Ph$CH_2C(BH)_{10}$), 7.3 (br, ~1672 H, –PhCHO_2), 7.4 (br, ~772 H, –PhCHO_2). ^{13}C NMR (125 MHz, $CDCl_3$): δ (ppm) = 16.0 (–CH$_3$C, peripheral), 17.0 (CH$_3$C, internal), 19.0 (CH$_3$C, internal), 29.0 (–CH$_2$CHPh), 50.8 (–CH$_2C$HPh), 53.8 (–CH$_2C$HPh), 58.0 (–CH$_2C(BH)_{10}$), 64.4 (–CH$_2$OCHPh), 75.0 (–CH$_2$OCHPh), 101.7 (–CHO$_2$Ph), 126.0 (–CH=CCH$_2C(BH)_{10}$ and –CH=CH–CCHO$_2$), 128.2 (–CH=CH–CCH$_2C(BH)_{10}$ and –CH=CCHO$_2$), 129.0 (–CH=C–CH$_2C(BH)_{10}$ and –CH=CH–CH=CCHO$_2$), 134.0 (–CH=CH–CH=CCHO$_2$), 137.8 (–CCHCH$_2$ and –CCHO$_2$), 172.9 (–COC(OCH$_2$)$_2$CH$_3$,

internal), 193.7 (–*C*OC(OCH$_2$)$_2$CH$_3$, peripheral). SEC (THF, eluent), M_w = 3.0 × 10^4 Da, PDI = 1.18.

2.4.18. [G4]-(OH)$_{16}$-CPS (2.17)

Deprotection was carried out, as described in general procedures, including both hydrogenolysis and acid-catalyzed deprotection, with **2.16** (0.153 g, 5.10 × 10^{-6} mol) dissolved in 20 mL of 1:1 CH_2Cl_2:methanol. The Polymer (**2.17**) was isolated as a white foam (0.12 g, 97%). ^{1}H NMR (500 MHz, $CDCl_3$): δ (ppm) = 1.1 (br, ~902 H, –CH_3C), 1.2 (br, ~376 H, –CH_3C), 1.3 (br, ~294 H, –CH_3C), 2.7-2.9 (br, ~ 326 H, –CH_2C(BH)$_{10}$), 3.6 (br, ~ 1057 H, –CH_2OH), 4.1-4.3 (br, ~656 H, –CH_2OH), 6.0-6.8 (br, ~320 H, –Ph). ^{13}C NMR (125 MHz, $CDCl_3$): δ (ppm) =16.0 (–*C*H$_3$C), 17.0 (–*C*H$_3$C), 19.0 (–*C*H$_3$C), 29.0 (–*C*H$_2$CHPh), 50.2 (–*C*H$_2$C(BH)$_{10}$), 54.0 (–*C*CH$_3$), 58.0 (–C*C*H$_2$OH), 64.2 (–C*C*H$_2$OH), 75.0 (–C*C*H$_2$OH), 101.7 (–*C*HO$_2$Ph), 126.2 (–*C*H=CH–CCH$_2$(BH)$_{10}$), 128.8 (–CH=*C*H–CCH$_2$(BH)$_{10}$), 129.3 (–*C*=CH–CH=CCH$_2$(BH)$_{10}$), 137.8 (–CH=CH–*C*CH$_2$(BH)$_{10}$), 172.9 (–*C*OCCH$_3$) , 193.7 (–*C*OCCH$_3$). SEC (THF, eluent), M_w = 2.5 × 10^4 Da, PDI = 1.16.

2.4.19. [G1]-(Bn)-functionalized monomer (2.18)

A solution of monomer **2.7** (1.51 g, 5.79 × 10^{-3} mol) in THF (150 mL) was added to a flame-dried round-bottom flask (under argon atmosphere) equipped with a magnetic stir bar, and the flask was cooled to 0 °C. To this solution, *n*-BuLi (2.5 M) (0.54 mL, 5.76 × 10^{-3} mol) was added dropwise, and the solution was stirred for 1 h at 0 °C. The solution

was warmed up to room temperature and benzylidene anhydride (**2.2**) (2.45 g, 5.76×10^{-3} mol) was added. The solution was stirred for an extra 8 h at room temperature. Once TLC analysis showed no further change in the reaction product, the solvent was removed by rotary-evaporation and the crude product was purified by column chromatography on silica (CH_2Cl_2:Hexanes, 1:1) to yield the [G1]-(Bn)-functionalized macromonomer (**2.18**) as a white solid (1.85 g, 70%). ^{1}H NMR (500 MHz, $CDCl_3$): δ (ppm) = 0.9 (s, 3 H, –CH_3C), 2.9 (s, 2 H, –CH_2C(BH)$_{10}$), 3.4 (d, 2 H, J = 5.78, –CH_2OCHPh), 4.7 (d, 2 H, *J* = 5.78, –CH_2OCHPh), 5.2 (d, 1 H, *J* = 5.47, –*cis*-CH_2=CHPh), 5.4 (s, 1 H, –CHO_2Ph), 5.7 (d, 1 H, *J* = 8.77, –*trans*-CH_2=CHPh), 6.7 (dd, 1 H, *J* = 5.44, –CH=CH_2), 6.9 (d, 2 H, *J* = 4.04, –CH=C–CH=CH_2), 7.3 (m(br), 7 H, –PhCH_2C(BH)$_{10}$ and –PhCHO_2). ^{13}C NMR (125 MHz, $CDCl_3$): δ 17.4 (–*C*H_3C), 43.9 (–*C*H_2C(BH)$_{10}$), 49.7 (–*C*CH_3), 73.5 (–*C*H_2OCHPh), 102.2 (–*C*HO_2Ph), 114.0 (–*C*H_2=CPh), 126.3 (–*C*H=CCH=CH_2), 128.2 (–*C*H=CCH_2C(BH)$_{10}$), 129.9 (–CH=*C*–CH=CH_2), 136.3 (–CH_2=*C*Ph), 194.8 (–*C*OC$(OCH_2)_2CH_3$). Anal. Calc. C 59.46 %; H 6.94 %. Found : C 58.61%, H 7.07%. LRMS (EI+) m/z calc. for $C_{23}H_{32}B_{10}O_3$ [M+]: 464.33, found: 464.34.

2.4.20. [G1]-(Bn)-CPS (2.19)

The alkoxyamine initiator (**2.5**) (0.005 g, 1.35×10^{-5} mol), along with catalytic amounts of the free nitroxide radical (**2.8**) (0.1 mL of a 9.08 mM solution in chlorobenzene, 6.7×10^{-7} mol), and acetic anhydride (2.3 μL, 2.4×10^{-5} mol) were added to a flame-dried round-bottom flask charged with macromonomer **2.18** (0.504 g, 1.21×10^{-3} mol) in chlorobenzene (2.0 mL). The solution was degassed under N_2 for 1 h and

heated at 125 °C under N_2 for 7 h. The polymer was precipitated from methanol, filtered, and dried in a vacuum oven overnight to give **2.19** as a white powder: 0.4 g (80%). ^{1}H NMR (500 MHz, $CDCl_3$): δ (ppm) = 0.8-1.0 (br, ~160 H, $-CH_3C$), 2.5-2.7 (br, ~240 H, $-CH_2CHPh$), 2.7-3.0 (br, ~265 H, $-CH_2C(BH)_{10}$), 3.5 (br, ~112 H, $-CH_2OCHPh$), 4.4 (m, 2 H, $-CH_2OCHPh$), 4.7 (br, ~102 H, $-CH_2OCHPh$), 5.4 (br, ~50 H, $-CHO_2Ph$), 6.1-6.8 (br, ~220 H, $-PhCH_2C(BH)_{10}$), 7.3 (br, ~245 H, $-PhCHO_2$). ^{13}C NMR (125 MHz, $CDCl_3$): δ (ppm) = 17.5 ($-CH_3C$), 40.2 ($-CH_2CHPh$), 44.6 ($-CH_2CHPh$), 49.7 ($-CH_2C(BH)_{10}$), 58.4 ($-CH_2CHPh$), 73.5 ($-CH_2OCHPh$), 81.8 ($-CH_2CHPh$), 84.7 ($-CCH_3$), 102.2 ($-CHO_2Ph$), 126.4 ($-CH{=}CCH_2C(BH)_{10}$ and $-CH{=}CH-CCHO_2$), 128.2 ($-CH{=}CH-CCH_2C(BH)_{10}$ and $-CH{=}CCHO_2$), 129.0 ($-CH{=}C-CH_2C(BH)_{10}$ and $-CH{=}CH-CH{=}CCHO_2$), 137.7 ($-CCHCH_2$ and $-CCHO_2$), 193.6 ($-COC(OCH_2)_2CH_3$). SEC (THF eluent), $M_w = 1.3 \times 10^4$ Da, PDI = 1.08.

2.4.21. [G1]-$(OH)_2$-CPS (2.20)

Deprotection of **2.19** (0.303 g, 2.3×10^{-5} mol) in 30 mL of (1:1) CH_2Cl_2:methanol was accomplished by hydrogenolysis and acid-catalyzed deprotection as described in general procedures. The polymer (**2.20**) was recovered as a white foam (0.26 g, 96%). ^{1}H NMR (500 MHz, $CDCl_3$): δ (ppm) = 1.1 (br, ~145 H, $-CH_3C$), 2.7-3.0 (br, ~255 H, $-CH_2C(BH)_{10}$), 3.6 (br, ~108 H, $-CH_2OH$), 3.7 (br, ~98 H, $-CH_2OH$), 6.0-6.8 (br, ~220 H, –Ph). ^{13}C NMR (125 MHz, $CDCl_3$): δ (ppm) = 16.1 ($-CH_3C$), 29.7 ($-CH_2CHPh$), 40.1 ($-CH_2CHPh$), 44.5 ($-CH_2C(BH)_{10}$), 53.3 ($-CCH_3$), 58.3 ($-CCH_2OH$), 126.3 ($-CH{=}CH-$

$CCH_2(BH)_{10}$), 129.5 (–CH=*C*H–$CCH_2(BH)_{10}$), 134.0 (–CH=CH–*C*$CH_2(BH)_{10}$). SEC (THF, eluent), $M_w = 9.5 \times 10^3$ Da, PDI = 1.1.

2.4.22. [G2]-$(Bn)_2$-CPS (2.21)

The coupling was carried out, as described in general procedures, using [G1]-$(OH)_2$-CPS (**2.20**) (0.240 g, 2.53×10^{-5} mol), benzylidene-protected anhydride (**2.2**) (0.85 g, 1.99 x 10^{-3} mol), and DMAP (0.23 mL of a 10 mM solution in CH_2Cl_2, 2.25 x 10^{-6} mol) in a solution of 3:2 CH_2Cl_2/pyridine (25 mL), and stirring at room temperature for 24 h. Upon quenching, washing, precipitation, and drying, polymer **2.21** was isolated as a white powder (0.33 g, 90%). ^{1}H NMR (500 MHz, $CDCl_3$): δ (ppm) = 0.9 (br, ~285 H, –CH_3C, peripheral), 1.2 (br, ~128 H, –CH_3C, internal), 2.5-2.7 (br, ~235 H, –$CH_2C(BH)_{10}$), 3.6 (br, ~ 176 H, –CH_2OCHPh), 4.3 (br, ~ 94 H, –CH_2OCHPh), 4.4 (br, ~190 H, –CH_2OCHPh), 4.5 (br, ~102 H, –CH_2OCHPh), 5.4 (br, ~88 H, –CHO_2Ph), 6.0-6.8 (br, ~220 H, –$PhCH_2C(BH)_{10}$), 7.3 (br, ~280 H, –$PhCHO_2$), 7.4 (br, ~150 H, –$PhCHO_2$). ^{13}C NMR (125 MHz, $CDCl_3$): δ (ppm) = 17.6 (–*C*H_3C), 42.5 (–*C*H_2CHPh), 53.9 (–CH_2*C*HPh), 58.3 (–*C*$H_2C(BH)_{10}$), 64.5 (–*C*H_2OCHPh), 73.3 (–*C*H_2OCHPh), 101.7 (–*C*HO_2Ph), 126.2 (–*C*H=$CCH_2C(BH)_{10}$ and –*C*H=CH–$CCHO_2$), 128.1 (–*C*H=CH–$CCH_2C(BH)_{10}$ and –*C*H=$CCHO_2$), 128.8 (–CH=*C*–$CH_2C(BH)_{10}$ and –*C*H=CH–CH=$CCHO_2$), 129.3 (–CH=CH–CH=*C*CHO_2), 137.8 (–*C*H=CH–CH=$CCHO_2$), 172.9 (–*C*$OC(OCH_2)_2CH_3$, internal), 193.7 (–*C*$OC(OCH_2)_2CH_3$, peripheral). SEC (THF, eluent), $M_w = 1.6 \times 10^4$ Da, PDI = 1.1.

2.4.23. [G2]-$(OH)_4$-CPS (2.22)

Deprotection of **2.21** (0.305 g, 1.91×10^{-5} mol) in 30 mL of (1:1) CH_2Cl_2:methanol was carried out by both hydrogenolysis and acid-catalyzed deprotection. The polymer (**2.22**) was recovered as a white foam (0.28 g, 99%). ^{1}H NMR (500 MHz, $CDCl_3$): δ = 1.1 (br, ~258 H, $-CH_3C$), 2.7-3.0 (br, ~248 H, $-CH_2C(BH)_{10}$), 3.5-3.7 (br, ~356 H, $-CH_2OH$), 4.2-4.3 (br, ~188 H, $-CH_2OH$), 6.1-6.8 (br, ~220 H, –Ph). ^{13}C NMR (125 MHz, $CDCl_3$): δ (ppm) = 16.0 ($-CH_3C$), 17.0 ($-CH_3C$), 29.0 ($-CH_2CHPh$), 50.2 ($-CH_2C(BH)_{10}$), 53.8 ($-CCH_3$), 58.8 ($-CCH_2OH$), 64.4 ($-CCH_2OH$), 75.0 ($-CCH_2OH$), 129.3 ($-C{=}CH-CH{=}CCH_2(BH)_{10}$), 134.0 ($-CH{=}CH-CCH_2(BH)_{10}$). SEC (THF, eluent), $M_w = 1.4 \times 10^4$ Da, PDI = 1.2.

2.4.24. [G3]-$(Bn)_4$-CPS (2.23)

The coupling was carried out, as described in general procedures, using [G2]-$(OH)_4$-CPS (**2.22**) (0.201 g, 1.44×10^{-5} mol), benzylidene-protected anhydride (**2.2**) (1.0 g, 2.7×10^{-3} mol), and DMAP (0.15 mL of a 10 mM solution in CH_2Cl_2, 1.5×10^{-6} mol) in a solution of 3:2 CH_2Cl_2/pyridine (25 mL), and stirring at room temperature for 48 h. Upon quenching, washing, precipitation, and drying, polymer **2.23** was isolated as a white powder (0.30 g, 75% yield). ^{1}H NMR (500 MHz, $CDCl_3$): δ (ppm) = 0.9 (br, ~508 H, $-CH_3C$, peripheral), 1.1 (br, ~244 H, $-CH_3C$, internal), 1.5 (br, ~118 H, $-CH_3C$, internal), 2.7-3.0 (br, ~242 H, $-CH_2C(BH)_{10}$), 3.6 (br, ~330 H, $-CH_2OCHPh$), 3.7 (br, ~174 H, $-CH_2OCHPh$), 3.8-4.1 (br, ~180 H, $-CH_2OCHPh$), 4.4 (br, ~322 H, $-CH_2OCHPh$), 4.6 (br, ~180 H, $-CH_2OCHPh$), 5.4 (br, ~170 H, $-CHO_2Ph$), 6.0-6.8 (br, ~220 H, $-CHO_2Ph$), 7.3

(br, ~945 H, –$PhCHO_2$), 7.4 (br, ~472 H, –$PhCHO_2$). ^{13}C NMR (125 MHz, $CDCl_3$): δ (ppm) = 16.0 (–CH_3C, peripheral), 17.0 (CH_3C, internal), 19.0 (CH_3C, internal), 29.0 (–CH_2CHPh), 50.8 (–CH_2CHPh), 53.8 (–CH_2CHPh), 58.0 (–$CH_2C(BH)_{10}$), 64.4 (–CH_2OCHPh), 75.0 (–CH_2OCHPh), 101.7 (–CHO_2Ph), 126.0 (–$CH{=}CCH_2C(BH)_{10}$ and –$CH{=}CH{-}CCHO_2$), 128.2 (–$CH{=}CH{-}CCH_2C(BH)_{10}$ and –$CH{=}CCHO_2$), 129.0 (–$CH{=}C{-}CH_2C(BH)_{10}$ and –$CH{=}CH{-}CH{=}CCHO_2$), 134.0 (–$CH{=}CH{-}CH{=}CCHO_2$), 137.8 (–$CCHCH_2$ and –$CCHO_2$), 172.9 (–$COC(OCH_2)_2CH_3$, internal), 193.7 (–$COC(OCH_2)_2CH_3$, peripheral). SEC (THF, eluent), $M_w = 2.0 \times 10^4$ Da, PDI = 1.18.

2.4.25. [G3]-$(OH)_8$-CPS (2.24)

Deprotection of **2.23** (0.203 g, 1.02 x 10^{-5} mol) in 30 mL of (1:1) CH_2Cl_2:methanol was carried out using both hydrogenolysis and acid-catalyzed deprotection as detailed in general procedures. The polymer (**2.24**) was recovered as a white foam (0.15 g, 96%). ^1H NMR (500 MHz, $CDCl_3$): δ (ppm) = 1.1 (br, ~768 H, –CH_3C), 1.2 (br, ~118 H, –CH_3C), 2.7-2.9 (br, ~238 H, –$CH_2C(BH)_{10}$), 3.6 (br, ~692 H, –CH_2OH), 4.1-4.3 (br, ~522 H, –CH_2OH), 6.0-6.8 (br, ~220 H, –Ph). ^{13}C NMR (125 MHz, $CDCl_3$): δ (ppm) =16.0 (–CH_3C), 17.0 (–CH_3C), 19.0 (–CH_3C), 29.0 (–CH_2CHPh), 50.2 (–$CH_2C(BH)_{10}$), 54.0 (–CCH_3), 58.0 (–CCH_2OH), 64.2 (–CCH_2OH), 75.0 (–CCH_2OH), 101.7 (–CHO_2Ph), 126.2 (–$CH{=}CH{-}CCH_2(BH)_{10}$), 128.8 (–$CH{=}CH{-}CCH_2(BH)_{10}$), 129.3 (–$C{=}CH{-}CH{=}CCH_2(BH)_{10}$), 137.8 (–$CH{=}CH{-}CCH_2(BH)_{10}$), 172.9 (–$COCCH_3$), 193.7 (–$COCCH_3$). SEC (THF, eluent), $M_w = 1.7 \times 10^4$ Da, PDI = 1.23.

2.4.26. [G4]-$(Bn)_8$-CPS (2.25)

The coupling was carried out, as described in general procedures, using [G3]-$(OH)_8$-CPS (**2.24**) (0.150 g, 8.82 x10^{-6} mol), benzylidene-protected anhydride (**2.2**) (1.7 g, 3.97 × 10^{-3} mol), and DMAP (88.0 μL of a 10 mM solution in CH_2Cl_2, 8.8 × 10^{-7} mol) in a solution of 3:2 CH_2Cl_2/pyridine (30 mL), and stirring at room temperature for 72 h. Upon quenching, washing, precipitation, and drying, polymer **2.25** was isolated as a white powder (0.18 g, 70% yield). ^{1}H NMR (500 MHz, $CDCl_3$): δ (ppm) = 0.9 (br, ~1025 H, –CH_3C, peripheral), 1.1 (br, 455~ H, –CH_3C, internal), 1.5 (br, ~105 H, –CH_3C, internal), 2.7-3.0 (br, ~245 H, –$CH_2C(BH)_{10}$), 3.6 (br, ~612 H, –CH_2OCHPh), 4.3 (br, ~625 H, –CH_2OCHPh), 4.4 (br, ~598 H, –CH_2OCHPh), 4.6 (br, ~438 H, –CH_2OCHPh), 5.4 (br, ~298 H, –CHO_2Ph), 6.0-6.8 (br, ~220 H, –$PhCH_2C(BH)_{10}$), 7.3 (br, ~1640 H, –$PhCHO_2$), 7.4 (br, ~1298 H, –$PhCHO_2$). ^{13}C NMR (125 MHz, $CDCl_3$): δ (ppm) = 16.0 (–*C*H_3C, peripheral), 17.0 (*C*H_3C, internal), 19.0 (*C*H_3C, internal), 29.0 (–*C*H_2CHPh), 50.8 (–CH_2*C*HPh), 53.8 (–CH_2*C*HPh), 58.0 (–*C*$H_2C(BH)_{10}$), 64.4 (–*C*H_2OCHPh), 75.0 (–*C*H_2OCHPh), 101.7 (–*C*HO_2Ph), 126.0 (–*C*H=C$CH_2C(BH)_{10}$ and –*C*H=CH–CCHO_2), 128.2 (–*C*H=CH–C$CH_2C(BH)_{10}$ and –*C*H=CCHO_2), 129.0 (–CH=*C*–$CH_2C(BH)_{10}$ and –*C*H=CH–CH=CCHO_2), 134.0 (–*C*H=CH–CH=CCHO_2), 137.8 (–*C*$CHCH_2$ and –*C*CHO_2), 172.9 (–*C*$OC(OCH_2)_2CH_3$, internal), 193.7 (–*C*$OC(OCH_2)_2CH_3$, peripheral). SEC (THF, eluent), M_w = 2.9 × 10^4 Da, PDI = 1.23.

2.4.27. [G4]-$(OH)_{16}$-PSC (2.26)

Deprotection was carried out, as described in general procedures, using both hydrogenolysis and acid-catalyzed deprotection, with **2.25** (0.151 g, 5.21×10^{-6} mol) in 30 mL of (1:1) CH_2Cl_2:methanol. The polymer (**2.26**) was recovered as a white foam (0.10 g, 90%). ^{1}H NMR (500 MHz, $CDCl_3$): δ (ppm) = 1.1 (br, ~895 H, $-CH_3C$), 1.2 (br, ~674 H. $-CH_3C$), 1.3 (br, ~90 H, $-CH_3C$), 2.7-2.9 (br, ~218 H, $-CH_2C(BH)_{10}$), 3.6 (br, ~1200 H, $-CH_2OH$), 4.1-4.3 (br, ~895 H, $-CH_2OH$), 6.0-6.8 (br, ~220 H, –Ph). ^{13}C NMR (125 MHz, $CDCl_3$): δ (ppm) =16.0 ($-CH_3C$), 17.0 ($-CH_3C$), 19.0 ($-CH_3C$), 29.0 ($-CH_2CHPh$), 50.2 ($-CH_2C(BH)_{10}$), 54.0 ($-CCH_3$), 58.0 ($-CCH_2OH$), 64.2 ($-CCH_2OH$), 75.0 ($-CCH_2OH$), 101.7 ($-CHO_2Ph$), 126.2 ($-CH{=}CH-CCH_2(BH)_{10}$), 128.8 ($-CH{=}CH-CCH_2(BH)_{10}$), 129.3 ($-C{=}CH-CH{=}CCH_2(BH)_{10}$), 137.8 ($-CH{=}CH-CCH_2(BH)_{10}$), 172.9 ($-COCCH_3$), 193.7 ($-COCCH_3$).

2.5. References

(1) Jiang, W.; Knobler, C. B.; Mortimer, M. D.; Hawthorne, M. F. *Angew. Chem.* **1995**, *34*, 1332-1334.
(2) Taylor, H. J.; Goldhaber, M. *Nature* **1935**, *135*, 341.
(3) Herzog, A.; Maderna, A.; Harakas, G. N.; Knobler, C. B.; Hawthorne, M. F. *Chem. Eur. J.* **1999**, *5*, 1212-1217.
(4) Locher, G. L. *Am. J. Roentgenol. Radium Ther.* **1936**, *36*, 1-13.
(5) Diaz, A. Z.; Coderre, J. A.; Chanana, A. D.; Ma, R. *Ann. Med.* **2000**, *32*, 82-85.
(6) Yanagie, H.; Maruyama, K.; Takizawa, T.; Ishida, O.; Ogura, K.; Matsumoto, T.; Sakurai, Y.; Kobayashi, T.; Shinohara, A.; Rant, J.; Skvarc, J.; Ilic, R.; Kuhne, G.; Chiba, M.; Furuya, Y.; Sugiyama, H.; Hisa, T.; Ono, K.; Kobayashi, H.; Eriguchi, M. *Biomed. Pharmacother.* **2006**, *60*, 43-50.
(7) Alam, F.; Soloway, A. H.; Mcguire, J. E.; Barth, R. F.; Carey, W. E.; Adams, D. *J. Med. Chem.* **1985**, *28*, 522-525.
(8) Ma, L.; Hamdi, J.; Wong, F.; Hawthorne, M. F. *Inorg. Chem.* **2006**, *45*, 278-285.
(9) Tietze, L. F.; Bothe, U.; Nakaichi, M.; Hasegawa, T.; Nakamura, H.; Yamamoto, Y. *ChemBioChem* **2001**, *2*, 236-334.
(10) Soloway, A. H.; Tjarks, W.; Barnum, B. A.; Rong, F. G.; Barth, R. F.; Codogni, I. M.; Wilson, J. G. *Chem. Rev.* **1998**, *98*, 1515-1562.
(11) Tomita, T.; Watanabe, M.; Takahashi, T.; Kumai, K.; Tadakuma, T.; Yasuda, T. *Biochim. Biophys. Acta* **1989**, *978*, 185-190.
(12) Tietze, L. F.; Griesbach, U.; Bothe, U.; Nakamura, H.; Yamamoto, Y. *ChemBioChem* **2002**, *3*, 219-225.
(13) Newkome, G. R.; Keith, J. M.; Baker, G. R.; Escamilla, G. H.; Moorefield, C. N. *Angew. Chem. Int. Ed.* **1994**, *33*, 666-668.
(14) Qualmann, B.; Kessels, M. M.; Musiol, H. J.; Sierralta, W. D.; Jungblut, P. W.; L., M. *Angew. Chem. Int. Ed.* **1996**, *35*, 909-911.
(15) Armspach, D.; Cattalini, M.; Constable, E. C.; Housecroft, C. E.; Phillips, D. *Chem. Commun.* **1996**, 1823-1824.
(16) Barth, R. F.; Adams, D. M.; Soloway, A. H.; Alam, F.; Darby, M. V. *Bioconjugate Chem.* **1994**, *5*, 58-66.
(17) Nunez, R.; Gonzalez, A.; Vinas, C.; Teixidor, F.; Sillanpaa, R.; Kivekas, R. *Org. Lett.* **2005**, *7*, 231-233.
(18) Parrott, M. C.; Marchington, E. B.; Valliant, J. F.; Adronov, A. *Macromol. Symp.* **2003**, *196*, 201-211.
(19) Parrott, M. C.; Valliant, J. F.; Adronov, A. *Langmuir* **2006**, *22*, 5251-5255.
(20) Parrott, M. C.; Marchington, E. B.; Valliant, J. F.; Adronov, A. *J. Am. Chem. Soc.* **2005**, *127*, 12081-12089.
(21) De Jesus, O. L. P.; Ihre, H. R.; Gagne, L.; Frechet, J. M. J.; Szoka, F. C. *Bioconjugate Chem.* **2002**, *13*, 453-461.
(22) Haag, R.; Kratz, F. *Angew. Chem. Int. Ed.* **2006**, *45*, 1198-1215.
(23) Schluter, A. D.; Rabe, J. P. *Angew. Chem. Int. Ed.* **2000**, *39*, 864-883.

(24) Yoshida, M.; Fresco, Z. M.; Ohnishi, S.; Frechet, J. M. J. *Macromolecules* **2005**, *38*, 334-344.
(25) Malkoch, M.; Carlmark, A.; Woldegiorgis, A.; Hult, A.; Malmstrom, E. E. *Macromolecules* **2004**, *37*, 322-329.
(26) Carlmark, A.; Malmstrom, E. E. *Macromolecules* **2004**, *37*, 7491-7496.
(27) Lee, C. C.; Yoshida, M.; Frechet, J. M. J.; Dy, E. E.; Szoka, F. C. *Bioconjugate Chem.* **2005**, *16*, 535-541.
(28) Ihre, H. R.; De Jesus, O. L. P.; Frechet, J. M. J. *J. Am. Chem. Soc.* **1998**, *123*, 5908-5917.
(29) Benoit, D. C., V.; Braslau, R.; Hawker, C. J. *J. Am. Chem. Soc.* **1999**, *121*, 3904-3920.
(30) Ihre, H. R.; Omayra, L.; De Jesus, O. L. P.; Frechet, J. M. J. *J. Am. Chem. Soc.* **2001**, *123*, 5908-5917.

Chapter 3: Protein Resistance of Surfaces Prepared by Chemisorption of Mono-Thiolated Poly(ethylene glycol) to Gold and Dendronization with Aliphatic Polyester Dendrons: Effect of Hydrophilic Dendrons

Abstract

Protein adsorption to surfaces prepared by chemisorption of thiol-terminated poly(ethylene glycol) (HS-PEG_{650}-OH) to gold-coated silicon wafers followed by functionalization of the terminal PEG OH-groups with aliphatic polyester dendrons was investigated. Chemisorption of HS-PEG_{650}-OH to the gold surfaces was carried out under cloud-point conditions to give a chain density of approximately 3.7 chains/nm^2, as calculated from AFM film thickness measurements. Dendronization of the PEG-functionalized surfaces with aliphatic polyester dendrons, generation 1 to 4, was achieved using divergent dendron growth. The hydrophilicity of the surfaces increased significantly with increasing dendron generation as shown by water contact angle data. The effect of the hydrophilic dendrons on protein adsorption from phosphate-buffered saline (PBS) and plasma are reported. Adsorption of both ^{125}I-radiolabled fibrinogen and lysozyme onto the dendronized surfaces showed that protein adsorption increases upon introduction of dendrons to the PEG-functionalized surfaces. The similarity between fibrinogen and lysozyme adsorption suggests that resistance of the dendronized surfaces to proteins follows the same trend regardless of protein size. This chapter has been reproduced in part with permission from *Macromolecules* **2008**, 2567-2576. Copyright 2008 American Chemical Society.

3.1. Introduction

Among the biomaterials under investigation, polymers constitute a versatile class that has received attention in various biological applications due to the vast flexibility in their synthesis and facile modification to suit specific physical and mechanical properties of a wide range of tissues. In comparison to natural polymers, the use of synthetic polymers as biomaterials is a relatively recent phenomenon.[1] A variety of polymers, including polyurethanes, polyethylene, poly(ethylene terephthalate), silicones, and various polyacrylates have been used in applications such as blood contacting devices, hip joint replacement, and intraocular lenses.[1] Even though the application of biostable polymeric materials has played an important role in the advancement of modern health care, many of these materials are limited by their lack of long-term biocompatibility.

Protein adsorption is known to be the first event that occurs following implantation of biomaterials, and is therefore important in initiating events that determine host responses such as blood coagulation, thrombus formation, platelet activation, bacterial infection, and other undesirable responses.[2,3] Surfaces that resist the nonspecific protein adsorption are useful in numerous applications, including sensors, materials for contact lenses, implantable devices in blood contacting applications,[2] and drug delivery devices.[4] A common approach for minimizing problems arising from protein adsorption involves coating the surface with a material that inhibits non-specific interactions. A number of such materials have been used, including heparin,[5] dextran,[6] and poly(ethyloxazoline).[7,8] However, the most prominent and commonly used material for protein adsorption resistance is poly(ethylene glycol) (PEG).[9] While a number of different

PEG-functionalized surfaces have been studied,[10-15] a molecular-level understanding of their protein-repelling mechanisms is still a matter of debate.[16-18] For example, Nishiumi and coworkers suggested that protein resistance of the PEG-modified surfaces is directly attributed to the highly dynamic nature of the segments in water.[19] Based on a model study by Andrade and de Gennes to rationalize the protein resistance of surfaces grafted with PEG, it was found that the conformational flexibility of the grafted PEG plays an important role in this process.[14,15,20] In separate studies, Grunze and co-workers[17,21] found that the conformation of PEG chains at the interface and their interaction with water is an important determinant of protein resistance, whereas Brash and coworkers have reported that chain density is one of the key contributors to this phenomenon.[3,12,22,23]

While these studies have thoroughly investigated the protein-resistant properties of linear hydrophilic polymers, focusing on hydrophilicity/hydration, conformation, molecular weight, and surface density, relatively little attention has been given to the effect of polymer branching on protein repulsion. Although branched polymers and dendrimers have attracted significant interest as drug delivery vehicles,[24-27] investigation of their anti-fouling properties on surfaces has been limited to the use of PAMAM dendrimers and polyglycerol hyperbranched polymers.[28-30] In the case of PAMAM dendrimers, protein resistance was significantly diminished as a result of their polycationic nature under physiological pH.[31,32] Non-specific protein adsorption is known to be exacerbated on cationic surfaces relative to neutral surfaces.[33] Hyperbranched polyglycerols, on the other hand, are neutral under physiological conditions. These structures were shown to exhibit protein resistance that is practically

equivalent to a PEG monolayer on gold.[30] However, the polymerization mechanism precludes precise control of polymer size, architecture, and degree of branching in these materials. Here, we present the synthesis and characterization of model dendronized gold surfaces, which combine the linear PEG with aliphatic polyester dendrons based on the 2,2-bis(hydroxymethyl)propionic acid (bis-MPA) building block. Similar to the hyperbranched polyglycerols, the polyester dendrons exhibit charge neutrality under physiological conditions and a well-defined structure that arises from their step-wise synthesis. In addition, the dendrons investigated here have been shown to be biocompatible, making them ideal for biological applications.[34,35] The focus of this study was therefore to investigate the effect of surface functionalization with hydrophilic bis-MPA-based polyester dendrons on protein adsorption at each dendrimer generation, and to compare this system with more traditional PEG-grafted surfaces.

3.2. Results and Discussion

3.2.1. Surface grafting with HS-PEG650-OH

Surface dendronization was preceded by the chemisorption of monothiolated PEG, HS-PEG_{650}-OH, onto the gold surfaces. Conditions for the chemisorption of HS-PEG_{650}-OH were optimized by varying the ionic strength of the chemisorption solution as well as the chemisorption time at 25 °C. This strategy was based on the previously reported premise that higher chain densities should be obtained when chemisorption is carried out under cloud-point conditions.[38] The surface grafting was evaluated by water

contact angle measurements. Based on the results from advancing contact angle measurements, higher chain densities were obtained in the high ionic strength (IS = 2.9, pH = 7.4) chemisorption solution after 4 h or longer at 25 °C, as reflected by the decrease in the contact angle (Table 3.1). Based on these results, all subsequent chemisorptions were carried out using a solution of 5 mM of HS-PEG_{650}-OH in high IS PBS for 4 h at 25 °C.

3.2.2. Divergent dendron synthesis

Growth of aliphatic polyester dendrons up to the fourth generation was accomplished using a divergent synthetic approach[39] with the acetonide-protected anhydride of 2,2-bis(hydroxylmethyl)propionic acid (bis-MPA) (**3.1**) as the building block (Scheme 3.1). The reactivity of this anhydride has proven to be useful for the synthesis of dendrimers,[36,40-43] dendronized polymers,[25,44-50] and dendronized surfaces.[24,51-53] The first generation dendrons were introduced via an esterification reaction carried out on the terminal hydroxyl groups of PEG_{650}-functionalized gold surfaces with excess acetonide anhydride (**3.1**) and a catalytic amount of DMAP in a mixture of CH_2Cl_2:pyridine (3:2 v/v). This step was followed by removal of the acetonide protecting groups to give the hydroxyl-terminated first generation dendrons. The deprotection step was carried out following a literature procedure, using the acidic resin DOWEX 50W-X2 in methanol at 50 °C for 1 h.[24] Iterative esterification and deprotection reactions allowed surface dendronization up to the fourth generation (Scheme 3.1).

Scheme 3.1. Synthesis of G1-G4 dendronized surfaces.

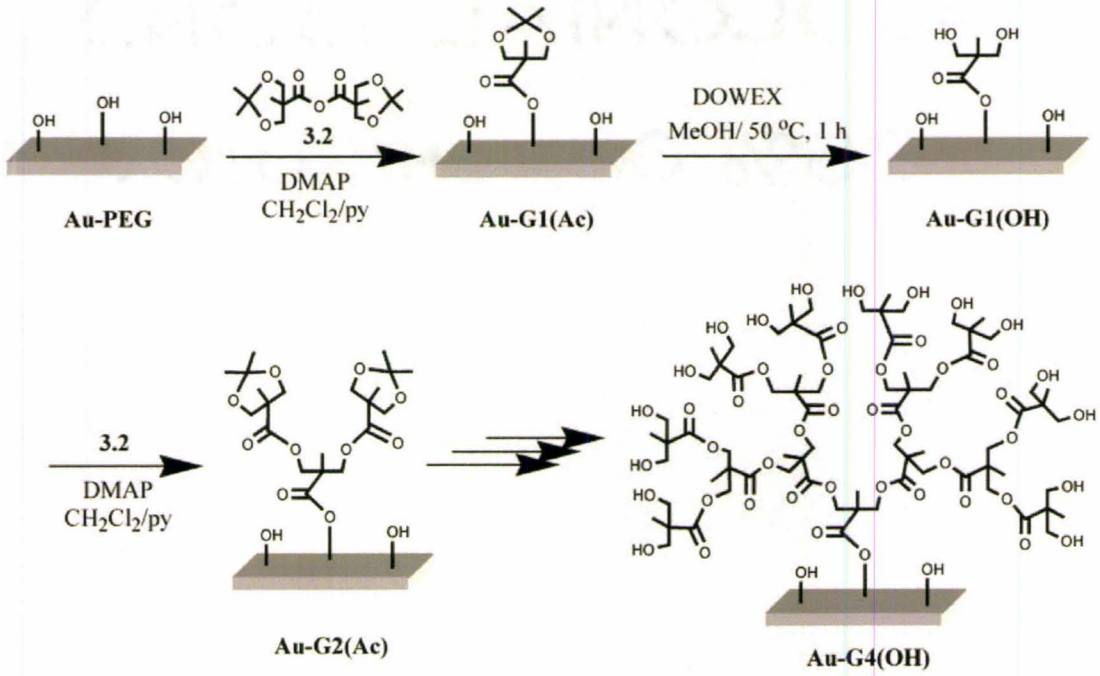

3.2.3. Water contact angle measurements

Water contact angles were measured before and after surface grafting with PEG and further dendronization with the aliphatic polyester dendrons of generation 1-4. It is apparent from the results (Table 3.1, Figure 3.1) that the surfaces grafted with HS-PEG_{650}-OH show a significant decrease in contact angle when compared to the unmodified gold surfaces. The advancing and receding angles on unmodified gold were 70 ± 3° and 40 ± 8°, respectively. Following chemisorption with PEG, the angles decreased significantly for all chemisorption conditions reflecting the hydrophilic nature imparted by the grafted PEG on the gold surfaces (Table 3.1).

Table 3.1. Water contact angles (°) under various chemisorption conditions: Effect of ionic strength and time on surface grafting density.

Chemisorption Conditions*	Advancing contact angle (°)	Receding contact angle (°)	Ionic strength (M)
Bare Au	70 ± 3	40 ± 8	
High IS (low solubility), 30 min	45 ± 2	15 ± 5	2.9
High IS, 2 h	41 ± 3	17 ± 4	2.9
High IS, 4 h	**38 ± 2**	**15 ± 6**	**2.9**
High IS, 12 h	36 ± 1	15 ± 3	2.9
Low IS (high solubility), 30 min	58 ± 4	25 ± 3	0.26
Low IS, 2 h	55 ± 3	26 ± 1	0.26
Low IS, 4 h	47 ± 2	28 ± 2	0.26
Low IS, 12 h	46 ± 3	27 ± 4	0.26

*5 mM chemisorption solution of HS-PEG_{650}-OH in PBS at pH = 7.4

Water contact angles were also utilized to characterize the surfaces after each esterification and deprotection step of the divergent growth of dendrons at every generation. The results, summarized in Table 3.2 and Figure 3.1, show that the advancing contact angles for the protected dendritic generations ranged between 51 ± 3° and 58 ± 1°, and the receding angles ranged between 26 ± 5° and 33 ± 3° for generations 1 to 4. These increasing contact angle values reflect the hydrophobic character of the dendrons bearing the acetonide groups at their periphery (Table 3.2, Figure 3.1).

Table 3.2. Water contact angles of unmodified Au, Au-PEG, and Au-G1(Ac) to G4(Ac).

Surface	Advancing contact angle (°)	Receding contact angle (°)
Bare Au	70 ± 3	40 ± 8
Au-PEG_{650}*	42 ± 4	36 ± 2
Au-G1(Ac)	51 ± 3	26 ± 5
Au-G2(Ac)	54 ± 2	31 ± 2
Au-G3(Ac)	57 ± 4	24 ± 2
Au-G4(Ac)	58 ± 1	33 ± 3

*5 mM chemisorption solution of HS-PEG_{650}-OH in PBS at pH = 7.4 and high IS for 4 h.

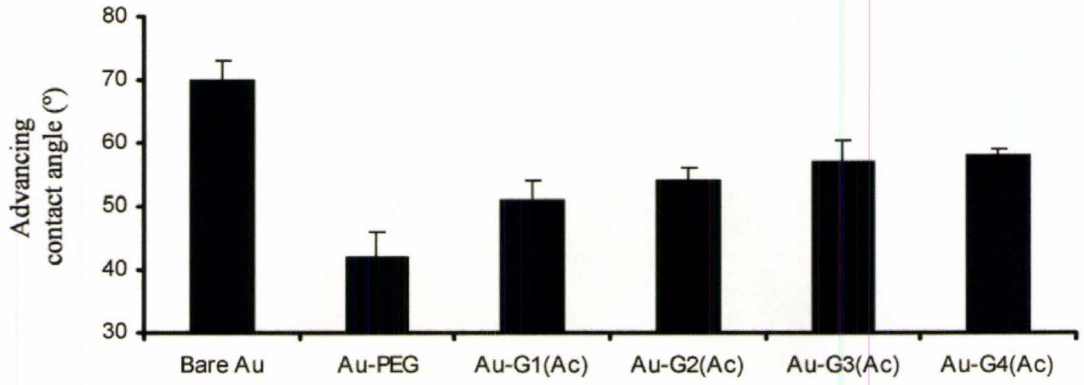

Figure 3.1. Advancing contact angles of Au, Au-PEG, and Au-G1(Ac) to G4(Ac) surfaces.

In contrast, the contact angles obtained after deprotection of the acetonide groups show a significant decrease when compared to the PEG-functionalized gold surfaces (Table 3.3, Figure 3.2). The advancing contact angles for the OH-terminated dendritic generations 1 to 4 ranged between 40 ± 2° and 30 ± 2°, and the receding angles ranged between 22 ± 3° and 13 ± 1°. These results reflect the hydrophilic character of the OH-terminated dendron periphery after removal of the acetonide groups. This hydrophilic character increases with increasing dendron generation as a result of the theoretical doubling in number of hydroxyl groups at the periphery from one generation to the next.

Table 3.3. Water contact angles of unmodified Au, Au-PEG, and Au-G1(OH) to G4(OH).

Surface*	Advancing contact angle (°)	Receding contact angle (°)
Bare Au	70 ± 3	40 ± 8
Au-PEG_{650}	42 ± 4	36 ± 2
Au-G1(OH)	40 ± 2	22 ± 3
Au-G2(OH)	36 ± 2	15 ± 1
Au-G3(OH)	32 ± 1	10 ± 1
Au-G4(OH)	30 ± 2	13 ± 1

*5 mM chemisorption solution of HS-PEG_{650}-OH in PBS at pH = 7.4 and high IS for 4 h.

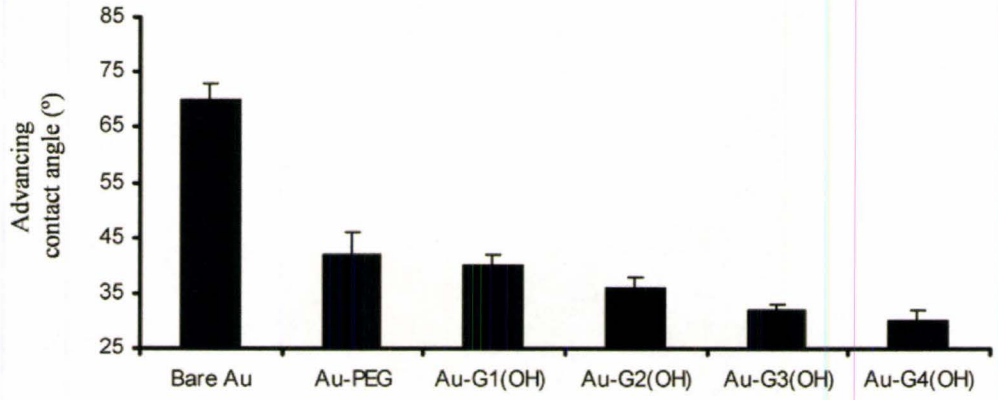

Figure 3.2. Advancing contact angles of Au, Au-PEG, and Au-G1(OH) to G4(OH) surfaces.

3.2.4. X-ray photoelectron spectroscopy (XPS)

High-resolution XPS data for sulfur and carbon within each of the samples are summarized in Figure 3.3 The S2*p* photoelectron peak at ~162 eV was assigned to the gold-bound sulfur atoms (S-Au) obtained for both PEG-grafted and G4-dendronized surfaces (Figure 3.3.b and c). The C1*s* peak at 284.6 eV, observed on the bare gold

surfaces (used as a control), was assigned to aliphatic carbon contamination on gold, which was also seen with the low-resolution data (not included). Such surface contamination with carbonaceous material is extremely common and difficult to avoid.[54] Deconvolution of the C1*s* peak of the PEG-modified surfaces revealed two distinct peaks shown in Figure 3.3.e. The presence of the new major peak at 286 eV, assigned to the ether carbons within each repeat unit of PEG, clearly demonstrated the presence of PEG at the surface (Figure 3.3.d). Similarly, analysis of the G4(Ac) dendronized surfaces revealed two major signals at 284.6 eV and 286 eV after deconvolution of the C1*s* peak, as well as minor peaks at 287 eV and 290 eV corresponding to higher oxidation state carbons (Figure 3.3.f). The main difference between the PEG-functionalized surface and the G4(Ac)-dendronized surface was the reversal in the intensity of the deconvoluted C1*s* peaks corresponding to the aliphatic and ether carbons. In the case of the Au-PEG surface, the ratio of ether to aliphatic carbons is greater than 1, whereas in the case of Au-G4(Ac) surface, this ratio is less than 1 due to the larger number of aliphatic carbons resulting from multiple acetonide groups at the dendron periphery (data for Au-G1(Ac) to Au-G3(Ac) is given in Appendix I, Figure 3.I.1). Furthermore, for a more quantitative evaluation of surface functionalization, the ratios of the deconvoluted peaks obtained from the high-resolution C1*s* analysis for each carbon environment were calculated and compared to the expected theoretical values (Table 3.4). The ratios were calculated for four specific carbon environments at binding energies of 284.6, 286, 287 and 290 eV, corresponding to aliphatic bis-MPA carbons, ether carbons (*C*-O-), ester carbons (-*C*H_2OCO-), and carbonyl carbons (-CH_2O*C*O-), respectively. These four carbon

environments were specifically chosen to provide a direct comparison between the PEG carbons and the dendron carbons. All ratios were calculated in reference to the aliphatic bis-MPA C atoms. For instance, the ratio of the aliphatic carbons, present only in the dendrons, to the ether carbons, present only in the PEG chains, would be expected to increase as the dendron generation increases. The XPS data shows that, as dendron generation increases, the agreement between measured and theoretically calculated ratios generally improves (Table 3.4).

Table 3.4. Atomic composition % ratios from high-resolution C1*s* XPS data for various surfaces.

Surface	Takeoff angle (°)	(284.6: 286 eV) *C** : *C*-O		(284.6 : 290 eV) *C** : *C*OO		(284.6 : 287 eV) *C** : *C*H_2OCO	
		Calc.	Found	Calc.	Found	Calc.	Found
Au	90	0	3.26	0	5.56	0	4.80
	20	0	3.47	0	8.09	0	6.45
Au-PEG	90	0	0.88	0	3.54	0	2.75
	20	0	0.67	0	2.78	0	1.56
Au-G1(Ac)	90	0.18	2.50	5	6.88	2.5	5.44
	20	0.18	2.47	5	5.47	2.5	4.91
Au-G2(Ac)	90	0.36	1.92	3.33	4.57	1.67	4.49
	20	0.36	2.06	3.33	3.37	1.67	3.37
Au-G3(Ac)	90	0.71	1.68	2.86	3.66	1.43	3.57
	20	0.71	1.06	2.86	4.01	1.43	2.92
Au-G4(Ac)	90	1.42	1.67	2.67	2.19	1.33	2.66
	20	1.42	1.39	2.67	2.12	1.33	1.88

* Alipahtic carbons of the acetonide protecting groups within the dendrons.

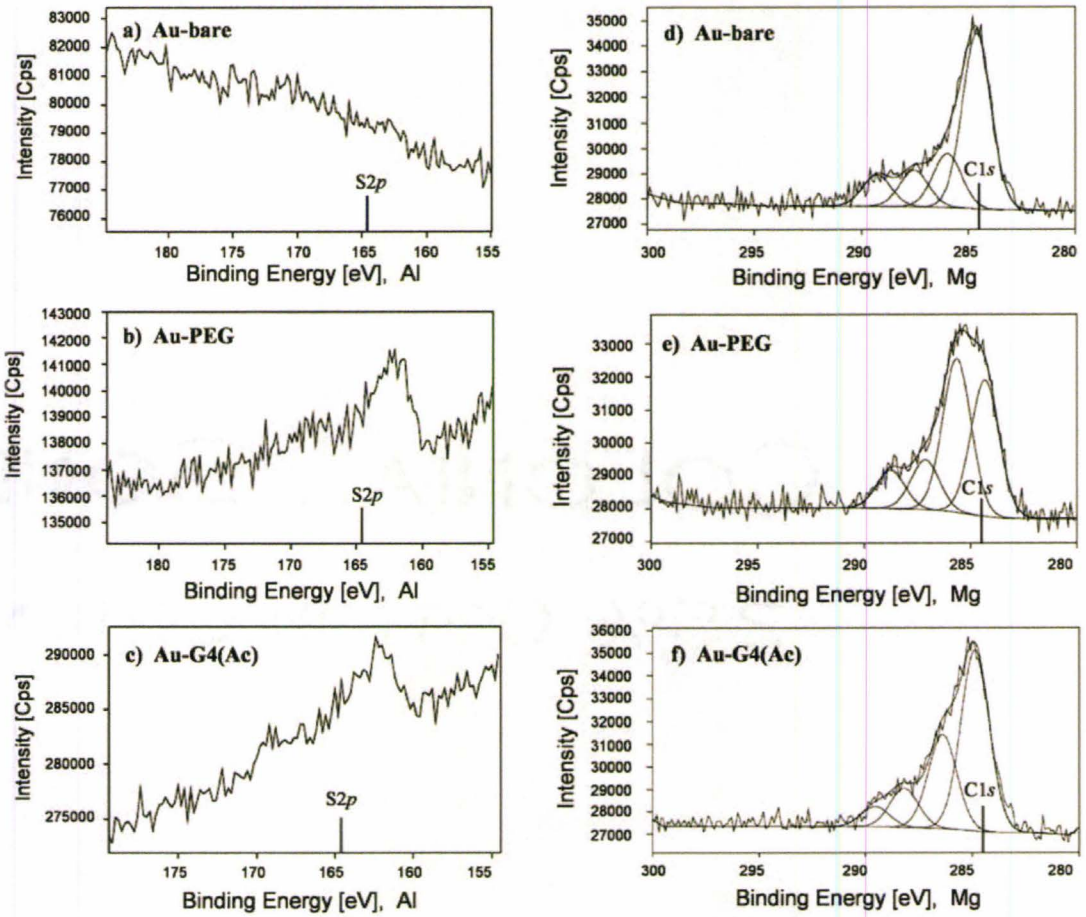

Figure 3.3. High-resolution S2p XPS data at 90° takeoff angle for: (a) Bare Au, (b) Au-PEG, (c) Au-G1(Ac), and C1s data at 90° takeoff angle for: (d) Bare Au, (e) Au-PEG, (f) Au-G4(Ac).

3.2.5. Time-of-Flight Secondary Ion Mass Spectroscopy (TOF-SIMS)

In order to further characterize the surface functionalization, all the surfaces were analyzed in detail using TOF-SIMS in both positive and negative modes. The major advantage of TOF-SIMS over XPS measurements is the ability to analyze only the outermost surface layer (~ 5 Å) of a sample, and provide not only information on the

elemental composition of the surface, but also the chemical structure of species on the surface. The positive ion TOF-SIMS spectra of the bare Au, Au-G1(Ac), Au-G1(OH), and Au-G2(Ac), are shown in Figure 3.4 for two different mass ranges corresponding to two fragments specific to the immobilized dendrons. These two fragments, with molecular formula of $C_5H_9O_4^+$ (MW = 133.12 Da) and $C_8H_{13}O_4^+$ (MW = 173.19 Da), correspond to the deprotected and acetonide-protected bis-MPA units, respectively. Therefore, analyzing the TOF-SIMS spectra at these specific mass values for the various surfaces provided direct evidence of functionalization with the aliphatic polyester dendrons (the full TOF-SIMS spectra over the entire mass range are included in Appendix I, Figure 3.I.2). For each surface, the observed molecular fragments corresponded to the species expected at the dendron periphery. For example, after reaction of the surfaces with the anhydride (**3.1**) at any dendron growth step, the TOF-SIMS spectra indicate the presence of the expected acetonide-protected fragment at 173 Da (Figure 4 B(ii), D(ii), F(ii), and H(ii)). After any deprotection step, the spectra indicate the presence of a fragment at 133 Da, corresponding to the expected diol fragment (Figure 3.4 C(i), E(i), G(i), and I(i)). Importantly, for the first three generations, the observed signals are mutually exclusive (i.e., the fragment at 133 Da is not observed in the samples measured after reaction with **3.1**, and the fragment at 173 is not observed after deprotection steps). Low intensity signals observed in several samples were identified as fragments of PEG chains and small amounts of unreacted lower-generation dendrons.

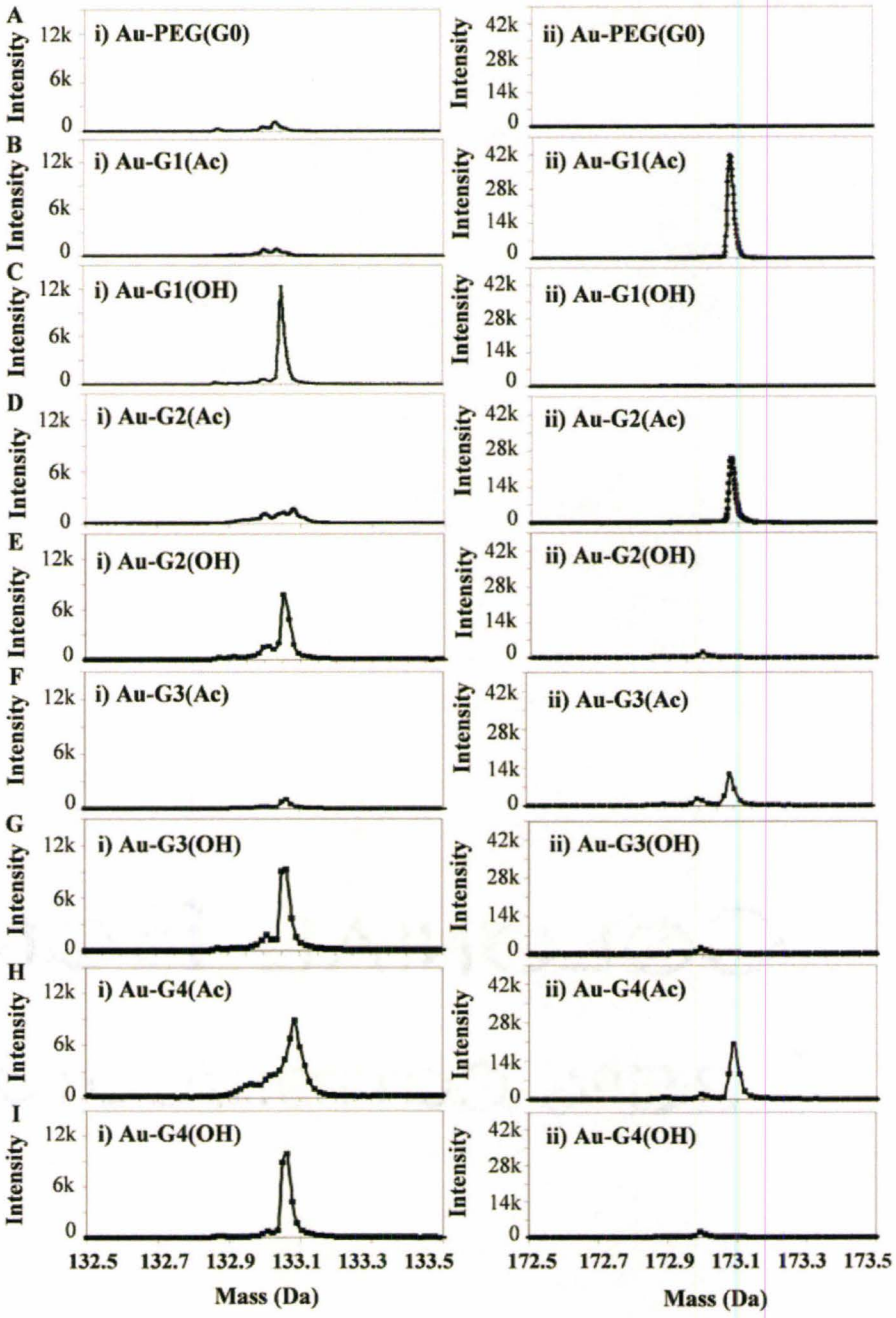

Figure 3.4. Normalized negative ion TOF-SIMS spectra of various surfaces for two mass ranges; i) mass range corresponding to the deprotected G1(OH) fragment ($C_5H_9O_4$), ii) mass range corresponding to the acetonide-protected fragment ($C_8H_{13}O_4$).

From the data for higher generations, it is clear that dendron growth from G3 to G4 on the surfaces does not go to completion, as a significant signal is observed for the deprotected fragments (133 Da) at this stage. This decreased efficiency of the coupling step at higher generations is likely a result of increasing steric hindrance arising from the presence of bulky dendrons on the surface. Nevertheless, along with the XPS and contact angle results, this data illustrates that dendronization of the PEG-functionalized surfaces and subsequent divergent dendron growth using the iterative deprotection and coupling protocol (Scheme 3.1) were carried out successfully.

3.2.6. AFM Analysis

Ex situ ellipsometry is the most widely used technique for film thickness measurement on smooth surfaces. However, the rough nature of gold surfaces (1-2 nm surface roughness) and the relatively small adsorbate thicknesses limited its use in the present work. Therefore, film thickness measurements of the chemisorbed PEG layer on gold were accomplished by Tapping Mode™ AFM height measurements using the "scratch" method. The average thickness of the gold layer measured on a clean surface prior to functionalization was found to be ~111.4 nm ± 0.6 nm, which is in good agreement with the expected thickness of 100 nm, as reported by the manufacturer. This result indicated that the scratch introduced onto the surface prior to functionalization penetrated the entire gold layer. This was important, since any gold remnants within the scratch could be grafted with PEG chains in the chemisorption step, resulting in inaccurate film thickness measurements. The film thickness data of the PEG-grafted

surfaces (Au-PEG) show that the average thickness, measured at numerous points using the average mode calculation in the AFM Nanoscope-(R) III software, was ~115.3 ± 0.4 nm (see Appendix I, Figure 3.I.3). Therefore, the thickness of the PEG chain layer was 3.9 ± 1 nm, which is in close agreement with the theoretical value of 4.1 nm calculated for the film thickness of a PEG_{650} layer based on the characteristic monomer length of 2.78 Å for the ethylene oxide repeat unit.[55]

The AFM thickness data obtained for the G1(Ac)-G4(Ac) dendronized surfaces show very little difference compared to the PEG layer thickness (Figure 3.5). These results were not surprising since the theoretical height of the grafted dendrons is expected to be less than 1 nm, which is within the error of the AFM measurements.

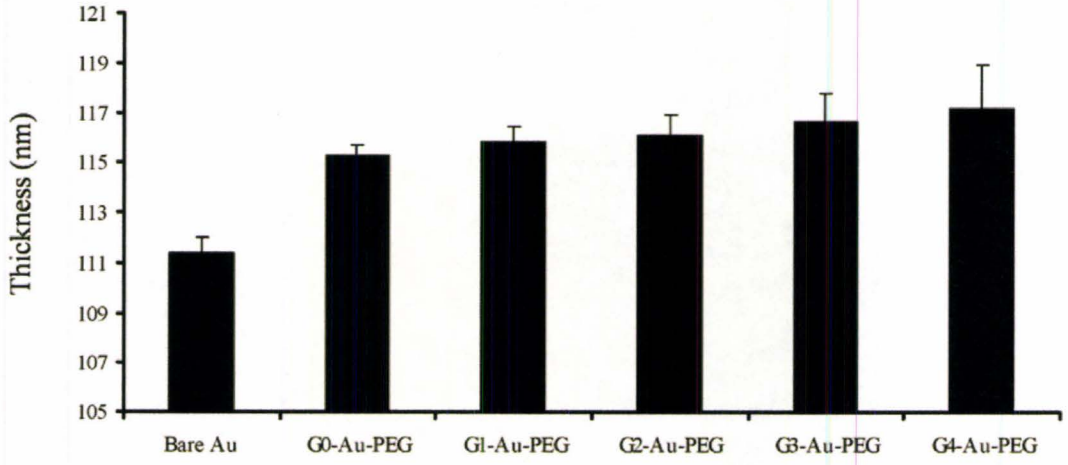

Figure 3.5. Film thickness measurement using Tapping ModeTM AFM height analysis.

The surface topographies of the scratched gold surface prior to and after functionalization were also examined by AFM. The results from the 3D AFM amplitude

images illustrated in Figure 3.6 show that the control gold surface prior to functionalization was relatively smooth, with a mean roughness (Ra) value of 1.26 nm (Figure 3.6.a). In contrast, the surface roughness of the PEG-grafted surface increased to 2.27 nm (Figure 3.6.b). The surface roughness increased considerably upon dendronization, with values ranging between 2.41 nm and 5.42 nm for the G1 to G4 dendronized surfaces (Figure 3.6.c-f, Table 3.5).

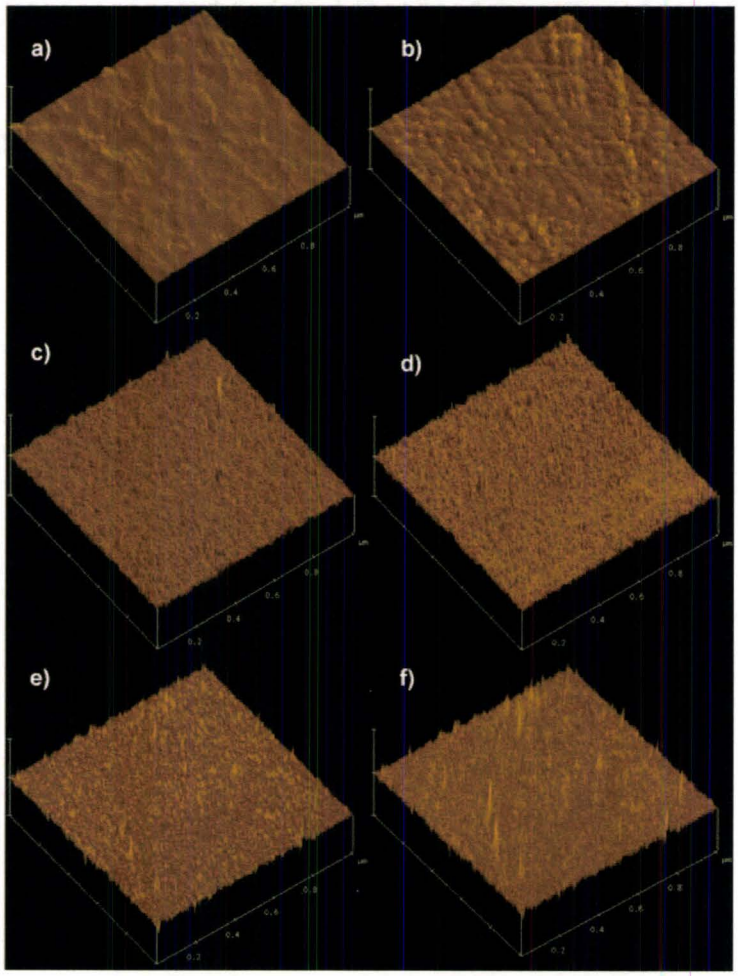

Figure 3.6. AFM amplitude images of (a) bare Au, (b) Au-PEG, (c) Au-G1(Ac), (d) Au-G2(Ac), (e) Au-G3(Ac), (f) Au-G4(Ac). (Image size: 1 × 1 μm^2).

The increase in surface roughness upon PEG-functionalization is believed to be a result of PEG aggregation into phase-separated domains on the surface. Similar AFM results on PEG-modified surfaces were reported previously.[56,57] The continued increase in surface roughness upon dendronization is likely caused by additional local aggregation of hydrophobic acetonide-protected dendrons as their size increases. Furthermore, the general dendron shape and the incomplete surface dendronization at higher generations can both lead to increased surface roughness and heterogeneity.

Table 3.5. Root-mean-square (Rms) roughness of bare and modified gold surfaces obtained from AFM data.

Surface	Rms (nm)
Bare gold	1.26
Au-PEG_{650}	2.27
Au-G1(Ac)	2.41
Au-G2(Ac)	3.57
Au-G3(Ac)	4.04
Au-G4(Ac)	5.42

3.2.7. Fibrinogen adsorption

The effect of surface modification with PEG and its subsequent dendronization on protein adsorption was investigated. Fibrinogen (Fg) was selected for these studies due to the crucial role it plays in wound healing,[58] clot formation,[59] and platelet adhesion/activation.[56] Adsorption onto various surfaces was studied from both PBS-NaI buffer and plasma. Prior to adsorption, the protein was radiolabeled with ^{125}I, which enabled quantitative estimation of the amount of protein adsorbed onto the surfaces in

units of $\mu g/cm^2$. This study was based on the previously reported results showing significant protein adsorption resistance of surfaces functionalized with PEG chains of various molecular weights.[3,12] Although the mechanism of protein repulsion in the presence of PEG is not fully understood, this effect was attributed to several factors, including chain density, length, flexibility, and PEG hydration due to its hydrophilic nature.[14,15,20,33,59] In the present work, we set out to determine whether or not the increased hydrophilicity introduced by dendron grafting could improve protein repulsion.

The results from the Fg adsorption studies show that the dendronized surfaces exhibit an opposite effect on protein adsorption to the one originally expected. The results obtained show that protein adsorption increased upon introducing the G1(OH) dendrons compared to the PEG-modified surfaces. Furthermore, protein adsorption continued to increase with increasing dendron generation as shown in Figure 3.7, despite the increase in surface hydrophilicity imparted by the dendrons. It has been proposed that one of the contributing factors to protein resistance on PEG-modified surfaces is PEG chain flexibility and dynamics, where it is believed that higher chain flexibility enhances protein repulsion.[3,12] In our studies, the increase in protein adsorption as a result of surface dendronization can potentially be explained by this hypothesis, as a decrease in PEG chain mobility can result from intra- and inter-molecular hydrogen-bonding of the grafted dendrons. The fact that protein adsorption increases with increasing dendron generation is consistent with this hypothesis, as higher dendron generations exhibit a greater number of peripheral OH-groups, increasing the extent of inter- and intra-molecular "locking" interactions.

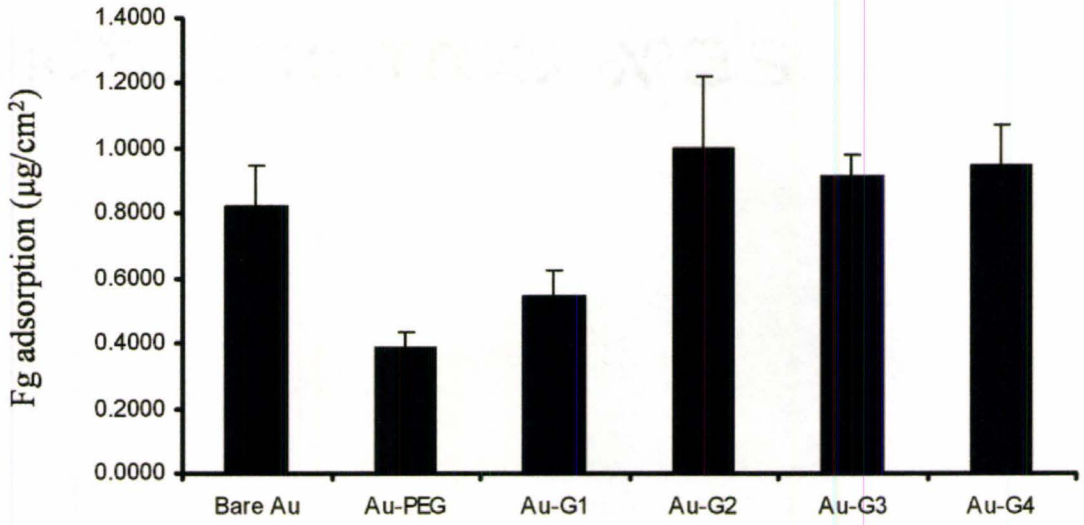

Figure 3.7. Fibrinogen adsorption from PBS buffer: effect of surface modification with PEG and dendronization with aliphatic polyester dendrons G1-G4.

Fibrinogen adsorption from plasma was also studied with 2.5% radioiodinated fibrinogen following the same procedure used with PBS-NaI buffer. The results from these experiments show that the trend of adsorption from plasma is similar to the one observed from PBS-NaI solution (Table 3.6, Figure 3.8). Once again, the data show that PEG-modified surfaces significantly enhance fibrinogen repulsion with about 75% reduction compared to the control gold surfaces. However, functionalization of the PEG chains with the aliphatic polyester dendrons increases protein adsorption (Table 3.6 and Figure 3.8).

Table 3.6. Fibrinogen reduction from PBS-NaI and plasma of various surfaces.

Surface	Fg PBS-NaI ($\mu g/cm^2$)	Reduction vs Control (%)[†]	Fg Plasma ($\mu g/cm^2$)	Reduction vs Control (%)[†]
Bare Au	0.82 ± 0.12		0.20 ± 0.05	
Au-PEG_{650}	0.28 ± 0.05	66	0.05 ± 0.02	75
Au-G1(OH)	0.54 ± 0.08	34	0.32 ± 0.09	-60[*]
Au-G2(OH)	1.00 ± 0.20	-22[*]	0.51 ± 0.03	-155[*]
Au-G3(OH)	0.91 ± 0.06	-11[*]	0.54 ± 0.15	-170[*]
Au-G4(OH)	0.94 ± 0.14	-15[*]	0.42 ± 0.01	-110[*]

[†] The value for bare Au was used as the control

[*] Negative values indicate a higher protein adsorption relative to bare Au.

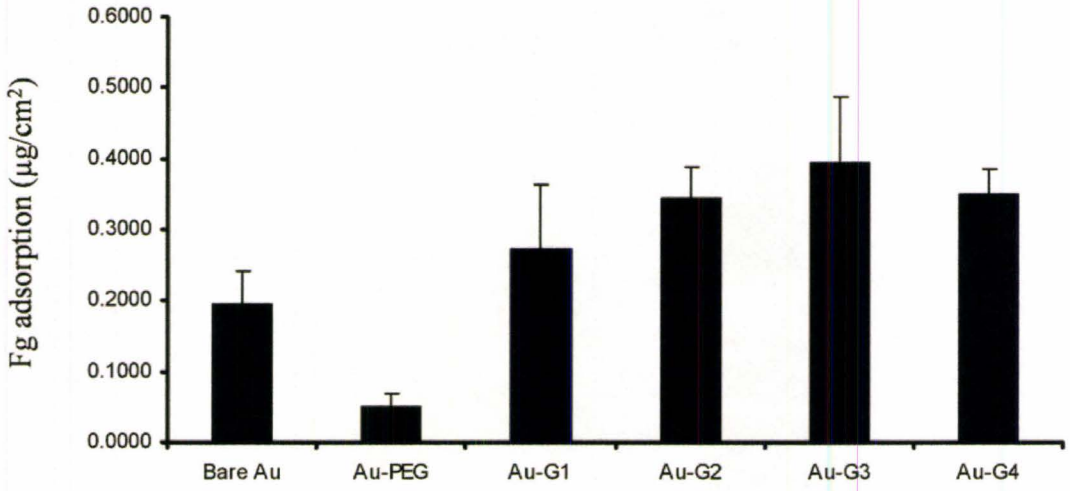

Figure 3.8. Fibrinogen adsorption from plasma: Effect of surface modification with PEG and dendronization with aliphatic polyester dendrons G1-G4.

3.2.8. Lysozyme Adsorption

Lysozyme was also selected for these studies in order to investigate the effect of protein size on adsorption to dendronized surfaces. Lysozyme is a relatively small protein (14.6 kDa) compared to fibrinogen (340 kDa), and therefore its adsorption onto the

modified surfaces could be facilitated by easier diffusion through the dendronized PEG film. The results obtained from protein adsorption from PBS-NaI buffer show that the trend of protein resistance to lysozyme is similar to the one observed with fibrinogen (Figure 3.9). Based on this data, it is clear that the molar quantity of lysozyme deposited on the various surfaces is much higher than that of fibrinogen, as expected due to the difference in protein size. The molar ratios of adsorbed Ly:Fg are given in Table 3.7, and range from 12.8 to 29.2.

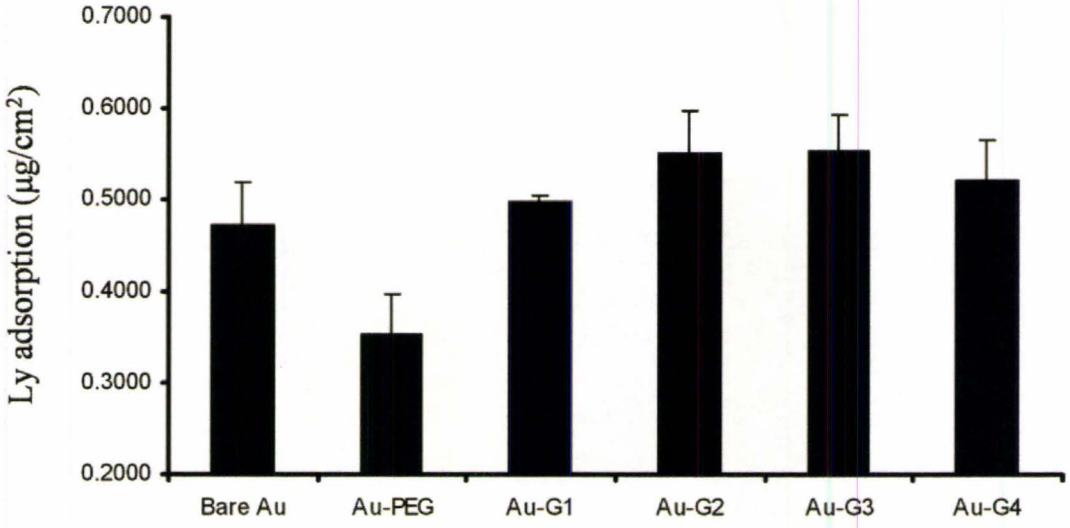

Figure 3.9. Lysozyme adsorption from PBS buffer: Effect of surface modification with PEG and dendronization with aliphatic polyester dendrons G1-G4.

Table 3.7. Comparison between fibrinogen and lysozyme adsorption.

Surface	Fibrinogen ($\mu g/cm^2$)	Reduction vs. control (%)[†]	Lysozyme ($\mu g/cm^2$)	Reduction vs. control (%)[†]	Molar ratio Ly:Fg
Bare Au	0.82 ± 0.1		0.47 ± 0.05		13.4
Au-PEG_{650}	0.28 ± 0.05	66	0.35 ± 0.04	26	29.2
Au-G1(OH)	0.54 ± 0.08	34	0.50 ± 0.01	-6[*]	21.5
Au-G2(OH)	1.00 ± 0.2	-22[*]	0.55 ± 0.05	-17[*]	12.8
Au-G3(OH)	0.91 ± 0.06	-11[*]	0.55 ± 0.04	-17[*]	14.1
Au-G4(OH)	0.94 ± 0.14	-15[*]	0.52 ± 0.04	-11[*]	12.9

[†] The value for bare Au was used as the control
[*] Negative values indicate a higher protein adsorption relative to bare Au.

3.3. Conclusions

Modification of gold-coated silicon wafers with mono-thiolated PEG_{650} was carried out using high ionic strength (IS = 2.9 M) chemisorption solutions for 4 h. Following chemisorption with PEG, the advancing water contact angles decreased significantly compared to the control gold surfaces, indicating an increase in hydrophilicity associated with the PEG chains. High-resolution C1*s* XPS data indicated the presence of a new peak at 286 eV corresponding to ether linkages following chemisorption of the gold surfaces with HS-PEG_{650}-OH. High-resolution S2*p* data showed a photoelectron peak at ~162 eV corresponding to the gold-bound sulfur atoms on the surfaces following PEG grafting, providing further evidence for the presence of PEG chains covalently attached to the surfaces. Further modification of the PEG-grafted surfaces was achieved via divergent dendron growth to introduce aliphatic polyester dendrons, generation 1 to 4, at the PEG-OH chain ends. Characterization of the G1-G4 dendronized surfaces using water contact angles showed a decrease in contact angle with increasing dendron generation for the deprotected OH-terminated dendrons, indicating an

increase in hydrophilicity imparted by the gradually increasing number of peripheral OH groups. The TOF-SIMS results provided detailed structural information of the functionality on the surface. Looking at the signals corresponding to specific peaks belonging to the dendron structure, the transition from the PEG-grafted surfaces to the dendronized ones was clearly demonstrated. In agreement with previously reported protein adsorption studies, PEG-modified surfaces exhibited a decrease in protein adsorption compared to the control gold surfaces. However, it was found that protein adsorption increased upon dendronization of the PEG-modified surfaces, suggesting that PEG chain flexibility may be one of the key factors in the mechanism of protein resistance. This chain flexibility is impeded by introducing dendrons with multiple peripheral OH-groups, which can lock the PEG chains via inter- and/or intra-molecular H-bonding. Future studies will focus on functionalization of the peripheral OH-groups of dendronized surfaces with PEG chains in order to increase surface coverage with PEG and retrieve chain flexibility.

3.4. Experimental

3.4.1. General

DOWEX50W-X2 ion-exchange resin, 4-(Dimethylamino)pyridine (DMAP) (99%), 2,2-Bis(hydroxymethyl)-propionic acid (bis-MPA), 2,2-dimethoxy propane, *p*-toluene-sulfonic acid monohydrate (TsOH), and *N,N'*-dicyclohexylcarbodiimide (DCC) were purchased from Aldrich. Thiol-terminated poly(ethylene glycol) (HS-PEG_{650}-OH)

was purchased from Polymer Source, Inc. Dichloromethane (CH_2Cl_2), ethyl acetate (EtOAc), and hexanes were purchased from CALEDON. Acetonide protected anhydride of bis-MPA (**3.2**) was prepared according to literature procedures.[36] All reagents were used as received.

Gold substrates prepared by electron beam evaporation of silicon wafers with an adhesive titanium tungstate (TiW) layer (300 Å) followed by a layer of gold (1000 Å), were purchased from Thin Film Technology, Buellton, CA, and diced into 1.0 × 1.0 cm^2 pieces. Prior to chemisorption, the surfaces were cleaned, using a literature procedure by immersing them in chromosulfuric acid (H_2SO_4 > 92%, CrO_3 > 1.3%) for 1 h to remove any organic contaminants, followed by ultrasonication in both Milli-Q water and ethanol for 10 minutes, and extensive rinsing with Milli-Q water.[24] Sessile-drop water contact angles were determined using water droplets with a 1-2 μl volume. Advancing and receding angles were obtained using a Ramé–Hart NRL 100-00 goniometer (Mountain Lakes, NJ). All dendronization reactions were carried out on a VWR™ S-500 orbital shaker since no stirring was possible.

X-ray photoelectron spectroscopy (XPS) data were obtained using a Leybold (Specs, Berlin) MAX 200 XPS system employing a non-monochromated Al*Kα* source operating at 15 kV and 20 mA. Low resolution spectra (pass energy = 192 eV) were used to determine atomic compositions; high-resolution C1*s* spectra (pass energy = 48 eV) provided additional surface structural information. Specslab (Specs, Berlin) software was used for spectral fitting. Spectra were taken at two takeoff angles: 90° and 20° relative to

the surface. The respective spot sizes were 4 × 7 and 1 × 1 mm; the smaller area at 20° was used to ensure that the beam footprint remained on the samples.

Time-of-Flight Secondary Ion Mass Spectrometry (TOF-SIMS) measurements were obtained with an ION-TOF TOF-SIMS IV (ION-TOF Gmbh, Germany) instrument using 25 keV Ga^+ primary ions (average current of 2.5 pA) in high current bunched mode. The data was acquired over a 500 × 500 μm^2 area and low-energy electron flooding was used for charge compensation. The primary ion dose was kept below 10^{12} ions cm^{-2} to ensure static SIMS condition. The mass calibrations of the positive and negative ion spectra were performed internally using CH_3^+, $C_2H_3^+$, $C_2H_5^+$, and $C_5H_7^+$ peaks and C^-, CH^-, C_2H^-, C_3H^-, and C_4H^- peaks, respectively. A complementary approach of the hypothesized structure of the surface has been used to identify and assign specific fragments.

Atomic force microscopy (AFM) analyses were carried out using a Digital Instruments NanoScope IIIa Multimode AFM equipped with a vertical engage "E" scanner with 15 μm full range scan. The images were recorded with standard tips in tapping mode at a scan rate of 0.5 Hz.

3.4.2. Proteins

Fibrinogen was purchased from Calbiochem (La Jolla, CA), dialyzed against Tris buffer, pH 7.4, aliquoted, and stored at -70 °C. The molecular weight and dimensions of fibrinogen are 3.4×10^5 Da and 450 × 90 × 90 $Å^3$, respectively, and its isoelectric point is 5.5. Lysozyme was obtained from Calbiochem (La Jolla, CA) and used as received. The

molecular weight and dimensions of lysozyme are 1.43×10^4 Da and $45 \times 30 \times 30$ Å^3, respectively, and its isoelectric point is 11.0.

3.4.3. Chemisorption of surfaces with HS-PEG$_{650}$-OH

After cleaning, the surfaces were immediately transferred to 24-well plates containing the chemisorption solution. This solution consisted of 5 mM of HS-PEG$_{650}$-OH in phosphate-buffered saline (PBS) at pH 7.4. The chemisorption was carried out for various time periods at 25 °C with two different ionic strengths (IS), adjusted using sodium chloride (NaCl), in order to optimize the conditions for surface chain density. Following chemisorption, the surfaces were transferred to vials containing Milli-Q water and ultrasonicated for 10 min. This was followed by ultrasonication in ethanol for 10 min, and finally extensive rinsing with Milli-Q water (~20 mL). The surfaces were dried with a stream of nitrogen (N_2) prior to contact angle, XPS, and AFM analysis.

3.4.4. General esterification reaction: preparation of Au-G1(Ac) surfaces

To flame-dried 15 mL vials under argon, each charged with a PEG$_{650}$-functionalized surface in a solution of CH_2Cl_2:pyridine (3:2 v/v, 3 mL), excess acetonide anhydride (**3.1**) (0.1 g, 3.03×10^{-4} mol) along with a catalytic amount of DMAP (10 mg, 8.18×10^{-5} mol) was added and the vials were shaken for 24 h at room temperature using an orbital shaker since no stirring was possible. The surfaces were transferred to new individual vials containing CH_2Cl_2 (5 mL) and ultrasonicated for 10 min to remove the unreacted acetonide anhydride. This was followed by ultrasonication of the surfaces in

Milli-Q water (~5 mL) for 10 min, and extensive rinsing with Milli-Q water (~20 mL) and ethanol (~20 mL), and finally drying with a stream of N_2 prior to analysis. For subsequent dendronization steps, all reagent quantities remained the same except for the amount of acetonide (**3.2**), the amount of DMAP, and the reaction time, which were as follows: Au-G2(Ac): 0.12 g of **3.2**, 12 mg of DMAP, 36 h; Au-G3(Ac): 0.15 g of **3.2**, 15 mg of DMAP, 48 h; Au-G4(Ac): 0.2 g of **3.2**, 20 mg of DMAP, 72 h.

3.4.5. General deprotection reaction: preparation of Au-G1(OH) surfaces

The G1(Ac)-functionalized surfaces were individually placed in 5 mL vials charged with methanol (5 mL). To these vials was added the acidic resin DOWEX 50W-X2 (~0.50 g) such that complete coverage of the grafted surfaces was achieved. The vials were transferred to an oil bath at 50 °C and incubated for 1h. The surfaces were transferred to new vials charged with methanol (5 mL) and ultrasonicated for 10 min. This step was followed by extensive rinsing with methanol (~20 mL), and immersion in methanol overnight. The surfaces were then dried with a stream of N_2 prior to the next esterification reaction. Deprotection of higher generation dendronized surfaces was done identically to the above.

3.4.6. AFM analysis

The AFM analyses were carried out using the "scratch" method, where a scratch was introduced on a clean gold surface prior to functionalization. To assure that the scratch penetrated the entire gold layer, scratch thickness was measured by AFM at

numerous points along the scratch, and compared to the known gold layer thickness from the manufacturer (100 nm). If the "trench" produced by scratching the surface was equal to or greater than 100 nm, the surface was used for subsequent experiments. On one side, across the scratch, the gold surface was coated with a temporary layer of poly(styrene) (PS) to prevent chemisorption of HS-PEG_{650}-OH, leaving this half unfunctionalized. After chemisorption on the exposed side, the surface was rinsed extensively with THF (~50 mL) to remove the PS film. The partially functionalized surface was ultrasonicated for 10 min in both Milli-Q water and ethanol and dried with N_2 prior to AFM analysis. AFM step-height measurements were carried out at multiple points (15 × 15 μm^2) of both unfunctionalized and PEG-grafted parts of the surface. Using the average mode in the AFM Nanoscope-(R) III Digital Instruments-version 5.30 program at each image collected, the PEG film thickness was calculated as the difference in average height between the two parts of the surface. Similar height measurements were carried out on the same surface after esterification of PEG-OH to introduce the first generation protected dendrons, and at each step of dendronization up to the fourth generation.

3.4.7. Protein Adsorption

Fibrinogen and lysozyme (Calbiochem, La Jolla, CA) were radiolabeled with $Na^{125}I$ (ICN, Irvine, CA) using the iodine monochloride method and passed through a column packed with AG® 1-X4 resin (Bio-Rad Laboratories, Inc.) in Tris buffer saline (TBS, pH 7.4) to remove unbound ^{125}I (held to <1% of total solution radioactivity). Prior to protein adsorption experiments, gold-coated silicon wafers were equilibrated in PBS-

NaI buffer overnight; "cold" NaI was added to the buffer to prevent uptake of unbound ^{125}I to the gold.[37] Protein adsorption experiments were performed in PBS-NaI buffer (pH 7.4) at a protein concentration of 1 mg/mL (10% labeled, 90% "cold"/PBS, and 2.5% labeled, 97.5% "cold"/plasma). The surfaces were placed in the wells of 24-well plates and incubated in a 1 mL solution of ^{125}I-labeled protein in PBS-NaI for 3 h at room temperature (22 °C). It was determined that no further adsorption occurred at times longer than 3 h.[3] The surfaces were rinsed three times (10 min each) with fresh PBS-NaI to remove any loosely bound protein. Surface radioactivity was determined, using a Perkin Elmer™ WIZARD™ 3'' 1480 automatic gamma counter. The percent reduction of adsorption on the PEO-functionalized and dendronized surfaces relative to the unmodified gold was determined.

3.5. References

(1) Castner, D. G.; Ratner, B. D. *Surf Sci* **2002**, *500*, 28-60.
(2) Kane, R. S.; Deschatelets, P.; Whitesides, G. M. *Langmuir* **2003**, *19*, 2388-2391.
(3) Unsworth, L. D.; Sheardown, H.; Brash, J. L. *Langmuir* **2005**, *21*, 1036-1041.
(4) Santini, J. T.; Cima, M. J.; Langer, R. *Nature* **1999**, *397*, 335-338.
(5) Xu, F. J.; Li, Y. L.; Kang, E. T.; Neoh, K. G. *Biomacromolecules* **2005**, *6*, 1759-1768.
(6) Frazier, R. A.; Matthijs, G.; Davies, M. C.; Roberts, C. J.; Schacht, E.; Tendler, S. J. B. *Biomaterials* **2000**, *21*, 957-966.
(7) Rabinow, B. E.; Ding, Y. S.; Qin, C.; Mchalsky, M. L.; Schneider, J. H.; Ashline, K. A.; Shelbourn, T. L.; Albrecht, R. M. *J Biomat Sci-Polym E* **1994**, *6*, 91-109.
(8) Lehmann, T.; Ruhe, J. *Macromol Symp* **1999**, *142*, 1-12.
(9) Heyes, C. D.; Groll, J.; Moeller, M.; Nienhaus, G. U. *Mol Biosyst* **2007**, *3*, 419-430.
(10) Sofia, S. J.; Premnath, V.; Merrill, E. W. *Macromolecules* **1998**, *31*, 5059-5070.
(11) Yang, Z. H.; Galloway, J. A.; Yu, H. U. In *Langmuir* 1999; Vol. 15, p 8405-8411.
(12) Unsworth, L. D.; Sheardown, H.; Brash, J. L. *Biomaterials* **2005**, *26*, 5927-5933.
(13) Zolk, M.; Eisert, F.; Pipper, J.; Herrwerth, S.; Eck, W.; Buck, M.; Grunze, M. *Langmuir* **2000**, *16*, 5849-5852.
(14) Jeon, S. I.; Andrade, J. D. *J Colloid Interf Sci* **1991**, *142*, 159-166.
(15) Jeon, S. I.; Lee, J. H.; Andrade, J. D.; de Gennes, P. G. *J Colloid Interf Sci* **1991**, *142*, 149-158.
(16) Albertsson, A. C.; Karlsson, S. *J Macromol Sci Pure Appl Chem* **1996**, *A33*, 1565-1570.
(17) Wang, R. L. C.; Kreuzer, H. J.; Grunze, M. *J Phys Chem B* **1997**, *101*, 9767-9773.
(18) Morra, M. *J Biomat Sci-Polym E* **2000**, *11*, 547-569.
(19) Nagaoka, S.; Mori, Y.; Takiuchi, H.; Yokota, K.; Tanzawa, H.; Nishiumi, S. *in Polymers as Biomaterials (Eds.: S.W. Shalaby, A. S. Hoffman, B. D. Ratner, T. A. Horbett), Plenum, New York* **1984**, 661-374.
(20) Andrade, J. D.; Hlady, V. *Adv Polym Sci* **1986**, *79*, 1-63.
(21) Harder, P.; Grunze, M.; Dahint, R.; Whitesides, G. M.; Laibinis, P. E. *J Phys Chem B* **1998**, *102*, 426-436.
(22) Unsworth, L. D.; Tun, Z.; Sheardown, H.; Brash, J. L. *J Colloid Interf Sci* **2006**, *296*, 520-526.
(23) Wojciechowski, P.; Tenhove, P.; Brash, J. L. *J Colloid Interf Sci* **1986**, *111*, 455-465.
(24) Ostmark, E.; Macakova, L.; Auletta, T.; Malkoch, M.; Malmstrom, E.; Blomberg, E. *Langmuir* **2005**, *21*, 4512-4519.
(25) Gillies, E. R.; Frechet, J. M. J. *J Am Chem Soc* **2002**, *124*, 14137-14146.
(26) Haag, R.; Sunder, A.; Stumbe, J. F. *J Am Chem Soc* **2000**, *122*, 2954-2955.
(27) Lee, C. C.; MacKay, J. A.; Frechet, J. M. J.; Szoka, F. C. *Nat Biotechnol* **2005**, *23*, 1517-1526.
(28) Yam, C. M.; Deluge, M.; Tang, D.; Kumar, A.; Cai, C. Z. *J Colloid Interf Sci* **2006**, *296*, 118-130.

(29) Sunder, A.; Mulhaupt, R.; Haag, R.; Frey, H. *Adv Mater* **2000**, *12*, 235-239.
(30) Siegers, C.; Biesalski, M.; Haag, R. *Chem-Eur J* **2004**, *10*, 2831-2838.
(31) Hong, M. Y.; Yoon, H. C.; Kim, H. S. *Langmuir* **2003**, *19*, 4866-4866.
(32) Hong, M. Y.; Kim, Y. J.; Lee, J. W.; Kim, K.; Lee, J. H.; Yoo, J. S.; Bae, S. H.; Choi, B. S.; Kim, H. S. *J Colloid Interf Sci* **2004**, *274*, 41-48.
(33) Ostuni, E.; Chapman, R. G.; Holmlin, R. E.; Takayama, S.; Whitesides, G. M. *Langmuir* **2001**, *17*, 5605-5620.
(34) Ihre, H. R.; De Jesus, O. L. P.; Szoka, F. C.; Frechet, J. M. J. *Bioconjugate Chem* **2002**, *13*, 443-452.
(35) De Jesus, O. L. P.; Ihre, H. R.; Gagne, L.; Frechet, J. M. J.; Szoka, F. C. *Bioconjugate Chem* **2002**, *13*, 453-461.
(36) Malkoch, M.; Malmstrom, E.; Hult, A. *Macromolecules* **2002**, *35*, 8307-8314.
(37) Du, Y. J.; Cornelius, R. M.; Brash, J. L. *Colloid Surf B* **2000**, *17*, 59-67.
(38) Kingshott, P.; Thissen, H.; Griesser, H. J. *Biomaterials* **2002**, *23*, 2043-2056.
(39) Ihre, H.; De Jesus, O. L. P.; Frechet, J. M. J. *J Am Chem Soc* **2001**, *123*, 5908-5917.
(40) Vestberg, R.; Nystrom, A.; Lindgren, M.; Malmstrom, E.; Hult, A. *Chem Mater* **2004**, *16*, 2794-2804.
(41) Wu, P.; Malkoch, M.; Hunt, J. N.; Vestberg, R.; Kaltgrad, E.; Finn, M. G.; Fokin, V. V.; Sharpless, K. B.; Hawker, C. J. *Chem Commun* **2005**, 5775-5777.
(42) Vestberg, R.; Westlund, R.; Eriksson, A.; Lopes, C.; Carlsson, M.; Eliasson, B.; Glimsdal, E.; Lindgren, M.; Malmstrom, E. *Macromolecules* **2006**, *39*, 2238-2246.
(43) Yim, S. H.; Huh, J.; Ahn, C. H.; Park, T. G. *Macromolecules* **2007**, *40*, 205-210.
(44) Goh, S. L.; Francis, M. B.; Frechet, J. M. J. *Chem Commun* **2002**, 2954-2955.
(45) Liang, C. O.; Helms, B.; Hawker, C. J.; Frechet, J. M. J. *Chem Commun* **2003**, 2524-2525.
(46) Malkoch, M.; Carlmark, A.; Wodegiorgis, A.; Hult, A.; Malmstrom, E. E. *Macromolecules* **2004**, *37*, 322-329.
(47) Malkoch, M.; Thibault, R. J.; Drockenmuller, E.; Messerschmidt, M.; Voit, B.; Russell, T. P.; Hawker, C. J. *J Am Chem Soc* **2005**, *127*, 14942-14949.
(48) Lee, C. C.; Frechet, J. M. J. *Macromolecules* **2006**, *39*, 476-481.
(49) Hietala, S.; Nystrom, A.; Tenhu, H.; Hult, A. *J Polym Sci Part A Polym Chem* **2006**, *44*, 3674-3683.
(50) Nystrom, A.; Malkoch, M.; Furo, I.; Nystrom, D.; Unal, K.; Antoni, P.; Vamvounis, G.; Hawker, C.; Wooley, K.; Malmstrom, E.; Hult, A. *Macromolecules* **2006**, *39*, 7241-7249.
(51) Ihre, H.; Hult, A.; Frechet, J. M. J.; Gitsov, I. *Macromolecules* **1998**, *31*, 4061-4068.
(52) Ling, F. H.; Lu, V.; Svec, F.; Frechet, J. M. J. *J Org Chem* **2002**, *67*, 1993-2002.
(53) Lonnberg, H.; Zhou, Q.; Brumer, H.; Teeri, T. T.; Malmstrom, E.; Hult, A. *Biomacromolecules* **2006**, *7*, 2178-2185.
(54) King, D. E. *J Vac Sci Technol A* **1995**, *13*, 1247-1253.
(55) Malmsten, M.; Emoto, K.; Van Alstine, J. M. *J. Colloid Interface Sci.* **1998**, *202*, 507.
(56) Chen, H.; Brook, M. A.; Sheardown, H. *Biomaterials* **2004**, *25*, 2273-2282.

(57) McGurk, S. L.; Green, R. J.; Sanders, G. H. W.; Davies, M. C.; Roberts, C. J.; Tendler, S. J. B.; Williams, P. M. *Langmuir* **1999**, *15*, 5136-5140.
(58) Unsworth, L. D.; Sheardown, H.; Brash, J. L. *Langmuir* **2005**, *21*, 1036-1041.
(59) Shen, M. C.; Horbett, T. A. *J Biomed Mater Res* **2001**, *57*, 336-345.

Chapter 4: Protein Resistance of PEG-Functionalized Dendronized Surfaces: Effect of PEG Molecular Weight and Dendron Generation

Abstract

Dendronized surfaces were prepared by chemisorption of poly(ethylene glycol) mono-thiol (HS-PEG_{650}-OH) onto gold-coated silicon wafers followed by functionalization of the PEG terminal OH-group with aliphatic polyester dendrons, generation 1 to 4, using divergent dendron growth. PEG mono-methyl ether (PEG-OMe) chains of various molecular weight (MW) were covalently attached to the peripheral hydroxyl groups of the dendronized surfaces via EDC coupling, and investigated for protein adsorption. Protein adsorption studies were carried out using fibrinogen (Fg) and lysozyme (Lys) as model proteins from phosphate buffered saline (PBS) (Fg, Lys) and plasma (Fg). In the first part of this study, the effect of functionalization of the peripheral hydroxyl groups with PEG-OMe oligomers (M_n = 350 Da) on protein adsorption was investigated. Results showed that adsorption of both Fg and Lys was reduced when dendronized surfaces were grafted with PEG-OMe oligomers. To investigate the effect of molecular weight on protein adsorption, PEG-OMe chains of greater length (750, 2000, and 5000 Da) were coupled to first generation dendronized surfaces (Au-G1(OH)). Results showed that protein adsorption decreased with increasing PEG-OMe MW up to 2000 Da. To further investigate the effect of dendron generation on protein resistance, dendronized surfaces of generation 1 to 4 were coupled with PEG_{2000}-acid. Subsequent protein studies showed a decrease in Fg and Lys adsorption with increasing dendron

generation. This chapter has been reproduced in part with permission from *Macromolecules* **2008**, 4817-4823. Copyright 2008 American Chemical Society.

4.1. Introduction

Development of surfaces with anti-fouling properties is of significant interest in biomedical applications, where biocompatibility of materials continues to be the primary issue.[1-8] Non-specific protein adsorption, known as the first event that follows implantation of biomaterials, is very important in initiating further events that determine host responses, such as blood coagulation, thrombus formation, and bacterial infection.[9,10] In the past two decades a number of studies investigating low-fouling surfaces have been reported in the literature, however, only few materials exhibit a significant reduction in non-specific protein adsorption sufficient to prevent such adverse events as platelet adhesion.[6,9,11-15] A number of experimental studies showed that surfaces displaying poly(ethylene glycol) (PEG) are known for their resistance to protein adsorption and cell adhesion.[5-10] It is believed that the effectiveness of PEG for repelling proteins is related to its highly hydrated nature under physiological conditions, and formation of a steric barrier by the PEG chains.[16-18] Several theories have been reported in the literature on the mechanism of protein resistance of PEG-functionalized surfaces, but a fundamental understanding of protein resistance at the molecular level has yet to be achieved.[19-26] From the various literature-reported protein-repelling surfaces modified with short or long segments of PEG, a number of criteria responsible for protein repulsion have been identified. Several of these reports attribute protein repulsion to the high dynamics of the PEG chains in water,[27] and molecular conformation of the segments at the interface.[28,29] Other criteria for enhanced protein resistance were reported by Whitesides and co-workers, and included high hydrophilicity, the presence of hydrogen-bond acceptors, and

the absence of hydrogen-bond donors.[30] However, other studies have demonstrated that good protein resistance can be achieved with molecules comprising a large number of hydrogen-bond donors, such as hydroxyl groups and carboxylic acid groups.[31,32]

When analyzing the reported structural properties of protein-resistant surfaces, as well as previous results by Haag and co-workers,[33] and Zhu and co-workers,[34] it became apparent that the presence of highly flexible and hydrophilic groups, combined with a highly branched architecture, can lead to good protein resistance. Based on these findings, we have prepared a series of gold surfaces coated with hydrophilic aliphatic polyester dendrons, in an attempt to study their protein resistance properties.[35] By analogy to previous results reported on branched architectures,[36] the aim of our study was to covalently functionalize PEG-grafted surfaces with aliphatic polyester dendrons to improve the overall surface coverage and surface hydrophilicity, which would potentially lead to enhanced protein resistance based on previous observations.[33,34,36] As expected, the hydrophilicity of the resulting surfaces increased with increasing dendron generation, as a result of the numerous hydroxyl groups at the periphery. However, contrary to our expectation, protein resistance was found to decrease when the surfaces were covalently functionalized with the hydrophilic dendrons.[35] It was postulated that several factors could be responsible for the increased protein adsorption to the dendronized surfaces, including increased surface area, the introduction of hydrogen-bond donor groups,[14,30] and a decrease in the mobility of the surface-grafted polymers as a result of inter- and intra-molecular hydrogen bonding between the numerous hydroxyl groups at the dendron periphery. To circumvent these confounding phenomena, while maintaining surface

hydrophilicity, we have chosen to covalently attach PEG-OMe chains of various molecular weight to the peripheral hydroxyl groups of first to fourth generation dendronized surfaces. Here we report the synthesis and characterization of the resulting surfaces, functionalized with PEG-OMe star polymers having 2, 4, 8, and 16 arms, and PEG-OMe molecular weight of 350, 750, 2000, and 5000 Da. We present the results of protein adsorption studies to these surfaces using fibrinogen and lysozyme.

4.2. Results and Discussion

Building on our results with dendronized surfaces, we set out to investigate the reason for increased protein adsorption on the previously reported surfaces. As stated in the introduction, the possible reasons for increased fouling could be the presence of hydrogen-bond donors (OH-groups) and a rigidifying effect of the underlying PEG layer due to inter- and intra-molecular hydrogen-bonding of the dendrons. Haag and coworkers have shown that methylation of the hydroxyl groups of surfaces functionalized with hyperbranched polyglycelrols slightly improves protein resistance.[33] We initially chose a similar approach using acetonide-protected G1 to G4 dendrons. However, protein adsorption increased likely due to increased hydrophobicity imparted by the methyl groups at the periphery of the protected dendrons (data given in Appendix I, Figures 4.I.3 and 4.I.4). Clearly any attempt to eliminate hydrogen-bonding must be done in a way that maintains the initial surface hydrophilicity. Therefore, we chose to investigate the introduction of short PEG-OMe oligomers to first generation dendronized surfaces. These

structures do not exhibit hydrogen-bond donating groups, but retain the hydrophilicity required.

4.2.1. Synthesis

The synthesis of dendronized surfaces was performed by divergent growth of aliphatic polyester dendrons as previously described.[35] The resulting hydroxyl terminated dendrons were subsequently functionalized with PEG mono-methyl ether (PEG-OMe) chains of different molecular weight using 1-(3-dimethylaminopropyl)-3-ethylcarbodiimide hydrochloride (EDC) coupling with a PEG-acid derivative (Scheme 4.1). This was accomplished by first converting the terminal hydroxyl group of PEG-mono methyl ether (PEG-OMe) to a carboxylic acid group using the TEMPO-mediated oxidation reported by Masson et al.[40] The peripheral hydroxyl groups of the dendronized surfaces were subsequently reacted with excess PEG-acid of specific molecular weight in the presence of EDC and a catalytic amount of 4-(dimethylamino)pyridine/*p*-toluene sulphonic acid (DPTS). The coupling reaction was carried out for 72 h at room temperature.

Scheme 4.1. EDC coupling of PEG-acid to a G1(OH)-dendronized surface.

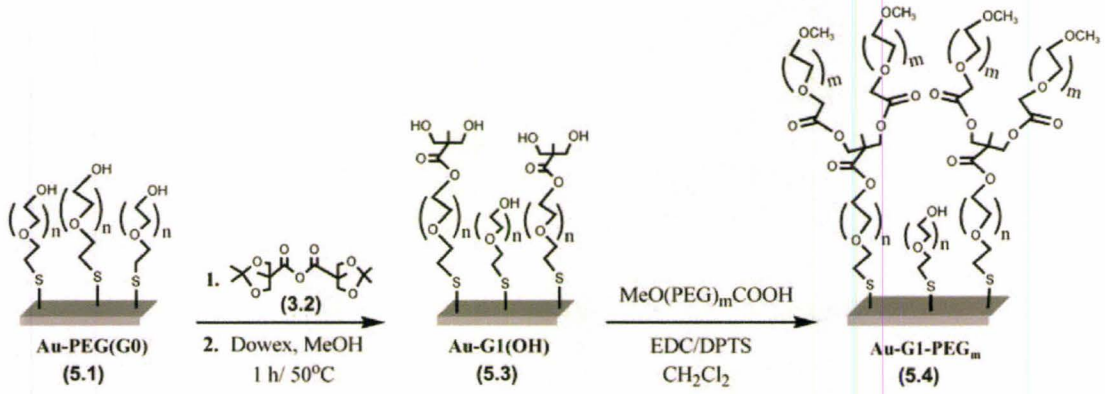

4.2.2. Modification of dendronized surfaces with PEG mono-methyl ether (PEG-OMe) oligomers

A preliminary study was carried out by coupling PEG-acid oligomers (M_n = 350 Da) to first generation (G1) dendronized surfaces. The results from contact angles showed that the hydrophilicity of the original G1-dendronized surface was retained after coupling of the peripheral hydroxyl groups with PEG-acid oligomers (Table 4.1). More importantly, protein adsorption results showed that fibrinogen and lysozyme adsorption decreased as a result of this modification (Figures 4.2.4).

Encouraged by this result, we decided to investigate longer PEG-OMe chains (M_n = 750 Da, 2000 Da, 5000 Da) to determine the effect of molecular weight on protein adsorption. Upon functionalization of the peripheral hydroxyl groups with PEG-acid chains of various MW, the effect of PEG-OMe length on surface hydrophilicity was measured by contact angle goniometry. The results, summarized in Table 4.1 and Figure 4.1, showed that the advancing contact angles for the PEG-functionalized G1-dendronized surfaces ranged between 41° ± 2° and 19° ± 2°, and the receding angles

ranged between 20° ± 4° and 12° ± 2° for PEG MWs of 350 Da to 5000 Da, respectively. These results reflect the hydrophilicity of the PEG-grafted G1-dendronized surfaces, which increased with increasing PEG-OMe chain length (Table 4.1, Figure 4.1). The data also indicate that the hydrophilic nature of the original G1-dendronized surfaces was retained and improved after coupling of the PEG-OMe chains, which was a requirement for the present study.

Table 4.1. Water contact angles (°) of PEG-grafted G1-dendronized surfaces: Effect of PEG molecular weight.

Surface	Advancing contact angle (°)	Receding contact angle (°)
Bare Au	65 ± 3	40 ± 8
Au-PEG_{650}*	42 ± 4	36 ± 2
Au-G1(OH)	40 ± 2	22 ± 3
Au-G1-PEG_{350}	41 ± 2	20 ± 4
Au-G1-PEG_{750}	38 ± 3	19 ± 4
Au-G1-PEG_{2000}	30 ± 5	12 ± 2
Au-G1-PEG_{5000}	19 ± 2	12 ± 2

*5 mM chemisorption solution of HS-PEG_{650}-OH in PBS at pH = 7.4

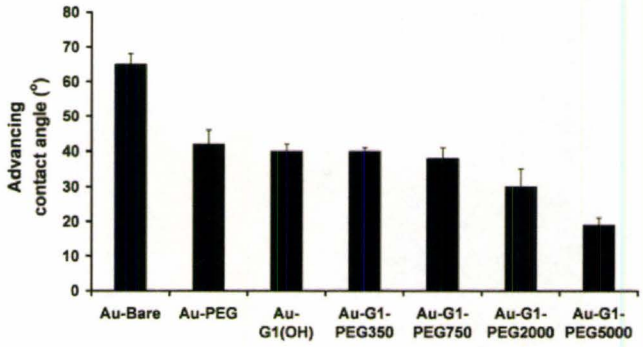

Figure 4.1. Advancing contact angles of Au, Au-PEG, Au-G1(OH), and Au-G1-$PEG_{350\text{-}5000}$ surfaces.

4.2.3. AFM Analysis

The topographies of the G1-dendronized surfaces prior to and after grafting with PEG-acid chains of various MW were examined by AFM. The results from the 3D AFM height images showed the presence of a large number of small bumps on the PEG-functionalized G1-dendronized surfaces. These observed features were absent in the control bare gold surface and Au-G1(OH) surface (Figure 4.I.1, Appendix I). Surface roughness was calculated and the results, presented in Table 4.2, showed an increase in surface roughness when G1-dendronized surfaces were coupled with PEG-acid chains, with values ranging between 3.42 nm for the Au-G1-PEG_{350} and 6.14 nm for Au-G1-PEG_{5000} surfaces. This increase in surface roughness is consistent with our previous results comparing the roughness of bare Au to PEG-functionalized and dendronized surfaces. Surface roughness increased with increasing surface functionalization, likely due to the formation of polymer-rich domains composed of PEG chains and dendrons on the gold.[18,43]

Table 4.2. Root-mean-square (Rms) roughness of PEG-functionalized dendronized surfaces obtained from AFM data: effect of PEG molecular weight.

Surface	Rms (nm)
Bare gold	1.26
Au-G1(OH)	3.27
Au-G1-PEG_{350}	3.42
Au-G1-PEG_{750}	4.97
Au-G1-PEG_{2000}	5.88
Au-G1-PEG_{5000}	6.14

4.2.4. Protein adsorption studies

4.2.4.1. Fibrinogen adsorption

The effect of surface functionalization with first-generation dendrons that were peripherally modified with PEG-OMe of various lengths on protein adsorption was investigated. In our previous study, it was found that protein adsorption increased upon surface dendronization with aliphatic polyester dendrons of generation 1 to 4 when compared to the control PEG-grafted surfaces.[35] To investigate the reason behind these results, we performed similar protein studies, but with G1-dendronized surfaces that were functionalized with PEG-OMe of different chain length. Initial studies using fibrinogen (Fg) were carried out from both phosphate buffered saline (PBS) and plasma (Figures 4.2 and 4.3, respectively). All protein experiments were repeated twice using triplicate samples at every functionalization step in order to confirm the observed trend of Fg adsorption onto the various surfaces. From these experiments, in contrast to OH-terminated dendronized surfaces, it was found that protein adsorption decreased when G1-dendronized surfaces were modified with PEG-OMe oligomers. This decrease in protein adsorption was even more significant when longer PEG-OMe chains were grafted to the dendronized surfaces reaching an optimum decrease at MW of 2000 Da (Figures 4.2 and 4.3). Interestingly, when the PEG-OMe MW was further increased to 5000 Da, protein repulsion did not improve. Although we cannot provide a definite explanation for this latter result, some contributing factors might include the difficulty for the system to achieve optimum chain density and mobility with longer PEG chains, an observation previously reported by Brash and co-workers.[44]

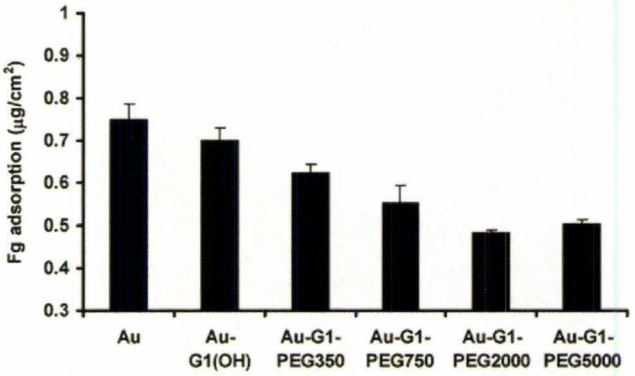

Figure 4.2. Fibrinogen adsorption from 1 mg/mL Fg-Fg-^{125}I in PBS-NaI on G1-dendronized surfaces functionalized with PEG chains of various molecular weight.

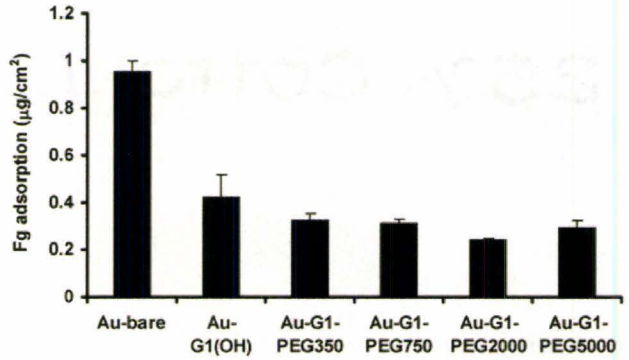

Figure 4.3. Fibrinogen adsorption from 1 mg/mL Fg-Fg-^{125}I in plasma on G1-dendronized surfaces functionalized with PEG chains of various molecular weight.

4.2.4.2. Lysozyme adsorption

To determine whether the degree of adsorption is influenced by the nature of the protein, we chose to also carry out these studies with Lysozyme (Lys), which is a much smaller protein relative to fibrinogen. Additionally, under our experimental conditions

(PBS, pH 7.4), lysozyme is positively charged while fibrinogen is negatively charged. Hence, it would be expected that these two proteins would respond to the PEG-functionalized dendronized surfaces in different ways. In our studies electrostatic interactions should not influence protein adsorption as the dendronized and PEG-functionalized surfaces are neutral under our conditions. Therefore, differences in size and surface functionality between the two proteins are expected to be dominant factors influencing adsorption. Moreover, the use of Lys allowed us to make quantitative comparisons with the results of Fg and Lys onto dendronized surfaces that we reported previously.[35] Similarly to fibrinogen, all protein studies were repeated twice using triplicate samples at every functionalization step to assure reproducibility of the results. From these experiments, it was again found that functionalization of the G1-dendronized surfaces with PEG-OMe chains enhanced protein resistance, but the improved resistance was only significant when PEG_{2000} and PEG_{5000} chains were grafted (Figure 4.4). Again, it was found that increasing PEG-OMe MW from 2000 to 5000 Da did not improve protein resistance, indicating a limit to the effective MW for protein resistance. Overall, these results show that grafting PEG-OMe to dendronized surfaces improves protein repulsion irrespective of the nature of the protein, which is in agreement with previous studies.[15,35,44] The requirement for higher PEG molecular weights (relative to results with fibrinogen) before appreciable decrease in adsorption was observed is likely a result of lysozyme's greater ability to diffuse through small openings within the PEG coating to reach and adsorb to the Au surface.

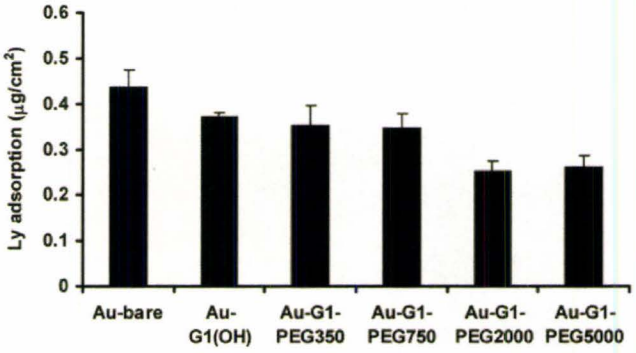

Figure 4.4. Lysozyme adsorption from 1 mg/mL Lys-Lys-^{125}I in PBS-NaI of G1-dendronized surfaces functionalized with PEG chains of various molecular weight.

4.2.5. Effect of dendron generation on protein adsorption

From the results obtained in the first part of this study, in which the effect of PEG-OMe MW on protein adsorption was investigated, it was found that surfaces functionalized with PEG_{2000}-OMe exhibited greatest protein resistance for both fibrinogen and lysozyme. Based on these results, PEG_{2000}-OMe was subsequently coupled to higher generation dendrons to produce PEG star-polymers having 2, 4, 8, and 16 arms. The synthesis of PEG star-polymers on the Au surfaces was carried out by esterification of the terminal hydroxyl groups of surface bound G1 to G4 dendrons with PEG_{2000}-acid (Scheme 4.2).

Initial characterization of the surface bound PEG star polymers was accomplished by contact angle measurements. The results, summarized in Table 4.3 and Figure 4.5, showed that the advancing contact angles for the PEG_{2000}-functionalized G1-G4-dendronized surfaces ranged between 33° ± 2° and 27° ± 3°, and the receding angles

ranged between 12° ± 2° and 10° ± 3° for G1-PEG_{2000} to G4-PEG_{2000} respectively. These results indicated that the hydrophilic character of the PEG-star functionalized surfaces was slightly superior to that of just the dendron-grafted surfaces at each generation (Table 4.3, Figure 4.5).[35]

Table 4.3. Water contact angles (°) of PEG_{2000}-grafted G1-G4 dendronized surfaces: Effect of dendron generation.

Surface	Advancing contact angle (°)	Receding contact angle (°)
Bare Au	65 ± 3	40 ± 8
Au-PEG_{650}*	42 ± 4	36 ± 2
Au-G1(OH)	40 ± 2	22 ± 3
Au-G1-PEG_{2000}	33 ± 2	12 ± 2
Au-G2-PEG_{2000}	30 ± 2	10 ± 2
Au-G3-PEG_{2000}	29 ± 2	9 ± 4
Au-G4-PEG_{2000}	27 ± 3	10 ± 3

*5 mM chemisorption solution of HS-PEG_{650}-OH in PBS at pH = 7.4

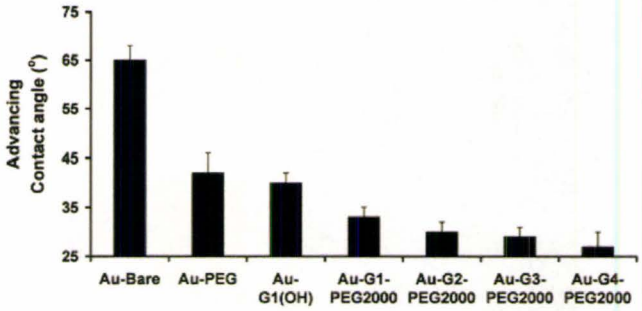

Figure 4.5. Advancing contact angles of Au, Au-PEG, Au-G1(OH), and Au-G1-PEG_{2000} to Au-G4-PEG_{2000} surfaces.

Scheme 4.2. EDC coupling of PEG_{2000}-acid to G1-G4-dendronized surfaces.

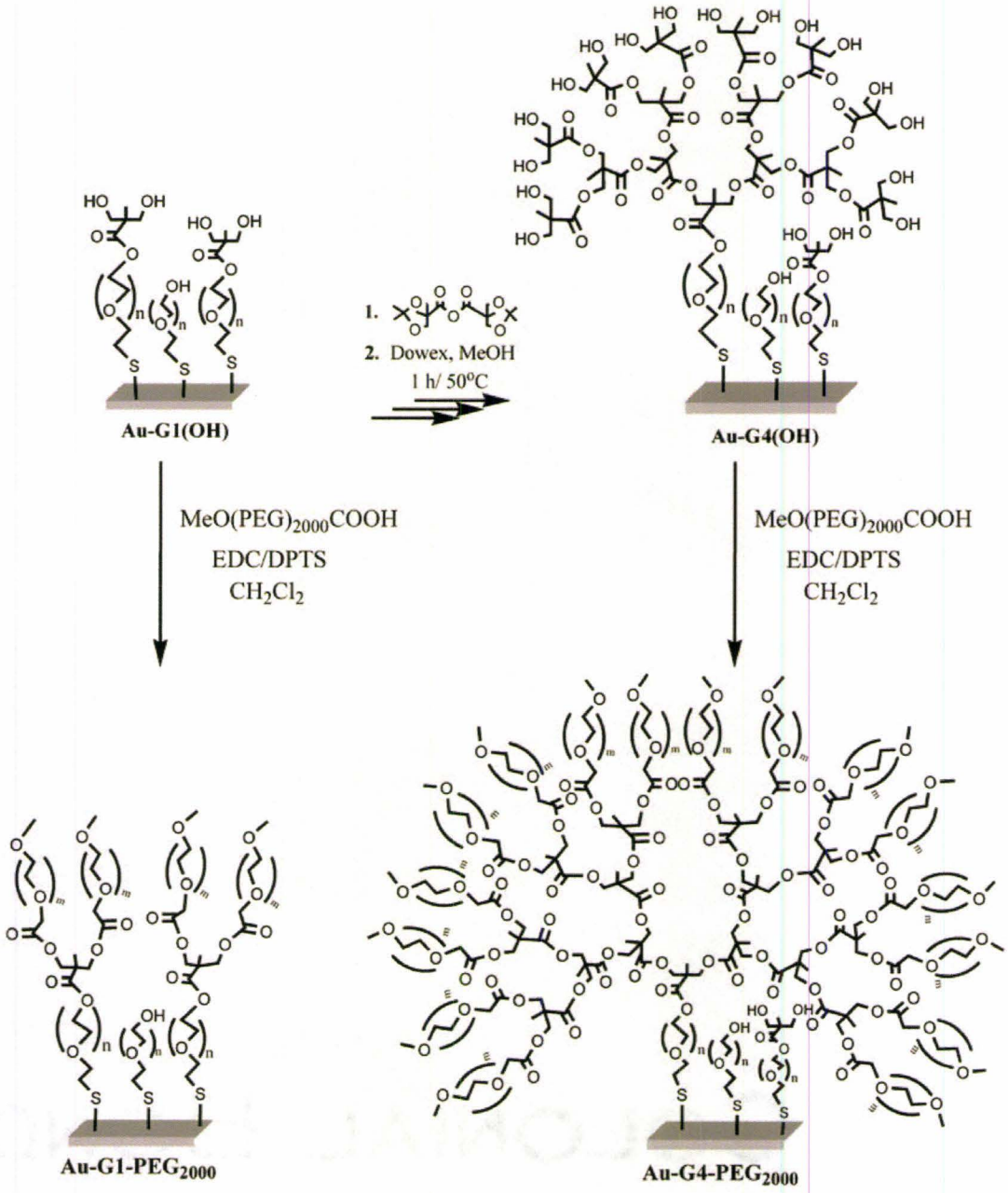

4.2.6. AFM analysis

The surface topographies of the functionalized gold surfaces prior to and after grafting of PEG_{2000}-acid to the G1-G4 dendronized surfaces were also examined by AFM. The 3D height images of the PEG_{2000}-functionalized dendronized surfaces showed the presence of a large number of small peaks and valleys, features that are absent on the control surface (Au-bare) and which became more significant with increasing dendron generation (Figure 4.I.2, Appendix I). The presence of these features resulted in a significant increase in surface roughness of the PEG_{2000}-grafted dendronized surfaces, which ranged between 5.88 nm for the Au-G1-PEG_{2000} and 10.64 nm for the Au-G4-PEG_{2000} (Table 4.4).

Table 4.4. Root-mean-square (Rms) roughness of PEG-functionalized dendronized surfaces obtained from AFM data: effect of dendron generation.

Surface	Rms (nm)
Bare gold	1.26
Au-PEG_{650}(G0)	5.47
Au-G1-PEG_{2000}	5.88
Au-G2-PEG_{2000}	7.10
Au-G3-PEG_{2000}	8.93
Au-G4-PEG_{2000}	10.64

4.2.7. Fibrinogen adsorption

Fibrinogen adsorption from PBS-NaI buffer decreased significantly on the PEG_{2000}-grafted dendronized surfaces compared to the control bare Au surface and the original Au-G1(OH) surface (Figure 4.6). However, no significant difference was noted

in the Fg adsorption from PBS on the various generation dendronized surfaces. In contrast, when the surfaces were incubated in a solution of Fg in plasma, a more significant decrease in protein adsorption was observed with increasing arm number of the star polymer (Figure 4.7). When comparing these results to the ones obtained with the G1-G4 dendronized surfaces,[35] it is clear that introducing PEG-OMe chains to the periphery of the dendronized surfaces results in a significant decrease in protein adsorption. By coupling PEG-OMe chains to the peripheral hydroxyl groups, the hydrogen bonding between the dendrons is eliminated, allowing the new system to exhibit greater chain mobility. Functionalization of the dendronized surfaces with PEG-OMe chains also eliminates the presence of hydrogen-bond donor groups, which may be an additional important contributing factor to the observed decrease in protein adsorption.

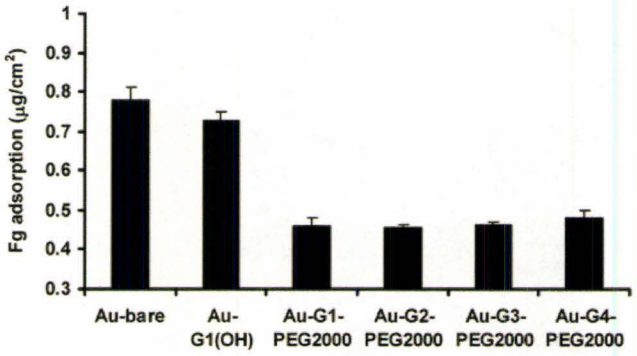

Figure 4.6. Fibrinogen adsorption from 1 mg/mL Fg-Fg-^{125}I in PBS-NaI of PEG_{2000}-grafted G1-G4-dendronized surfaces.

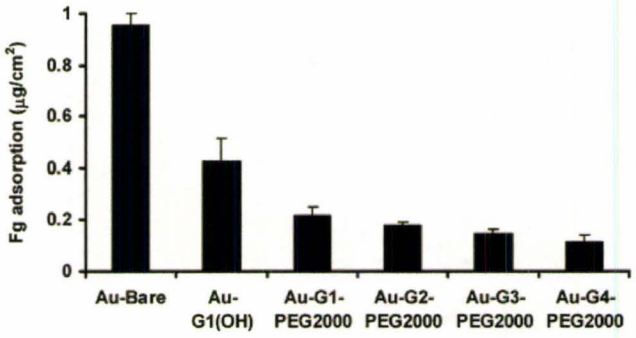

Figure 4.7. Fibrinogen adsorption from 1 mg/mL Fg-Fg-^{125}I in plasma of PEG_{2000}-grafted G1-G4-dendronized surfaces.

4.2.8. Lysozyme adsorption

Lysozyme adsorption from PBS-NaI onto PEG_{2000}-functionalized G1-G4 dendronzied surfaces followed a similar trend to the one observed for Fg adsorption from PBS. Protein adsorption on the PEG_{2000}-grafted dendronized surfaces was significantly lower compared to the control bare Au surface. However, no major difference was noted when the number of the PEG-OMe arms was increased with increasing dendron generation (Figure 4.8). The similarity of these results to the ones observed with fibrinogen is another indication that protein adsorption onto PEG-functionalized dendronized surfaces follows the same trend regardless of protein size.

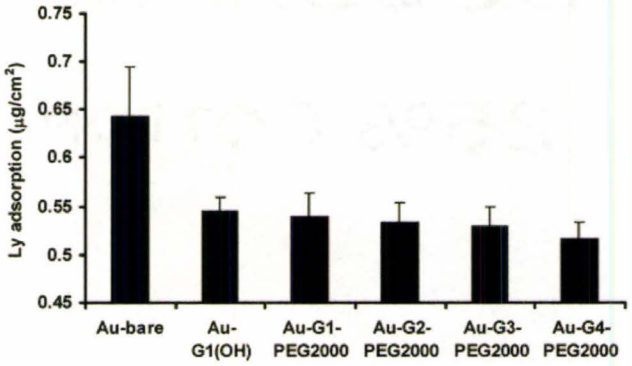

Figure 4.8. Lysozyme adsorption from PBS-NaI of PEG_{2000}-grafted G1-G4-dendronized surfaces.

4.3. Conclusions

Modification of dendronized surfaces with PEG-OMe chains was carried out via EDC coupling of the peripheral hydroxyl groups to the carboxyl end group of PEG-acid. In the first part of this study, the effect of functionalization of G1-dendronized surfaces with PEG-OMe oligomers on protein adsorption was investigated. Results from fibrinogen and lysozyme adsorption studies showed that protein adsorption onto the PEG-OMe grafted surfaces was lower than for the original dendronized surfaces. To further investigate the effect of PEG-OMe molecular weight on protein resistance, PEG-acid chains with molecular weight ranging between 350 Da and 5000 Da were used. Protein studies comparing the original G1-dendronized surfaces to the PEG-functionalized dendronized surfaces showed that protein adsorption gradually decreased with increasing MW of PEG-OMe chains. Results also showed that increasing PEG-OMe MW beyond 2000 Da did not result in better protein resistance. In the second part of this study, the

effect of dendron generation on protein adsorption was investigated using PEG_{2000}-acid. Protein studies showed a decrease in protein adsorption with increasing dendron generation regardless of protein size. The present results, when compared to our previous study,[35] showed that protein resistance was recovered when the dendronized surfaces were functionalized with PEG-OMe chains and both hydrogen bonding between the dendrons and the presence of hydrogen-bond donor groups were eliminated from the system. These results support previous studies indicating that chain mobility and dynamics in water may be critical to protein repulsion.[44,45] Additionally, this work shows that, when a surface incorporates a large number of hydrogen-bond donor groups that have a restricted motion at the water interface, it becomes more accessible to proteins and results in greater protein adsorption.

4.4. Experimental

4.4.1. General

DOWEX50W-X2 ion-exchange resin, 4-(dimethylamino)pyridine (DMAP, 99%), 2,2-Bis(hydroxymethyl)-propionic acid (bis-MPA, 98%), 2,2-dimethoxy propane (98%), *p*-toluene-sulfonic acid monohydrate (TsOH, 98%), TEMPO free radical (98%), iodobenzene diacetate (98%), and poly(ethylene glycol) methyl ether (M_n = 350 and 750 Da) were purchased from Aldrich. 1-(3-dimethylaminopropyl)-3-ethylcarbodiimide hydrochloride (EDC, 98+%) was purchased from Alfa Aesar. Poly(ethylene glycol) methyl ether (M_n = 2000 and 5000 Da) were purchased from Fluka. Thiol-terminated poly(ethylene glycol) (HS-PEG_{650}-OH) was purchased from Polymer Source, Inc.

Dichloromethane (CH_2Cl_2), ethyl acetate (EtOAc), hexanes, methanol (MeOH), diethyl ether, and ethanol (EtOH) were purchased from Caledon. All reagents were used as received. Acetonide-protected anhydride of bis-MPA (**3.2**)[37] and of 4-dimethylaminopyridine/*p*-toluene sulfonic acid (DPTS)[38] were prepared according to literature procedures.

Gold substrates prepared by electron beam evaporation of silicon wafers with an adhesive titanium tungstate (TiW) layer (300 Å) followed by a layer of gold (1000 Å), were purchased from Thin Film Technology, Buellton, CA, and diced into 1.0 × 1.0 cm^2 pieces. Prior to chemisorption, the surfaces were cleaned, using a literature procedure by immersing them in chromosulfuric acid (H_2SO_4 > 92%, CrO_3 > 1.3%) for 1 h to remove any organic contaminants, followed by ultrasonication in both Milli-Q water and ethanol for 10 minutes, and extensive rinsing with Milli-Q water.[39] All reactions on surfaces were carried out by placing reaction flasks on a VWR™ S-500 orbital shaker at a medium speed setting, since no stirring was possible.

4.4.2. Characterization

NMR spectra were measured on Avance 600 MHz spectrometers. ^1H spectra were recorded at 600 MHz, ^{13}C NMR spectra were recorded at 150 MHz in $CDCl_3$ or methanol-d_4. The non-deuterated solvent signal was used as the internal standard for both ^1H and ^{13}C spectra. Sessile-drop water contact angles were determined using water drops with a 1-2 μL volume. Advancing and receding angles were obtained using a Ramé–Hart NRL 100-00 goniometer (Mountain Lakes, NJ). Atomic force microscopy (AFM)

analyses were carried out using a Digital Instruments NanoScope IIIa Multimode AFM equipped with a vertical engage "E" scanner with 15 μm full range scan. The images were recorded with standard tips in tapping mode at a scan rate of 0.5 Hz.

4.4.3. Proteins

Fibrinogen was purchased from Calbiochem (La Jolla, CA), dialyzed against Tris buffer, pH 7.4, aliquoted, and stored at -70 °C. The molecular weight and dimensions of fibrinogen are 3.4×10^5 Da and $450 \times 90 \times 90$ Å^3, respectively, and its isoelectric point is 5.5. Lysozyme was obtained from Calbiochem (La Jolla, CA) and used as received. The molecular weight and dimensions of lysozyme are 1.43×10^4 Da and $45 \times 30 \times 30$ Å^3, respectively, and its isoelectric point is 11.0.

4.4.4. General Procedures

4.4.4.1. General procedure for surface dendronization

First generation aliphatic polyester dendrons (G1(Ac)) were covalently attached to the terminal hydroxyl groups of PEG_{650}-functionalized gold surfaces via an esterification reaction. In this reaction, excess acetonide anhydride (**3.2**) (0.1 g, 3.03×10^{-4} mol; excess/cm^2 of (**3.2**):PEG-OH = 5×10^4:1) was added along with a catalytic amount of DMAP (10 mg, 8.18×10^{-5} mol) in a mixture of CH_2Cl_2:pyridine (3:2 v/v, 5 mL). This step was followed by removal of the acetonide protecting groups to give the hydroxyl-terminated first generation dendrons. The deprotection step was carried out following a literature procedure, using the acidic resin DOWEX 50W-X2 in methanol at 50 °C for 1

h.[39] Subsequent esterification and deprotection reactions allowed surface dendronization up to the fourth generation as described previously.[35]

4.4.4.2. General procedure for oxidation of poly(ethylene glycol) mono-methyl ether (PEG-OMe)[40]

Poly(ethylene glycol) mono-methyl ether (PEG-OMe) (M_n = 2000 Da) (3.01 g, 1.51×10^{-3} mol) was introduced to a round-bottom flask equipped with a magnetic stir bar as a solution in a 1:1 mixture of water/acetonitrile (5 mL). TEMPO free radical (0.047 g, 3.0×10^{-4} mol) was added to the solution, followed by iodobenzene diacetate (1.45 g, 4.5×10^{-3} mol). The reaction mixture was stirred at room temperature for 6 h (or overnight to ensure a complete reaction). The mixture was then concentrated to dryness in vacuo and the residue was dissolved in a minimum amount of ethanol. The crude polymer was precipitated in cold diethylether, and recovered by filtration through a glass fritted funnel. After drying in a vacuum oven overnight, PEG_{2000}-acid was obtained as a white powder (2.9 g, 97%). ^{1}H NMR (600 MHz, CD_3OD): δ (ppm) = 3.36 (s, 3H, $-CH_3O$), 3.50-3.55 (m, 2H, $-CH_2OCH_3$), 3.55-3.69 (s-broad, 148H, $-CH_2CH_2O$), 3.69-3.72 (m, 2H, $-CH_2O$), 4.13 (s, 2H, $-CH_2CO_2H$). ^{13}C NMR (150 MHz, CD_3OD): δ (ppm) = 59.1 ($-CH_3O$), 69.15 ($-CH_2OCH_3$), 71.37 ($CH_3O-CH_2CH_2O$), 71.58 ($-CH_2CH_2O$), 72.97 ($-CH_2CO_2H$), 174.01 ($-CO_2H$).

4.4.4.3. Oxidation of poly(ethylene glycol)$_{350}$ mono-methyl ether (MeO-PEG$_{350}$-OH)

The oxidation was carried out, as described in the general procedures, using PEG-OMe (M_n = 350 Da) (3.06 g, 8.57×10^{-3} mol), TEMPO free radical (0.268 g, 1.71×10^{-3} mol), and iodobenzene diacetate (8.28 g, 2.57×10^{-2} mol) in a 1:1 mixture of water/acetonitrile (15 mL). The crude polymer was precipitated three times in cold diethylether, and filtered to isolate the desired product as a white powder (2.7 g, 90%). ^{1}H NMR (600 MHz, $CDCl_3$): δ (ppm) = 3.35 (s, 3H, $-CH_3O$), 3.53 (m, 2H, $-CH_2OCH_3$), 3.59-3.65 (s-broad, 22H, $-CH_2CH_2O$), 3.72 (m, 2H, $-CH_2O$), 4.13 (s, 2H, $-CH_2CO_2H$). ^{13}C NMR (150 MHz, $CDCl_3$): δ (ppm) = 59.1 ($-CH_3O$), 69.01 ($-CH_2OCH_3$), 70.62 ($-CH_2CH_2O$), 71.28 ($CH_3O-CH_2CH_2O$), 72.03 ($-CH_2CO_2H$), 172.72 ($-CO_2H$).

4.4.4.4. Oxidation of poly(ethylene glycol)$_{750}$ mono-methyl ether (MeO-PEG$_{750}$-OH)

The oxidation was carried out, as described in the general procedures, using PEG-OMe (M_n = 750 Da) (3.02 g, 4.03×10^{-3} mol), TEMPO free radical (0.127 g, 8.13×10^{-4} mol), and iodobenzene diacetate (3.86 g, 1.19×10^{-2} mol) in a 1:1 mixture of water/acetonitrile (20 mL). The crude polymer was precipitated three times in cold ether, and filtered through a fritted funnel to isolate the desired product as a white powder (2.84 g, 95%). ^{1}H NMR (600 MHz, CD_3OD): δ (ppm) = 3.27 (s, 3H, $-CH_3O$), 3.48-3.52 (m, 2H, $-CH_2OCH_3$), 3.52-3.65 (s-broad, 72H, $-CH_2CH_2O$), 3.65-3.68 (m, 2H, $-CH_2O$), 4.08 (s, 2H, $-CH_2CO_2H$). ^{13}C NMR (150 MHz, CD_3OD): δ (ppm) = 59.1 ($-CH_3O$), 69.26 ($-CH_2OCH_3$), 71.37 ($CH_3O-CH_2CH_2O$), 71.57 ($-CH_2CH_2O$), 72.98 ($-CH_2CO_2H$), 174.22 ($-CO_2H$).

4.4.4.5. Oxidation of poly(ethylene glycol)$_{5000}$ mono-methyl ether (MeO-PEG$_{5000}$-OH)

The oxidation was carried out, as described in the general procedures, using PEG-OMe (M_n = 5000 Da) (3.08 g, 6.16×10^{-4} mol), TEMPO free radical (0.019 g, 1.22×10^{-4} mol), and iodobenzene diacetate (0.582 g, 1.81×10^{-3} mol) in a solution of a 1:1 mixture of water/acetonitrile (10 mL). The crude polymer was precipitated in cold ether, and filtered to isolate the desired product as a white powder (2.94 g, 98%). ^{1}H NMR (600 MHz, CD_3OD): δ (ppm) = 3.36 (s, 3H, $-CH_3O$), 3.53-3.55 (m, 2H, $-CH_2OCH_3$), 3.56-3.69 (s-broad, 432H, $-CH_2CH_2O$), 3.69-3.72 (m, 2H, $-CH_2O$), 4.12 (s, 2H, $-CH_2CO_2H$). ^{13}C NMR (150 MHz, CD_3OD): δ (ppm) = 59.1 ($-CH_3O$), 69.26 ($-CH_2OCH_3$), 71.37 ($CH_3O-CH_2CH_2O$), 71.60 ($-CH_2CH_2O$), 72.98 ($-CH_2CO_2H$), 174.22 ($-CO_2H$).

4.4.4.6. General procedure for EDC-coupling of PEG-acid to the peripheral OH-groups of G1-G4 dendronized surfaces

First, the G1-G4 dendronized surfaces were synthesized using the divergent dendron growth, as described in detail in our previous work.[35] Then, flame-dried 15 mL vials were individually charged with Au-Gx(OH) (x = 1 to 4) surface in a solution of CH_2Cl_2:pyridine (3:2 v/v, 3 mL) under argon. Excess (50 mg) PEG-acid of specific MW (350, 750, 2000, and 5000 Da), along with 1-(3-dimethylaminopropyl)-3-ethylcarbodiimide hydrochloride (EDC) (10 mg, 5.22×10^{-5} mol), and a catalytic amount of 4-dimethylaminopyridine/*p*-toluene sulfonic acid (DPTS) (2.5 mg, 8.50×10^{-5} mol) were added, and the vials were shaken for 72 h at room temperature using a shaker since stirring was not possible. The surfaces were then transferred to new individual vials and

washed extensively with CH_2Cl_2 (~25 mL) to remove any unreacted EDC. This was followed by extensive rinsing with 1M $NaHSO_4$ (~20 mL), 10% Na_2CO_3 (~20 mL), and brine (~10 mL) to remove any unreacted PEG-acid and DPTS. Finally, the surfaces were washed extensively with Milli-Q water (~20 mL) and dried with a stream of N_2 prior to analysis.

4.4.4.7. Protein radiolabeling with ^{125}I

Fibrinogen (Fg) (Calbiochem, La Jolla, CA) was radiolabeled with $Na^{125}I$ (ICN, Irvine, CA) using the iodine monochloride method.[41] The solution containing the ^{125}I-radiolabeled Fg was passed through a column packed with AG® 1-X4 resin (Bio-Rad Laboratories, Inc.) in Tris Buffered Saline (TBS, pH 7.4) to remove unbound ^{125}I (held to <1% of total solution radioactivity). A free ^{125}I test was carried out on the ^{125}I-radiolabeled Fg using the trichloracetic acid (TCA) method, to determine the percent of unbound isotope following the iodination reaction. The same procedure was used to radiolabel lysozyme.

4.4.4.8. Protein Adsorption

Prior to protein adsorption experiments, gold-coated silicon wafers were equilibrated in PBS-NaI buffer overnight; "cold" NaI was added to the buffer to prevent uptake of unbound ^{125}I to the gold.[42] Protein adsorption experiments were performed in PBS-NaI buffer (pH 7.4) at a protein concentration of 1 mg/mL (10% labeled, 90% "cold"/PBS, and 2.5% labeled, 97.5% "cold"/plasma). The surfaces were placed in the

wells of 24-well plates and incubated in a 1 mL solution of ^{125}I-labeled protein in PBS-NaI for 3 h at room temperature (22 °C). It was previously determined that no further adsorption occurred at times longer than 3 h.[17] The surfaces were rinsed three times (10 min each) with fresh PBS-NaI to remove any loosely bound protein. Surface radioactivity was determined, using a Perkin Elmer™ WIZARD™ 3'' 1480 automatic gamma counter. The percent reduction of adsorption on the PEO-functionalized and dendronized surfaces relative to the unmodified gold was determined.

4.5. References

(1) Schiedermayer, D. L.; Shapiro, R. S. *J Heart Transplant* **1989**, *8*, 471-473.
(2) Cho, W. K.; Kong, B. Y.; Choi, I. S. *Langmuir* **2007**, *23*, 5678-5682.
(3) Dickinson, G. M.; Bisno, A. L. *Int J Artif Organs* **1993**, *16*, 749-754.
(4) Chen, C. S.; Mrksich, M.; Huang, S.; Whitesides, G. M.; Ingber, D. E. *Science* **1997**, *276*, 1425-1428.
(5) Snellings, G. M. B. F.; Vansteenkiste, S. O.; Corneillie, S. I.; Davies, M. C.; Schacht, E. H. *Adv Mater* **2000**, *12*, 1959-1962.
(6) Kim, H.; Doh, J.; Irvine, D. J.; Cohen, R. E.; Hammond, P. T. *Biomacromolecules* **2004**, *5*, 822-827.
(7) Xiao, D. Q.; Van Le, T.; Wirth, M. J. *Anal Chem* **2004**, *76*, 2055-2061.
(8) Fu, K.; Klibanov, A. M.; Langer, R. *Nat Biotechnol* **2000**, *18*, 24-25.
(9) Fukai, R.; Dakwa, P. H. R.; Chen, W. *J Polym Sci Pol Chem* **2004**, *42*, 5389-5400.
(10) Ratner, B. D. *J Biomed Mater Res* **1993**, *27*, 837-850.
(11) Chen, H.; Zhang, Z.; Chen, Y.; Brook, M. A.; Sheardown, H. *Biomaterials* **2005**, *26*, 2391-2399.
(12) Khademhosseini, A.; Jon, S.; Suh, K. Y.; Tran, T. N. T.; Eng, G.; Yeh, J.; Seong, J.; Langer, R. *Adv Mater* **2003**, *15*, 1995-2000.
(13) Holzl, M.; Tinazli, A.; Leitner, C.; Hahn, C. D.; Lackner, B.; Tampe, R.; Gruber, H. J. *Langmuir* **2007**, *23*, 5571-5577.
(14) Ostuni, E.; Chapman, R. G.; Holmlin, R. E.; Takayama, S.; Whitesides, G. M. *Langmuir* **2001**, *17*, 5605-5620.
(15) Prime, K. L.; Whitesides, G. M. *J Am Chem Soc* **1993**, *115*, 10714-10721.
(16) Li, L. Y.; Chen, S. F.; Zheng, J.; Ratner, B. D.; Jiang, S. Y. *J Phys Chem B* **2005**, *109*, 2934-2941.
(17) Unsworth, L. D.; Sheardown, H.; Brash, J. L. *Langmuir* **2005**, *21*, 1036-1041.
(18) McGurk, S. L.; Green, R. J.; Sanders, G. H. W.; Davies, M. C.; Roberts, C. J.; Tendler, S. J. B.; Williams, P. M. *Langmuir* **1999**, *15*, 5136-5140.
(19) Szleifer, I. *Curr Opin Colloid In* **1996**, *1*, 416-423.
(20) Szleifer, I. *Physica A* **1997**, *244*, 370-388.
(21) Szleifer, I. *Curr Opin Solid St M* **1997**, *2*, 337-344.
(22) Szleifer, I. *Biophys J* **1997**, *72*, 595-612.
(23) Halperin, A.; Fragneto, G.; Schollier, A.; Sferrazza, M. *Langmuir* **2007**, *23*, 10603-10617.
(24) Halperin, A. *Langmuir* **1999**, *15*, 2525-2533.
(25) Pertsin, A. J.; Grunze, M. *Langmuir* **2000**, *16*, 8829-8841.
(26) Zolk, M.; Eisert, F.; Pipper, J.; Herrwerth, S.; Eck, W.; Buck, M.; Grunze, M. *Langmuir* **2000**, *16*, 5849-5852.
(27) Nagaoka, S.; Mori, Y.; Takiuchi, H.; Yokota, K.; Tanzawaza, H.; Nishiumi, S. *in Polymers as Biomaterials (Eds.: S. W. Shalaby, A. S. Hoffman, B. D. Ratner, T. A. Horbett), Plenum, New York* **1984**, 361-374.
(28) Wang, R. C. L.; Kreuzer, H. J.; Grunze, M. *J Phys Chem B* **1997**, *101*, 9767-9773.

(29) Harder, P.; Grunze, M.; Dahint, R.; Whitesides, G. M.; Laibinis, J. *J Phys Chem B* **1998**, *102*, 426-436.
(30) Chapman, R. G.; Ostuni, E.; Takayama, S.; Holmlin, R. E.; Yan, L.; Whitesides, G. M. *J Am Chem Soc* **2000**, *122*, 8303-8304.
(31) Ajikumar, P. K.; Ng, J. K.; Tang, Y. C.; Lee, J. Y.; Stephanopoulos, G.; Too, H.-P. *Langmuir* **2007**, *23*, 5670-5677.
(32) Luk, Y.-Y.; Kato, M.; Mrksich, M. *Langmuir* **2000**, *16*, 9604-9608.
(33) Siegers, C.; Biesalski, M.; Haag, R. *Chem-Eur J* **2004**, *10*, 2831-2838.
(34) Zhao, Y. H.; Zhu, B. K.; Kong, L.; Xu, Y. Y. *Langmuir* **2007**, *23*, 5779-5786.
(35) Benhabbour, S. R.; Sheardown, H.; Adronov, A. *Macromolecules* **2008**, DOI: 10.1021/ma702074v.
(36) Hong, M.-Y.; Yoon, H. C.; Kim, H.-S. *Langmuir* **2003**, *19*, 416-421.
(37) Malkoch, M.; Malmstrom, E.; Hult, A. *Macromolecules* **2002**, *35*, 8307-8314.
(38) Moore, J. S.; Stupp, S. I. *Macromolecules* **1990**, *23*, 65-70.
(39) Ostmark, E.; Macakova, L.; Auletta, T.; Malkoch, M.; Malmstrom, E.; Blomberg, E. *Langmuir* **2005**, *21*, 4512-4519.
(40) Masson, C.; Scherman, D.; Bessodes, M. *J Polym Sci Pol Chem* **2001**, *39*, 4022-4024.
(41) Wagner, M. S.; Horbett, T. A.; Castner, D. G. *Biomaterials* **2003**, *24*, 1897-1908.
(42) Du, Y. J.; Cornelius, R. M.; Brash, J. L. *Colloid Surface B* **2000**, *17*, 59-67.
(43) Chen, H.; Brook, M. A.; Sheardown, H. *Biomaterials* **2004**, *25*, 2273-2282.
(44) Unsworth, L. D.; Sheardown, H.; Brash, J. L. *Biomaterials* **2005**, *26*, 5927-5933.
(45) Latour, R. A. *J Biomed Mater Res A* **2006**, *78A*, 843-854.

Chapter 5. Cell Adhesion and Proliferation on Dendronized Surfaces

Abstarct

Dendronized surfaces were prepared by chemisorption of poly(ethylene glycol)-mono-thiol (HS-PEG_{650}-OH) onto gold-coated silicon wafers followed by divergent dendronization of the terminal PEG OH-group with aliphatic polyester dendrons, generation 1 to 4. The adhesion and proliferation of human corneal epithelial cells (HCEC) and mouse 3T3 fibroblasts (M-3T3) as model cells on these hydroxyl-terminated dendronized surfaces were investigated. In addition, the effect of covalently attaching PEG mono-methyl ether (PEG-OMe) chains (M_n = 2000 Da) to the peripheral hydroxyl groups of G1 and G2 dendronized surfaces on adhesion and proliferation of the same cell lines was studied. Little or no HCEC adhesion was noted on gold surfaces modified with PEG mono-thiol (HO-PEG-SH) in serum-free medium. These cells showed a greater affinity for the dendronized surfaces compared to the control Au surfaces at early incubation stages (1 day). At longer incubation times, HCEC proliferation increased exponentially on the dendronized surfaces. However, when G1 and G2 dendronized surfaces were modified with PEG-OMe chains, adhesion of both HCEC and M-3T3 cells was significantly reduced. Cell studies with M-3T3 fibroblasts, carried out in serum-containing medium, showed that cell attachment was diminished for the PEG-grafted Au surfaces compared to the control Au and G1-G4 dendronized surfaces. This chapter has been reproduced in part with permission from *Biomaterials* **2008**. jbmt9200, ***In Press***, ***Corrected Proof***. Copyright 2008 Elsevier.

5.1. Introduction

The biological responses to implantation of biomaterials depends mainly on cellular interactions, which are mediated by the concentration, composition, and conformation of adsorbed proteins at the implant surface.[1] Therefore, protein adsorption to the surface is the dominant factor in determining the host response to implanted materials and tissue-engineered surfaces.[2-5] Numerous studies have been reported on cell adhesion to various surfaces with the aim of providing a better understanding of cellular interactions with biomaterials.[6] It has been shown that specific surface properties, including hydrophilicity, chemical composition, roughness, and surface energy influence protein adsorption and subsequent cell adhesion.[7-14] Among these properties, surface chemistry has been shown to influence the adhesion of a variety of cell types, including fibroblasts, endothelial cells, and epithelial cells through the adsorption of fibronectin and/or vitronectin derived from serum used to supplement the culture medium.[15-19] Several methods have been used to optimize cell adhesion and proliferation, including coating surfaces with cell adhesive proteins such as fibronectin, collagen, or laminin.[20,21] The use of natural proteins has several disadvantages, such as their propensity for degradation and need to be continuously refreshed, precluding their suitability for long-term applications.[19,22,23] Most of these limitations can be overcome by surface grafting with active oligopeptide fragments of the adhesive proteins that are involved in cell recognition.[24,25] However, the use of these peptides suffers from reduced activity of the oligopeptides when excised from the native biomacromolecules, their limited specificity among integrin adhesion receptors, and their potential to adopt conformational changes

that limit their ability to bind certain receptors, resulting in a substantial loss of biological activity.[26-30] These limitations and the need for a better understanding of factors which contribute to cellular responses to materials continue to drive numerous studies investigating the use of synthetic polymeric materials with enhanced biocompatibility for biomedical and tissue engineering applications.

One of the most widely used polymers for controlling cell-biomaterial interactions is poly(ethylene glycol) (PEG).[31,32] The effectiveness of PEG lies in its ability to suppress non-specific protein adsorption and, subsequently, non-specific cell adhesion to surfaces, since cells depend on specific proteins for anchorage.[33,34] Other examples include the use of hydrogels such as poly(hydroxyethyl methacrylate) (PHEMA),[35,36] PEG diacrylate,[37] poly(ethylene fumarate-*co*-ethylene glycol),[38] poly(vinyl alcohol),[39] and poly(2-hydroxypropyl methacrylamide),[40] which have also been extensively investigated for use in tailoring cell adhesion and proliferation. However, most synthetic hydrogels do not have built-in cell adhesive ligands and require chemical modifications to incorporate them. In addition, because of their highly hydrated nature, hydrogels prevent proteins or peptides from adhering to their surfaces, leading to very low or even suppressed cell adhesion.[41] Due to these limitations, there continues to be a need for development of new systems with controlled cell adhesion and proliferation.

The use of branched architectures in cell adhesion studies and tissue engineering applications has attracted attention,[42-44] although this field of study is still in its infancy. In the present work, we set out to investigate the effect of functionalizing gold surfaces with hydrophilic dendritic moieties on cell adhesion and proliferation.

In a previous paper, we have found that protein adsorption increased when gold surfaces were covalently functionalized with aliphatic polyester dendrons compared to the control PEG-grafted surfaces.[45] Here, we build upon these results by investigating whether the increased protein adsorption with the dendronized surfaces could lead to enhanced cell adhesion and proliferation. Two cell lines were chosen to carry out this study, human corneal epithelial cells (HCEC) and mouse 3T3 fibroblasts (M-3T3). Human corneal epithelial cells were selected because they can effectively adapt to serum free conditions through a mode of attachment that is independent of the adsorption of serum-derived fibronectin and vitronectin.[46] This endogenous attachment mechanism is directly affected by surface chemistry, providing a correlation between the substrates and their effect on cell adhesion.[47] However, since protein adsorption cannot be prevented *in vivo* when materials are in contact with various tissues and blood, we have also carried out studies using the M-3T3 cells in serum-containing medium, as these cells have previously proven difficult to grow without serum on a number of surfaces.[13,48,49]

5.2. Results and Discussion

5.2.1. Synthesis

The synthesis of dendronized surfaces was accomplished by divergent growth of aliphatic polyester dendrons as previously described.[45] The resulting hydroxyl terminated dendrons were subsequently functionalized with PEG mono-methyl ether (PEG-OMe) chains. This was achieved by first oxidizing the terminal hydroxyl group of PEG-OMe to a carboxylic acid derivative using a TEMPO-mediated oxidation.[53] The peripheral

hydroxyl groups of the dendronized surfaces were subsequently reacted with excess PEG_{2000}-acid in the presence of 1-(3-dimethylaminopropyl)-3-ethylcarbodiimide hydrochloride (EDC) and a catalytic amount of 4-(dimethylamino)pyridine/*p*-toluene sulphonic acid (DPTS) (Scheme 5.1) for 72 h at room temperature. All surfaces were characterized by contact angle measurements, AFM analysis, XPS, and TOF-SIMS analyses, as previously reported.[45] Since the surfaces studied here were chemically identical to ones previously used to carry out protein adsorption studies, it was possible to correlate the results of cell adhesion to the previously reported propensity for adsorption of proteins.[45,54]

Scheme 5.1. EDC coupling of PEG-acid to a G1(Ac)-dendronized surface.

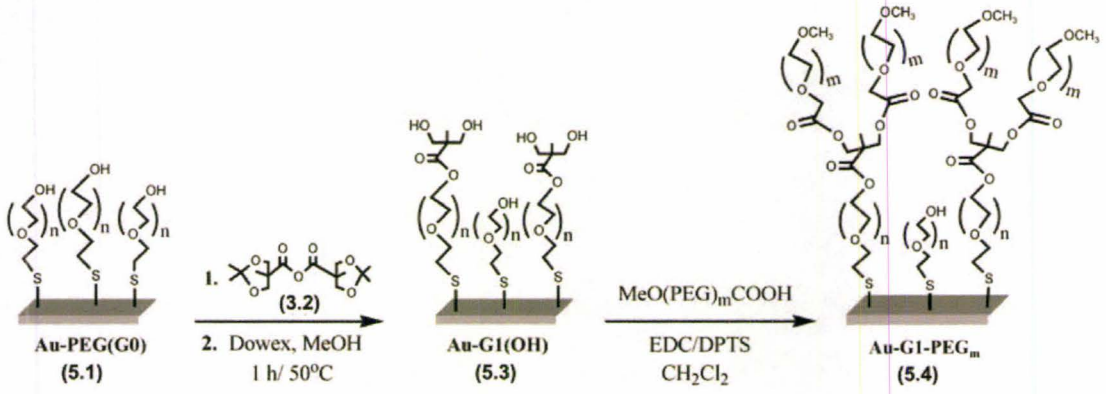

5.2.2. Detection of cell adhesion using unmodified gold surfaces

In the first control experiments, we wished to investigate whether the cells would grow and proliferate on bare Au surfaces. Control experiments were carried out for both human corneal epithelial cells (HCEC) and mouse 3T3 fibroblasts (M-3T3). Cells from

both cell lines were initially plated on the surfaces and incubated in serum-free media, with cell counts on the surfaces being measured after 1, 3, and 6 days of incubation. Results from these experiments showed that, over the 6 day incubation period, HCEC adhered onto the gold surfaces at early incubation stages and proliferated over longer periods. However, when the M-3T3 cells were incubated in serum-free medium, no cell attachment was noted at any stage of incubation. This control experiment was repeated using serum-containing medium for M-3T3 cells. Results indicated that in the presence of serum, the cells adhered to Au surfaces and proliferated over time. Therefore, all subsequent studies were performed in serum-free medium for the HCEC and in serum-containing medium for the M-3T3 cells.

5.2.3. Detection of cell adhesion to the modified gold surfaces

5.2.3.1. *In vitro* adhesion of human corneal epithelial cells (HCEC)

Gold surfaces modified with various thiol compounds have been widely used as a well-defined model system to study protein-surface interactions and cell adhesion.[55,56] Their properties, including the relative ease of modification with self-assembled monolayers (SAMs) using the thiol-gold bond, as well as their stability to physical and biological changes, provide the ability to study early biological responses to the biomaterial interface by controlling surface properties at the molecular level.[57] In this work, we exploited the thiol-gold chemistry to introduce PEG chains, which were further functionalized with G1-G4 aliphatic polyester dendrons. The presence of a large number of peripheral hydroxyl groups allowed us to subsequently couple PEG-OMe chains to the

dendronized surfaces, and investigate the effect of all these functionalities on cell adhesion and proliferation.

Prior to every cell adhesion study, gold surfaces functionalized with HS-PEG_{650}-OH, aliphatic polyester dendrons, and PEG-grafted dendrons were transferred to 24-well plates and incubated in KSFM overnight. The medium was removed, and the surfaces were seeded with 70 μL of a solution containing 20,000 cells in KSFM, followed by incubation for 20 min. Serum-free medium (KSFM, 1 mL) was added to each well, and surfaces were incubated for 1, 3, and 6 days. The medium was changed every 48 hours for the 6-day studies. Each study was repeated twice using triplicate samples of each functionalization step to assure reproducibility of the results. The first set of experiments was carried out with PEG-grafted surfaces and G1-G4 dendronized surfaces in order to study the effect of hydrophilic polyester dendrons on cell adhesion and proliferation. Cells were fixed and analyzed by optical microscopy following each adhesion study. The optical micrographs illustrated in Figure 5.1 show that cell attachment and proliferation occurred on the control Au surfaces, as well as the G1-G4 dendronized surfaces. However, no cell adhesion or proliferation was noted for the PEG-grafted gold surfaces (Figure 5.1). This was not surprising as PEG is well known to repel protein adsorption and cell adhesion.[45,56,58-62] In contrast to the PEG-grafted surfaces, the G1-G4 dendronized surfaces, which we previously found to promote protein adsorption,[45] exhibited a significant increase in cell adhesion and a typical exponential growth of cell population with time, in comparison to the original PEG-grafted surfaces (Figure 5.1.III-IV, Figure 5.2).

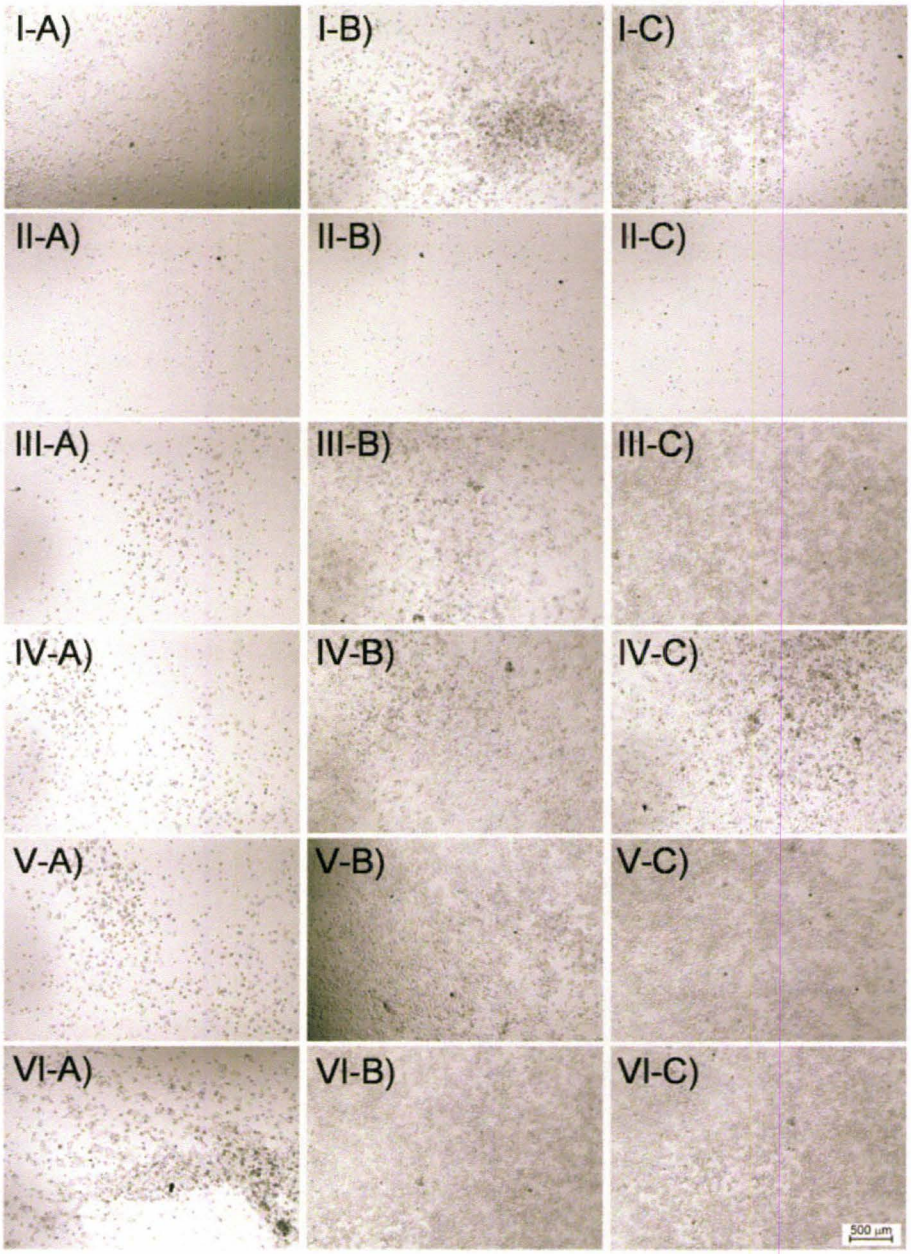

Figure 5.1. Optical micrographs (×2.5) showing HCEC cell numbers at various time points on various surfaces: I) bare Au, II) Au-PEG(G0), III) Au-G1(OH), IV) Au-G2(OH), V) Au-G3(OH), VI) Au-G4(OH), A) 1-day, B) 3-days, C) 6-days of incubation at 37°C.

Cell culture counts carried out following every cell adhesion study show that greater cell densities were calculated for the control Au and G1-G4 dendronized surfaces in comparison to the PEG-grafted surfaces (Figure 5.2). In addition, there was a gradual increase in cell densities with increasing incubation time, which became more noticeable for the higher generation dendronized surfaces. The difference in cell densities calculated for the control Au and dendronized surfaces became more pronounced at higher generations (G3 and G4), and at longer incubation time (3 days and 6 days) (Figure 5.2).

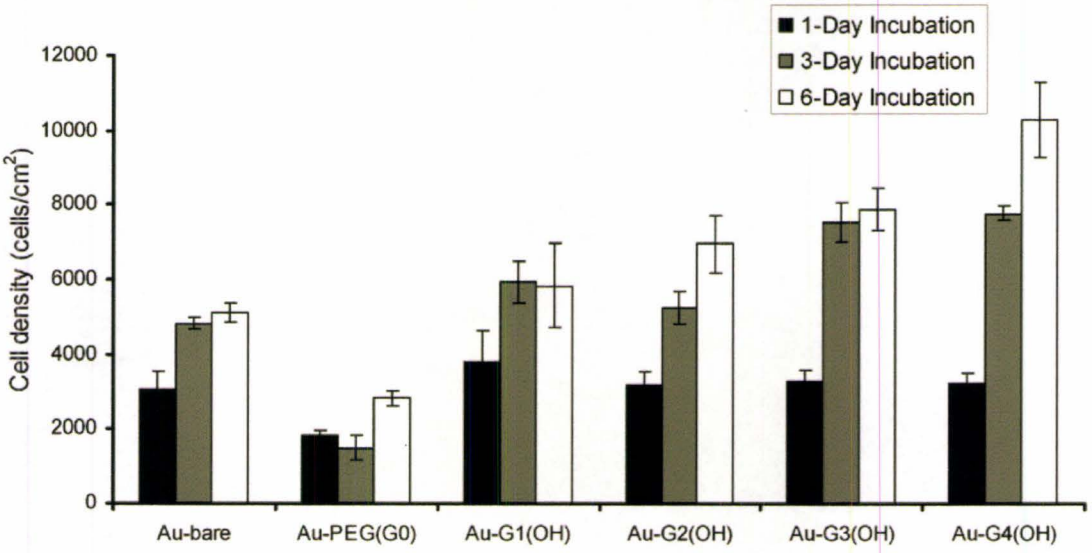

Figure 5.2. Human corneal epithelial cell response to the various surfaces: Effect of hydrophilic dendrons.

Assessing the fraction of cells able to attach and proliferate on a surface is important in determining the potential of a surface for biomedical applications. The percentage of cells attached to various surfaces was calculated and the results presented in

Figure 5.I.1 (Appendix I) indicate that the number of cells attached to various surfaces increased gradually at longer incubation periods. From the 20,000 cells seeded, less than 10% adhered to the PEG-grafted surfaces at the early incubation periods (1 day). After 6 days of incubation, no significant difference was noted in the percentage of cells attached to the PEG-grafted surfaces, estimated to be approximately 15% of the original number of cells plated on the surfaces. A greater percentage of cells adhered and proliferated on the control Au surfaces, with approximately 15% after 1 day of incubation, and a highest value of approximately 25% occurring after 6 days of incubation in serum-free medium. Over longer incubation periods, the highest generation (G4) dendronized surfaces showed the largest cell percentages, approaching 50% after 6 days of incubation (Figure 5.I.1).

To further confirm the effect of aliphatic dendrons on cell adhesion and proliferation, we grafted PEG-OMe chains (M_n = 2000 Da) to the peripheral hydroxyl groups of the dendrons using EDC-mediated coupling. The resulting PEG-grafted dendronized surfaces were tested for cell adhesion and proliferation following the procedures outlined above. The optical micrographs of cells fixed on the PEG-grafted surfaces after 1, 3, and 6 days of incubation are illustrated in Figure 5.3. Lower cell adhesion was obtained when the G1 dendronized surfaces were coupled with PEG-OMe chains. This behavior can be seen starting at early incubation stages (1 day), where the cells that adhered to the PEG-grafted G1-dendronized surfaces were significantly aggregated in what appeared to be a continuous gel (Figure 5.3.II.A). This difference in cell adhesion became more noticeable at the second generation, where a significantly lower number of cells adhered to the PEG-grafted dendronized surfaces compared to the

original G2 dendronized surfaces (Figure 5.3.IV). These results are in agreement with those previously observed for the original PEG-grafted surfaces prior to dendronization, and confirm that the presence of a high density of PEG chains results in cell-resistant surfaces due to the absence of proteins that provide cell anchorage to the surface. On the contrary, functionalization of the original PEG-grafted surfaces with branched hydrophilic dendrons, and the presence of a large network of peripheral hydroxyl groups, created a system with greater affinity for HCEC adhesion and proliferation.

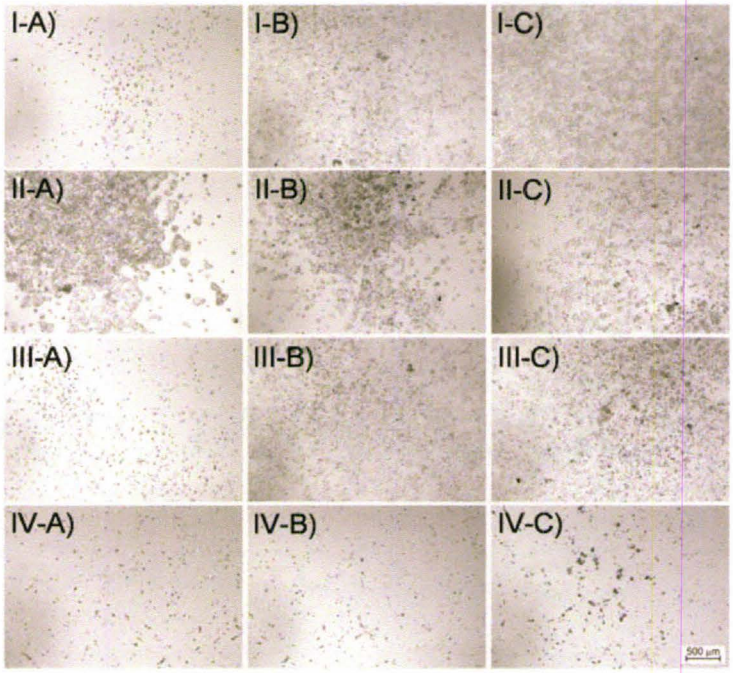

Figure 5.3. Optical micrographs (×2.5) illustrating the effect of PEGylation of G1 and G2 dendronized surfaces on response of human corneal epithelial cells to the various surfaces: I) Au-G1(OH), II) Au-G1-PEG_{2000}, III) Au-G2(OH), IV) Au-G2-PEG_{2000}, A) 1-day, B) 3-days, C) 6-days of incubation at 37ºC.

Based on the 1 day data, surface-specific differences in the number of cells adhered to the dendronized surfaces prior to and after coupling with PEG_{2000}-acid were also noted from cell counts. In agreement with the results obtained from the optical microscopy analyses, cell culture counts show that the densities of cells calculated for the PEG-grafted dendronized surfaces were significantly lower than those obtained for the hydroxyl-terminated dendronized surfaces (Figure 5.4).

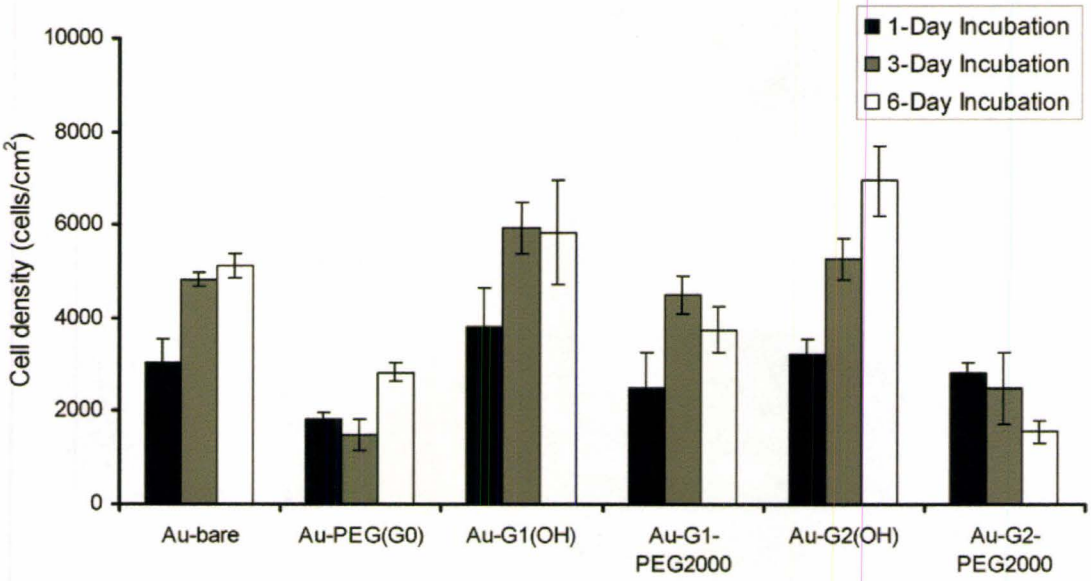

Figure 5.4. Evaluation of adhesion and proliferation of human corneal epithelial cells on various surfaces: Effect of PEGylation of G1 and G2 dendronized surfaces.

The percentage of cells present on the various surfaces was also calculated and the results presented in Figure 5.I.2 (Appendix I) indicate that fewer cells adhered to the PEG-grafted dendronized surfaces. From the 20,000 cells seeded on the surfaces studied, the percentage of cells present on the G1-dendronized surfaces after 6 days of incubation

was reduced from ~28% to ~18% after coupling with PEG-OMe chains. Similarly, after a 6-day incubation study, the percentage of cells present on the G2-dendronized surfaces, estimated to be approximately 35%, decreased to approximately 5% after functionalization of the peripheral hydroxyl groups with PEG-OMe chains (Figure 5.I.2). It is evident from these values that cell resistance became more pronounced at higher generations and with the presence of a larger number of PEG-OMe chains.

5.2.3.2. Cell viability measurement

Cell viability tests were conducted following each adhesion study for the various surfaces after 6 days of incubation. The cells were dislodged from the surfaces using trypsin-EDTA before adding an equal amount of serum-free medium to stop the enzymatic reaction. Calcein AM, which fluoresces only upon cellular uptake, was added to the solution containing the cells at a concentration of 2 μL/mL and incubated for 20 min. Following incubation, the solutions were analyzed by fluorescence microscopy, which clearly showed that no detectable amounts of living cells were lifted from the original PEG-grafted Au surfaces prior to dendronization (Figure 5.5). On the other hand, a larger number of living cells was detected in samples lifted from the higher generation (G2-G4) dendronized surfaces compared to the control Au surface. Moreover, comparison of G1 and G2 dendronized surfaces prior to and after coupling with PEG-OMe chains clearly demonstrates the higher affinity of cells for the dendronized surfaces without PEG (Figure 5.5).

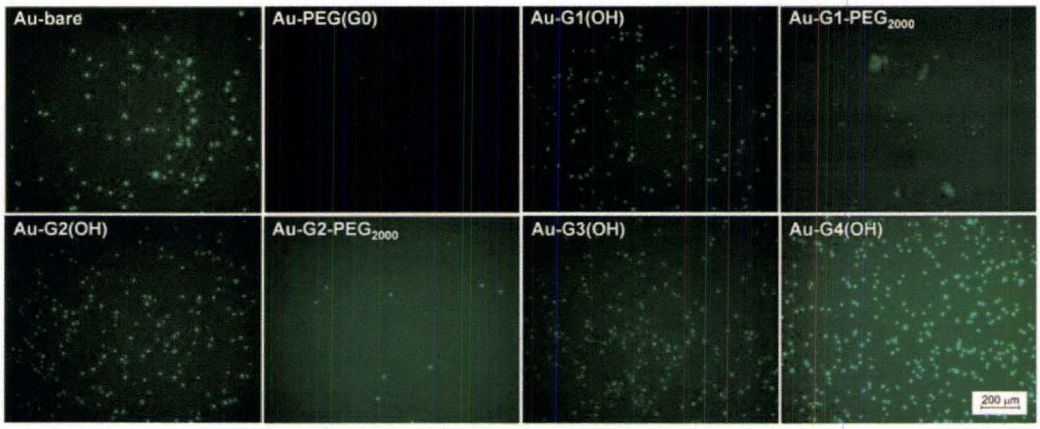

Figure 5.5. Fluorescence micrographs (×10) illustrating the effect of various substrates on the proliferation of human corneal epithelial cells using cell viability test after a 6-day incubation study.

5.2.3.3. *In vitro* adhesion studies of mouse 3T3 fibroblasts (M-3T3)

To further evaluate the potential application of dendronized surfaces in tissue engineering and blood-contacting applications, to examine the effect of the presence of serum proteins on cellular responses to these materials, and to build upon previous studies postulating that the formation of a confluent vascular endothelial cell monolayer significantly improves the blood-contacting properties of biomaterials,[49,63,64] we chose to study the adhesion of mouse 3T3 fibroblasts (M-3T3). The ability of the dendronized surfaces to support cell interactions in the presence of serum proteins, perhaps better simulating *in vivo* conditions, was investigated by conducting the adhesion studies of M-3T3 cells in serum-containing medium. Additionally, this allowed us to evaluate and compare the responses of the same set of surfaces to different cell types. We initially

investigated the effect of surface dendronization with hydrophilic polyester dendrons on M-3T3 cell adhesion and proliferation. Cell adhesion studies were carried out following the same procedure described for the HCEC. From the optical microscopy analyses of fixed cells, no major difference in cell adhesion and proliferation was observed for the various surfaces (Figure 5.6). Visual differences could only be seen at the early stages of incubation (1 day), where more cells seemed to adhere preferentially on the higher-generation-dendronized surfaces compared to the PEG-grafted and unmodified Au surfaces (Figure 5.6.A). The observed M-3T3 cell numbers showing very little difference between the surfaces studied, may be caused by cell adhesion that is mediated by the adsorption of proteins present in the serum-containing medium. This would result in greater cell adhesion/proliferation, and less discrimination between surfaces.

Cell densities calculated from culture counts provided a quantitative measure of the amount of M-3T3 cells attached (at early times) and proliferated (later times) on the various surfaces. These data indicated a clear difference between the number of cells attached to the dendronized surfaces and those attached to the PEG-grafted and unmodified Au surfaces (Figure 5.7). For example, after a 24 h incubation study, the cell density calculated for first generation dendronized surfaces, Au-G1(OH), was 68,000 ± 6,000 cells/cm^2, as opposed to 16,000 ± 7,000 cells/cm^2 calculated for PEG-grafted surfaces. Whereas the results from the optical microscopy analyses did not reveal any major differences between the various surfaces, the cell densities clearly followed a similar trend observed with the HCEC, where the dendronized surfaces prior to PEG grafting promoted cell adhesion and proliferation.

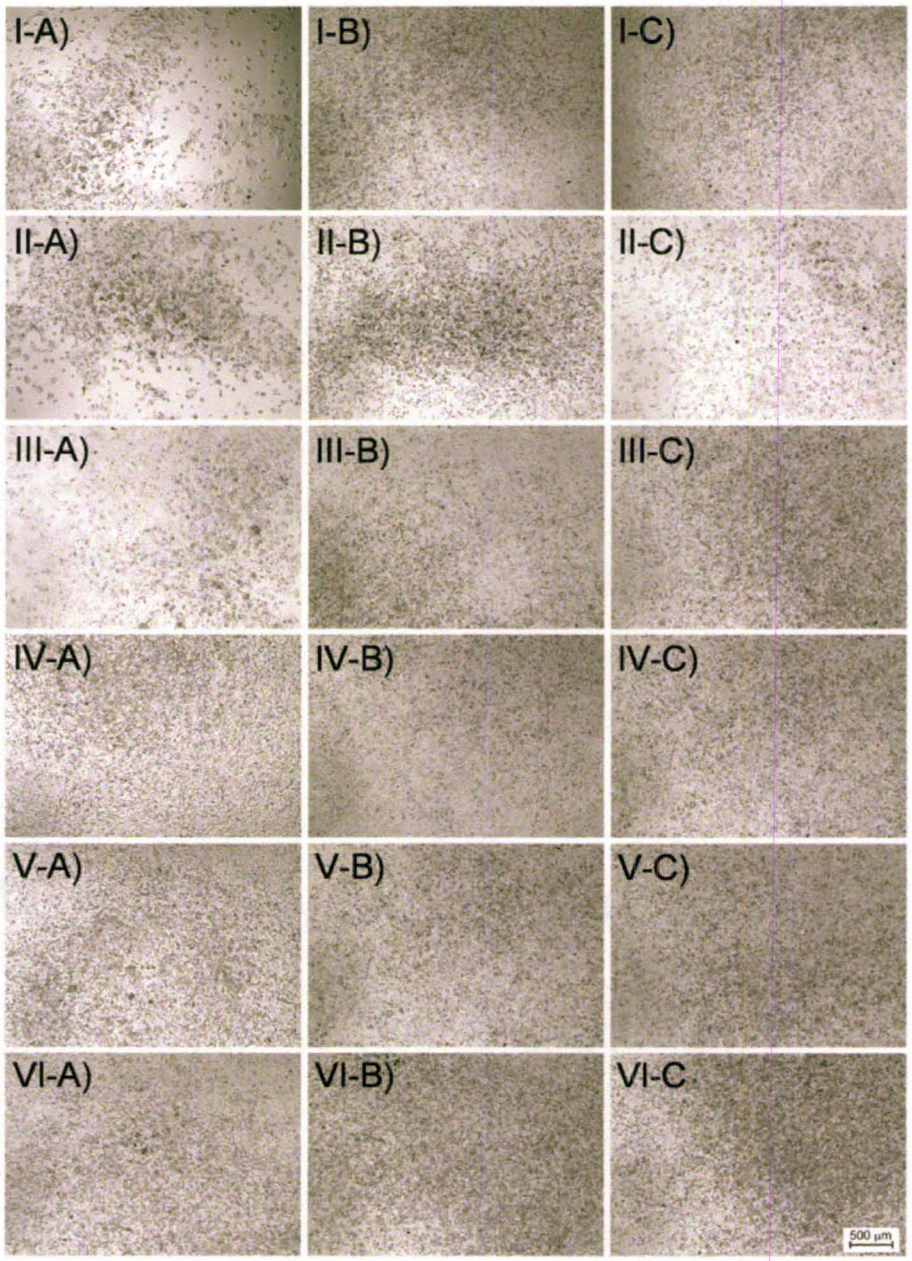

Figure 5.6. Optical micrographs (×2.5) showing the numbers of mouse 3T3 fibroblasts on various surfaces: I) bare Au, II) Au-PEG(G0), III) Au-G1(OH), IV) Au-G2(OH), V) Au-G3(OH), VI) Au-G4(OH), A) 1-day, B) 3-days, C) 6-days of incubation at 37 °C.

The difference between the optical microscopy analysis and cell densities is most likely due to the fact that when cells become confluent on a surface, it may be difficult to estimate the extent of cell confluency using qualitative visual techniques.

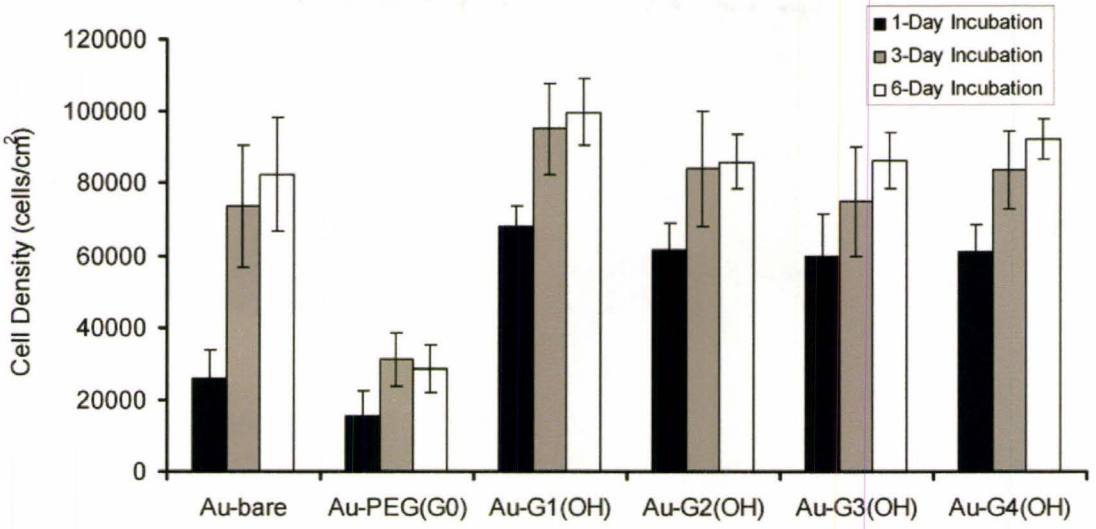

Figure 5.7. Cell density of mouse 3T3 fibroblasts on various surfaces: Effect of hydrophilic polyester dendrons.

Again, the percentage of cells attached at each incubation period was calculated, and indicated that cell attachment increased slightly at longer incubation times (Figure 5.I.3, Appendix I). The difference in cell attachment and proliferation to the dendronized surfaces and the original PEG-grafted surfaces is also accentuated by these results. From the 20,000 cells seeded on the surfaces, the percentage of cells present on the PEG-grafted surfaces reached a maximum of ~150% after 6 days of incubation. This was much lower than the number of cells present on the highest generation (G4) dendronized

surfaces in absence of PEG grafting, which reached approximately 450% for the same incubation period (Figure 5.I.3). Furthermore, when the dendronized surfaces were functionalized with PEG-OMe chains, a considerable reduction in cell density was observed (Figure 5.8). These results are consistent with the ones obtained with the HCEC and clearly demonstrate the greater ability of the dendronized surfaces to promote cell adhesion and proliferation.

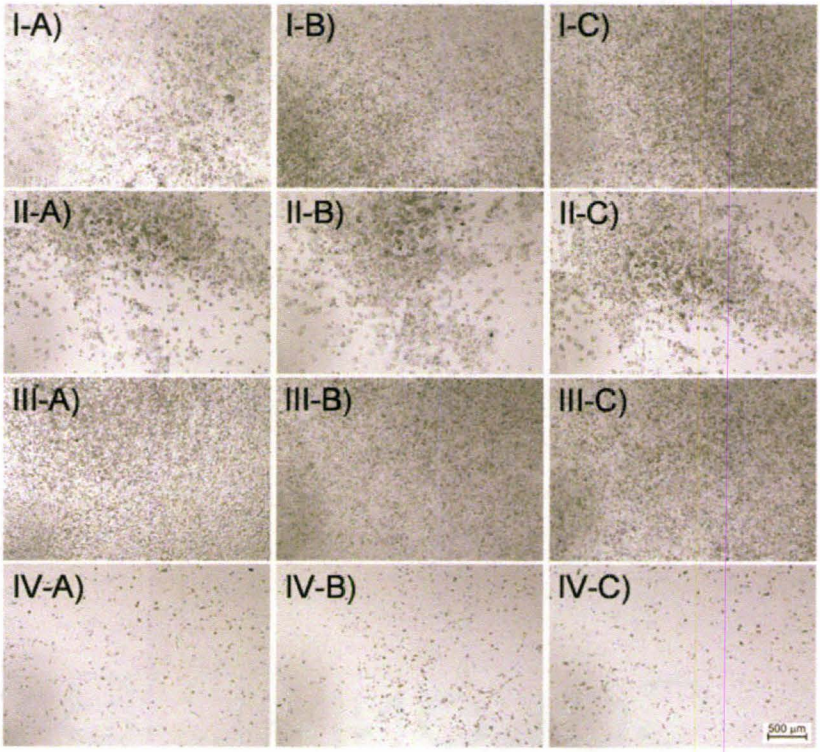

Figure 5.8. Optical micrographs (×2.5) illustrating the effect of PEGylation of G1 and G2 dendronized surfaces on density of mouse 3T3 fibroblasts: I) Au-G1(OH), II) Au-G1-PEG_{2000}, III) Au-G2(OH), IV) Au-G2-PEG_{2000}, A) 1-day, B) 3-days, C) 6-days incubation at 37 °C.

To support the results obtained from optical microscopy analyses, cell densities were calculated from the culture counts of cells lifted from the various surfaces. Once again, the results were in agreement with those obtained for the HCEC showing a significant reduction in cell densities when the peripheral hydroxyl groups were coupled with PEG-OMe chains (Figure 5.9). It is therefore clear that the presence of a high density of PEG moieties on a surface alters protein adsorption and cell adhesion significantly, regardless of the presence of serum in the medium. This is in agreement with a previously reported study by Nagahama *et al.* comparing adhesion of fibroblast cells on star-shaped 8-armed PEG-poly(L-lactide) block copolymer membranes to their linear analogues. Greater cell resistance was obtained with the star-shaped polymers, which was attributed to the presence of a large number of PEG chains and a more hydrated film surface.[42]

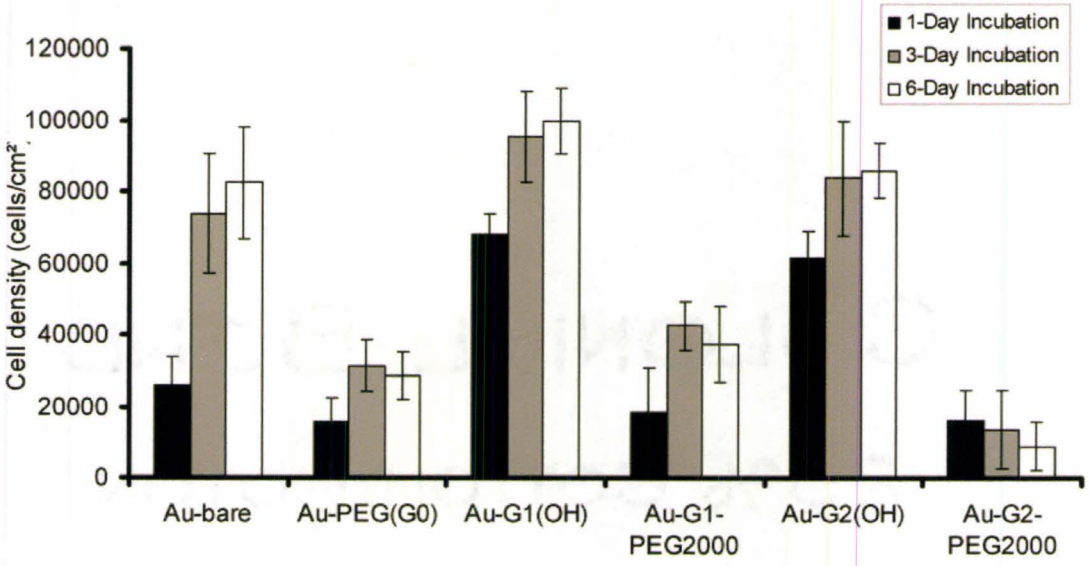

Figure 5.9. Mouse 3T3 fibroblast density on various surfaces: Effect of PEGylation of G1 and G2 dendronized surfaces.

Again, calculation of cell percentages remaining relative to the number initially plated on the surfaces indicated that the percentage of cells present on the G1-dendronized surfaces after 6 days of incubation was reduced from nearly 500% to approximately 180% after coupling of PEG-OMe chains (Figure 5.I.4, Appendix I). Similarly, after a 6-day incubation study, the number of M-3T3 cells present on G2-dendronized surfaces was estimated to be approximately 430% of the number originally seeded; this decreased to ~40% after PEGylation (Figure 5.I.4). When comparing the percentage of cells attached to the various surfaces for the two cell lines, the overall trend is very similar. At the early incubation stages (1 day), the highest percentage of HCEC attached was estimated to be approximately 20% for the Au-G1(OH) surfaces (Figure 5.I.1). In the case of M-3T3 cells, the highest cell density was also obtained with the Au-G1(OH) surfaces (Figure 5.I.3), however, this percentage reached over 300% of the original number of cells plated on the surfaces. The reason for this large difference between the two cell lines is mainly due to the presence of cell-adhesive proteins in the serum-containing medium used for the M-3T3 studies. The adsorption of serum proteins facilitates cell adhesion to the surfaces. In the absence of serum, i.e. for the HCEC, cell adhesion is mediated by proteins secreted by cells, such as fibronectin (FN), and deposited onto the surfaces. Therefore, substrates that have a high tendency to repel proteins, as in the case of PEG-functionalized surfaces, have the lowest capability to promote cell adhesion and proliferation. As we already demonstrated in our previous studies, dendronized surfaces induce greater protein adsorption, which is likely the reason

for the enhanced cell adhesion observed in the present work for the G1-G4 dendronized (non-PEGylated) surfaces.

5.2.3.4. Cell viability

Cell viability was again examined after each adhesion study for the various surfaces using the procedure described for HCEC. A greater number of living cells was again detected in the solutions of cells lifted from the dendronized surfaces compared to the control Au and PEG-grafted surfaces (Figure 5.10). Looking at the fluorescence images in Figure 5.10, it is apparent that there were very few living cells present in the solutions of cells dislodged from all surfaces presenting PEG chains. On the opposite side, the greatest densities of fluorescent spots appeared in the solutions of cells lifted from the G1-G4 dendronized surfaces, indicating once again the tendency of cells to preferentially attach and proliferate on the dendronized surfaces.

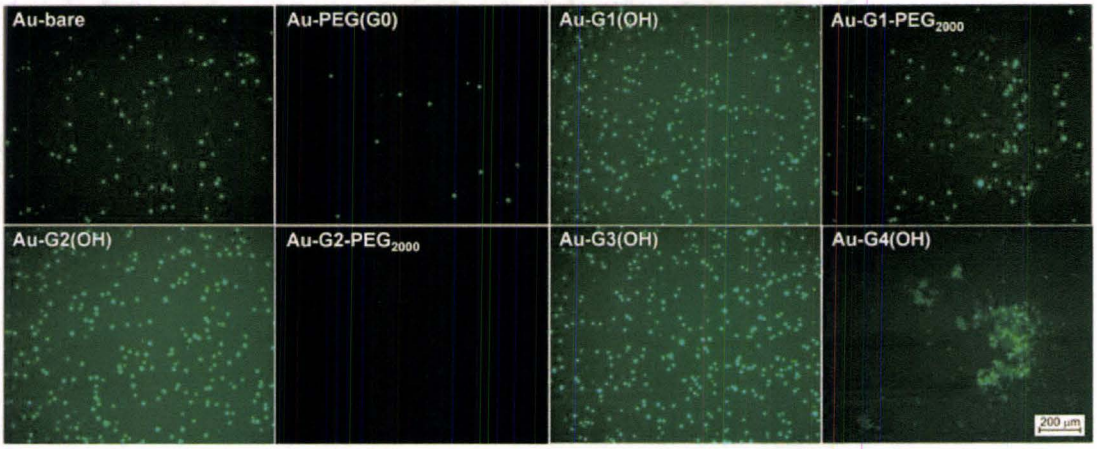

Figure 5.10. Fluorescence micrographs (×10) illustrating the effect of various substrates on the proliferation of mouse 3T3 fibroblast cells using a cell viability test after a 6-day incubation study.

5.3. Conclusions

The effect of functionalization of PEG-grafted gold surfaces with hydrophilic polyester dendrons on cell interactions was investigated. Cell studies using HCEC were carried out in serum-free medium to provide information on the response of the cells to the surfaces without the confounding effects of a protein layer. As expected, cell adhesion was significantly lower on the original PEG-grafted Au surfaces due to the protein-resistant nature of PEG moieties. On the other hand, the dendronized surfaces showed a significantly higher affinity for the cells, showing higher cell densities particularly at longer incubation periods. To further elucidate the effect of hydrophilic dendrons on the observed increase in cell adhesion, the peripheral hydroxyl groups of G1 and G2 dendronized surfaces were coupled with PEG-acid chains (M_n = 2000 Da). Cell studies comparing the original G1 and G2 dendronized surfaces to the PEG-functionalized dendronized surfaces indicated a significant reduction in cell adhesion upon functionalization of the peripheral alcohols with PEG-OMe chains. These results support the fact that the observed increase in HCEC cell density on the dendronized surfaces is directly related to the presence of the aliphatic polyester dendrons, which can promote the adsorption of cell-anchoring proteins to the surface. In the second part of this study, the ability of the surfaces to support preferential cell interactions was tested using mouse 3T3 fibroblasts. Based on the data collected from M-3T3 cell densities and percentages of cells attached to the surfaces, the trend observed among the various substrates was similar to the one obtained with the HCEC, although significantly higher percentages of M-3T3 cells attached to the various surfaces. These results were likely due to the rapid adsorption

of serum proteins in the medium, which provided a greater anchorage for cells to attach to the surfaces even in the presence of the PEG, showing lower discrimination between surfaces. The effect of PEG chains became more evident, even in the presence of serum, when the peripheral hydroxyl groups of G1 and G2 dendronized surfaces were coupled with PEG-OMe chains. The presence of PEG-OMe chains resulted in a significant reduction in cell density, regardless of the presence or absence of serum in the growth medium. More importantly, these results show that surfaces presenting a large number of hydroxyl groups in a branched network can be a potential alternative to the use of peptides to promote cell adhesion and proliferation. In order to support the possibility of exploiting the use of polyester dendrons for developing novel biomaterials, further experiments are needed to extrapolate these results to more biocompatible, flexible materials such as poly(dimethyl siloxane) (PDMS), and investigate their cell adhesion properties.

5.4. Experimental

5.4.1. General

DOWEX50W-X2 ion-exchange resin, 4-(dimethylamino)pyridine (DMAP, 99%), 2,2-bis(hydroxymethyl)-propionic acid (bis-MPA, 98%), 2,2-dimethoxy propane (98%), *p*-toluene-sulfonic acid monohydrate (TsOH, 98%), TEMPO free radical (98%), iodobenzene diacetate (98%), and poly(ethylene glycol) methyl ether (MW 350 and 750) were purchased from Aldrich. 1-(3-dimethylaminopropyl)-3-ethylcarbodiimide hydrochloride (EDC, 98+%) was purchased from Alfa Aesar. Poly(ethylene glycol)

methyl ether (M_n 2000 and 5000) was purchased from Fluka. Thiol terminated poly(ethylene glycol) (HS-PEG_{650}-OH) was purchased from Polymer Source, Inc. Dichloromethane (CH_2Cl_2), ethyl acetate (EtOAc), hexanes, methanol (MeOH), diethyl ether, and ethanol (EtOH) were purchased from CALEDON. All reagents were used as received. Acetonide-protected anhydride of bis-MPA (**2**)[50] and of 4-dimethylaminopyridine/*p*-toluene sulfonic acid (DPTS)[51] were prepared according to literature procedures.

Gold substrates prepared by electron beam evaporation of silicon wafers with an adhesive titanium tungstate (TiW) layer (300 Å) followed by a layer of gold (1000 Å), were purchased from Thin Film Technology, Buellton, CA, and diced into 1.0 × 1.0 cm^2 pieces. Prior to chemisorption, the surfaces were cleaned using a literature procedure by immersing them in chromosulfuric acid (H_2SO_4 > 92%, CrO_3 > 1.3%) for 1 h to remove any organic contaminants, followed by ultrasonication in both Milli-Q water and ethanol for 10 minutes, and extensive rinsing with Milli-Q water.[52]

5.4.2. Cells

Human corneal epithelial cells and mouse 3T3 fibroblasts (American Type Culture Collection, Rockville, Maryland) were used to determine the effect of surface modification with aliphatic polyester dendrons on cell adhesion and proliferation, including preferential interactions of the surfaces with one cell type over another. Prior to seeding on the surfaces, corneal epithelial cells were cultured in Keratinocyte Serum-Free Medium (KSFM) (Invitrogen Corp., Burlington, ON, Canada) supplemented with 10%

fetal bovine serum (FBS, Invitrogen Corp., ON, Canada) and 1% penicillin streptomycin solution (Invitrogen Corp., ON, Canada) at 37ºC and 5% CO_2. Fibroblasts were cultured in Dulbecco's Modified Eagle Medium (DMEM, Invitrogen Corp., Burlington, ON, Canada) supplemented with 10% FBS at 37°C and 5% CO_2.

5.4.3. Analysis

Optical microscopy analyses of fixed cells were carried out using an Olympus BX51 optical microscope equipped with a Q-Imaging/Retiga EXi camera. Fluorescence microscopy images were taken with a Zeiss Atto Arc. 2 HBO 100 W AxioCam MRC microscope equipped with an excitation filter set at 470 nm, and an emission filter set at 525 nm.

5.4.4. Synthesis

5.4.4.1. General procedure for surface dendronization. First generation aliphatic polyester dendrons (G1(Ac)) were covalently attached to the terminal hydroxyl groups of PEG_{650}-functionalized gold surfaces via an esterification reaction. The deprotection of the acetonide groups was carried out following a literature procedure, using the acidic resin DOWEX 50W-X2 in methanol at 50°C for 1 h.[52] Subsequent esterification and deprotection reactions allowed surface dendronization up to the fourth generation as previously described.[45]

5.4.4.2. EDC-coupling of PEG-acid to the peripheral OH-groups of dendronized surfaces

First and second generation hydroxyl-terminated dendronized surfaces were functionalized with PEG-OMe chains (M_n = 2000 Da). Prior to the coupling reaction, the terminal hydroxyl group of PEG-OMe was oxidized to a carboxyl end group using a TEMPO-mediated oxidation.[53] The PEG_{2000}-acid derivative was subsequently coupled to the peripheral hydroxyl groups of G1 and G2 dendronized surfaces using 1-(3-dimethylaminopropyl)-3-ethylcarbodiimide hydrochloride (EDC) coupling as described in our previous work.[54]

5.4.5. Cell adhesion

5.4.5.1. Adhesion of human corneal epithelial cells (HCEC)

Human corneal epithelial cells (~passage-12) were cultured under standard conditions (37°C, 95% relative humidity, 5% CO_2 in keratinocyte serum-free medium (KSFM) supplemented with 10% fetal bovine serum (FBS) and 1% penicillin/streptomycin). For cell adhesion and proliferation experiments, the confluent cells were trypsinized and centrifuged using a Beckman Coulter, Allegra^{TM} X-12R centrifuge at 900 rpm for 5 min. The resulting cell pellet was re-suspended in the required amount of serum-free medium (KSFM) to achieve a cell-plating density of 20,000 cells per 70 µL drop. The control bare Au and modified surfaces were incubated in KSFM overnight to equilibrate them prior to every cell adhesion study. The cells were plated onto the surfaces at a density of 20,000 cells/cm^2, and then incubated at 37°C in serum-

free medium for periods of 1 day, 3 days, and 6 days. Following each incubation period, the surfaces were rinsed with phosphate buffered saline (PBS) to remove loosely bound cells, and the adhered cells were fixed onto the surfaces by adding a solution of 10% neutral buffered formalin for optical microscopy analysis. Triplicate samples of each functionalization step were used to count the cells adhered to the various surfaces following every incubation period. The surfaces were transferred to new 24-well plates and a solution of Trypsin 0.25% EDTA (1.5 mL) was added to each well to lift the cells. After incubation for 10 min, the trypsin was neutralized with PBS (7.0 mL) and the cells were counted using a Beckman Z2™ Coulter Counter®. To ensure reproducibility of the results, cells were also counted using a Hausser Scientific hemacytometer for the various surfaces. Cell viability tests were carried out with the various surfaces for each adhesion study using Calcein AM, a fluorescence-based method for assaying cell viability and cytotoxicity.

5.4.5.2. Adhesion of mouse 3T3 fibroblasts (M-3T3)

Mouse 3T3 fibroblast (M-3T3) cells (~passage-2) were cultured under standard conditions (37°C, 95% relative humidity, 5% CO_2 in Dulbecco's Modified Eagle Medium (DMEM) supplemented with 10% FBS and 1% penicillin/streptomycin). Similarly to HCEC, the M-3T3 cells were plated onto the surfaces at a density of 20,000 cells/cm^2, incubated and kept at 37°C for periods of 1, 3, and 6 days. Following each experiment, the cells were fixed and analyzed by optical microscopy. For cell density measurement,

triplicate samples of each functionalization step were used and viability tests were also carried out as described for the HCEC.

5.5. References

(1) Tamada, Y.; Ikada, Y. *J Colloid Interf Sci* **1993**, *155*, 334-339.
(2) Andrade, J. D.; Hlady, V. *Adv Polym Sci* **1986**, *79*, 1-63.
(3) Langer, R.; Vacanti, J. P. *Science* **1993**, *260*, 920-926.
(4) Anderson, J. M.; Ziats, N. P.; Azeez, A.; Brunstedt, M. R.; Stack, S.; Bonfield, T. L. *J Biomat Sci-Polym E* **1995**, *7*, 159-169.
(5) Shen, M. C.; Horbett, T. A. *J Biomed Mater Res* **2001**, *57*, 336-345.
(6) Edwards, J. G. *Prog Surf Sci* **1983**, *13*, 125-196.
(7) Gray, D. S.; Tien, J.; Chen, C. S. *J Biomed Mater Res A* **2003**, *66A*, 605-614.
(8) Lee, J. N.; Jiang, X.; Ryan, D.; Whitesides, G. M. *Langmuir* **2004**, *20*, 11684-11691.
(9) Arima, Y.; Iwata, H. *Biomaterials* **2007**, *28*, 3074-3082.
(10) Karuri, N. W.; Liliensiek, S.; Teixeira, A. I.; Abrams, G.; Campbell, S.; Nealey, P. F.; Murphy, C. J. *J Cell Sci* **2004**, *117*, 3153-3164.
(11) Teixeira, A. I.; McKie, G. A.; Foley, J. D.; Berticsc, P. J.; Nealey, P. F.; Murphy, C. J. *Biomaterials* **2006**, *27*, 3945-3954.
(12) Whitesides, G. M.; Mathias, J. P.; Seto, C. T. *Science* **1991**, *254*, 1312-1319.
(13) Luk, Y. Y.; Kato, M.; Mrksich, M. *Langmuir* **2000**, *16*, 9604-9608.
(14) Romanova, E. V.; Oxley, S. P.; Rubakhin, S. S.; Bohn, P. W.; Sweedler, J. V. *Biomaterials* **2006**, *27*, 1665-1669.
(15) Vanwachem, P. B.; Mallens, B. W. L.; Dekker, A.; Beugeling, T.; Feijen, J.; Bantjes, A.; Detmers, J. P.; Vanaken, W. G. *J Biomed Mater Res* **1987**, *21*, 1317-1327.
(16) Steele, J. G.; Johnson, G.; Norris, W. D.; Underwood, P. A. *Biomaterials* **1991**, *12*, 531-539.
(17) Steele, J. G.; Johnson, G.; Underwood, P. A. *J Biomed Mater Res* **1992**, *26*, 861-884.
(18) Steele, J. G.; Dalton, B. A.; Johnson, G.; Underwood, P. A. *Biomaterials* **1995**, *16*, 1057-1067.
(19) Altankov, G.; Grinnell, F.; Groth, T. *J Biomed Mater Res* **1996**, *30*, 385-391.
(20) Howlett, C. R.; Evans, M. D. M.; Walsh, W. R.; Johnson, G.; Steele, J. G. *Biomaterials* **1994**, *15*, 213-222.
(21) Hynes, R. O. *Cell* **2002**, *110*, 673-687.
(22) Fields, G. B.; Lauer, J. L.; Dori, Y.; Forns, P.; Yu, Y. C.; Tirrell, M. *Biopolymers* **1998**, *47*, 143-151.
(23) Lhoest, J. B.; Detrait, E.; van den Bosch de Aguilar, P.; Bertrand, P. *J Biomed Mater Res* **1998**, *41*, 95-103.
(24) Boxus, T.; Touillaux, R.; Dive, G.; Marchand-Brynaert, J. *Bioorgan Med Chem* **1998**, *6*, 1577-1595.
(25) Neff, J. A.; Caldwell, K. D.; Tresco, P. A. *J Biomed Mater Res* **1998**, *40*, 511-519.
(26) Ruoslahti, E. *Annu Rev Cell Dev Bi* **1996**, *12*, 697-715.
(27) Huhtala, P.; Humphries, M. J.; Mccarthy, J. B.; Tremble, P. M.; Werb, Z.; Damsky, C. H. *J Cell Biol* **1995**, *129*, 867-879.

(28) Sastry, S. K.; Lakonishok, M.; Thomas, D. A.; Muschler, J.; Horwitz, A. F. *J Cell Biol* **1996**, *133*, 169-184.
(29) Garcia, A. J.; Vega, M. D.; Boettiger, D. *Mol Biol Cell* **1999**, *10*, 785-798.
(30) Mostafavi-Pour, Z.; Askari, J. A.; Parkinson, S. J.; Parker, P. J.; Ng, T. T. C.; Humphries, M. J. *J Cell Biol* **2003**, *161*, 155-167.
(31) Kingshott, P.; Griesser, H. J. *Curr Opin Solid St M* **1999**, *4*, 403-412.
(32) Liu, V. A.; Jastromb, W. E.; Bhatia, S. N. *J Biomed Mater Res* **2002**, *60*, 126-134.
(33) Lee, J. H.; Lee, H. B.; Andrade, J. D. *Prog Polym Sci* **1995**, *20*, 1043-1079.
(34) Nath, N.; Hyun, J.; Ma, H.; Chilkoti, A. *Surf Sci* **2004**, *570*, 98-110.
(35) Kiremitci, M.; Piskin, E. *Biomater Artif Cell* **1990**, *18*, 599-603.
(36) Ziegelaar, B. W.; Fitton, J. H.; Clayton, A. B.; Platten, S. T.; Maley, M. A. L.; Chirila, T. V. *Biomaterials* **1999**, *20*, 1979-1988.
(37) Hern, D. L.; Hubbell, J. A. *J Biomed Mater Res* **1998**, *39*, 266-276.
(38) Behravesh, E.; Zygourakis, K.; Mikos, A. G. *J Biomed Mater Res A* **2003**, *65A*, 260-270.
(39) Schmedlen, K. H.; Masters, K. S.; West, J. L. *Biomaterials* **2002**, *23*, 4325-4332.
(40) Woerly, S.; Pinet, E.; de Robertis, L.; Van Diep, D.; Bousmina, M. *Biomaterials* **2001**, *22*, 1095-1111.
(41) Tan, J.; Gemeinhart, R. A.; Ma, M.; Saltzman, W. M. *Biomaterials* **2005**, *26*, 3663-3671.
(42) Nagahama, K.; Ohya, Y.; Ouchi, T. *Macromol Biosci* **2006**, *6*, 412-419.
(43) Heyes, C. D.; Groll, J.; Moller, M.; Nienhaus, G. U. *Mol Biosyst* **2007**, *3*, 419-430.
(44) Yang, M.; Tsang, E. M. W.; Wang, Y. A.; Peng, X. G.; Yu, H. Z. *Langmuir* **2005**, *21*, 1858-1865.
(45) Benhabbour, S. R.; Sheardown, H.; Adronov, A. *Macromolecules* **2008**, *41*, 2567-2576.
(46) Evans, M. D. M.; Steele, J. G. *Exp Cell Res* **1997**, *233*, 88-98.
(47) Evans, M. D. M.; Steele, J. G. *J Biomed Mater Res* **1998**, *40*, 621-630.
(48) Zhu, A. P.; Fang, N.; Chan-Park, M. B.; Chan, V. *Biomaterials* **2006**, *27*, 2566-2576.
(49) McMillan, R.; Meeks, B.; Bensebaa, F.; Deslandes, Y.; Sheardown, H. *J Biomed Mater Res* **2001**, *54*, 272-283.
(50) Malkoch, M.; Malmstrom, E.; Hult, A. *Macromolecules* **2002**, *35*, 8307-8314.
(51) Moore, J. S.; Stupp, S. I. *Macromolecules* **1990**, *23*, 65-70.
(52) Ostmark, E.; Macakova, L.; Auletta, T.; Malkoch, M.; Malmstrom, E.; Blomberg, E. *Langmuir* **2005**, *21*, 4512-4519.
(53) Masson, C.; Scherman, D.; Bessodes, M. *J Polym Sci Pol Chem* **2001**, *39*, 4022-4024.
(54) Benhabbour, S. R.; Sheardown, H.; Adronov, A. *Macromolecules* **2008**, *ma-2008-004586*, Submitted.
(55) Prime, K. L.; Whitesides, G. M. *Science* **1991**, *252*, 1164-1167.
(56) Unsworth, L. D.; Sheardown, H.; Brash, J. L. *Langmuir* **2005**, *21*, 1036-1041.
(57) Kanagaraja, S.; Alaeddine, S.; Eriksson, C.; Lausmaa, J.; Tengvall, P.; Wennerberg, A.; Nygren, H. *J Biomed Mater Res* **1999**, *46*, 582-591.

(58) Chen, H.; Zhang, Z.; Chen, Y.; Brook, M. A.; Sheardown, H. *Biomaterials* **2005**, *26*, 2391-2399.
(59) Halperin, A.; Fragneto, G.; Schollier, A.; Sferrazza, M. *Langmuir* **2007**, *23*, 10603-10617.
(60) Herrwerth, S.; Eck, W.; Reinhardt, S.; Grunze, M. *J Am Chem Soc* **2003**, *125*, 9359-9366.
(61) Li, L. Y.; Chen, S. F.; Zheng, J.; Ratner, B. D.; Jiang, S. Y. *J Phys Chem B* **2005**, *109*, 2934-2941.
(62) Prime, K. L.; Whitesides, G. M. *J Am Chem Soc* **1993**, *115*, 10714-10721.
(63) Bradley, B. K.; Schnaar, R. L. *Anal. Biochem.* **1988**, *172*, 270-278.
(64) Massia, S. P.; Hubbell, J. A. *J Biomed Mater Res* **1991**, *25*, 223-242.

Chapter 6: Thesis Overall Conclusions and Recommendations for Future Work

6.1. General Conclusions

Dendronized polymers represent an effective way to develop highly boron-containing macromolecules as potential candidates for Boron Neutron Capture Therapy (BNCT) application. This strategy provides the ability to achieve high molecular weights that can exceed the renal cut off known to be in the range of 30-50 kDa. In Chapter 2, we demonstrated that by combining a simple polymerization method and the divergent dendrimer synthesis, we were able to incorporate 8-12% of boron atoms to high molecular weight (> 50 kDa) water soluble macromolecules without having to dendronize beyond the fourth generation. This synthetic strategy provides control over the shape and dimensions of the dendronized polymers and the ability to achieve high molecular weights with a significantly lower number of synthetic steps relative to dendrimers. Using aliphatic polyester dendrons, the resulting carborane-containing dendronized polymers can exhibit all the required properties for BNCT application including water solubility, biocompatibility, low toxicity, and biodegradability.

Development of novel low-fouling biomaterials continues to be the main focus of numerous studies. In the present work, we set out to investigate surface functionalization with aliphatic polyester dendrons on protein adsorption and cell adhesion and proliferation. Taking advantage of the unique properties of aliphatic polyester dendrons such as biocompatibility, biodegradability and their highly hydrophilic character, we

covalently functionalized PEG-grafted gold surfaces with these dendritic moieties with the aim of improving the overall hydrophilicity.

In Chapter 3 of this thesis, we have demonstrated via a series of characterization methods including contact angle goniometry, XPS, TOF-SIMS and AFM, that gold-coated silicon wafers were successfully grafted with PEG chains and further functionalized with aliphatic polyester dendrons of generation 1 to 4. Moreover, the main finding in this chapter was the fact that, contrary to our initial expectation, and despite their highly hydrophilic character (which was greater than the original PEG-grafted surfaces), dendronized surfaces exhibited greater protein adsorption of both fibrinogen and lysozyme in comparison to the original PEG-grafted surfaces. These results were mainly attributed to a decrease in chain mobility via intra- and inter-molecular hydrogen bonding between the peripheral hydroxyl groups of the dendronized surfaces as well as the presence of a large number of hydrogen bond donor groups on the surface.

Based on previous studies, the main contributing factors to enhanced fouling resistance are surface hydrophilicity, chain dynamics and mobility at the water interface, surface coverage, and charge neutrality. Additionally, Whitesides and co-workers have found that the presence of hydrogen-bond donor groups on the surface induces greater protein adsorption. Taking these main contributing factors into account, we decided to functionalize the peripheral hydroxyl groups of the dendronized surfaces with PEG chains and study the effect of PEGylation on protein adsorption.

In Chapter 4, we have demonstrated that functionalization of the original dendronized surfaces with PEG chains of various molecular weights resulted in a

decrease in protein adsorption on these PEGylated surfaces. These results showed that the absence of hydrogen bond donor groups and the presence of a large number of flexible PEG chains on a surface provide better protein resistance. Additionally, these results combined with the ones obtained from Chapter 3 demonstrated that although surface hydrophilicity is known to be one of the main contributing factors to proteins resistance, its contribution might not be as important as chain mobility and dynamics at the water interface and the absence of hydrogen bond donor groups on the surface.

In Chapter 5, we set out to investigate whether we could exploit the protein adsorbent character of the dendronized surfaces to promote cell adhesion and proliferation. Results from cell adhesion studies carried out using human corneal epithelial cells and mouse 3T3 fibroblasts demonstrated that the dendronized surfaces exhibited greater affinity for both cell lines. At longer incubation periods, the cells were almost confluent on the G1-G4 dendronized surfaces, as opposed to the original PEG-grafted surfaces which were found to significantly reduce cell adhesion.

The most important contribution of the present thesis resulted from the protein adsorption studies. This thesis demonstrates that improving surface hydrophilicity and surface coverage by introducing hydrophilic branched dendritic architectures does not provide better protein resistance. Achieving a better understanding of the main factors that play a key role in protein resistance and understanding the mechanisms involved in protein adsorption provide a better platform for designing effective low-fouling biomaterials. This thesis helps provide a better insight on the key requirements to improve protein resistance. These requirements include high chain dynamics and absence of

hydrogen bond donor groups. Hydrophilicity was found to play a less important role in enhancing protein resistance. We believe that these findings will help provide a better understanding of the most significant factors necessary to achieve better protein resistance and design future biomaterials with enhanced low-fouling properties.

6.2. Recommendations for Future Work

The next step in the study of carborane loaded dendronized polymers would focus on investigating the biodisctribution of these systems *in vivo*. The presence of the chloromethyl group at the polymer chain end wihtin these model systems provides the ability to attach a radiolabel or a fluorescent tag and study the biodistribution of these macromolecules using Single Photon Emission Computed Tomography (SPECT) imaging or fluorescent imaging respectively. Carrying out these biodistribution studies will provide a better insight on the structural relationship of these "rod-like" macromolecules to their pharmacokinetics and biodistribution *in vivo*. Comparison of the biodistibution properties of the carborane-containing dendronized polymers to previous results reported on linear polymers and carborane-containing dendrimers would also provide a significant insight into structural influence and importance in mediating selective accumulation of macromoles in tumor tissue.

Moreover, these model systems can serve as a platform for the development of novel carborane-containing dendronized polymers with biocompatible polymeric backbones such as poly(*p*-hydroxystyrene) or poly(hydroxyethyl methacrylate) (PHEMA), which have previously been investigated for biological applications.

Future work in the area of dendronized surfaces would mainly focus on taking advantage of the major findings of the present work in order to develop new strategies in designing better protein resistant surfaces and biomaterials. These strategies would take into account the important role that chain dynamics and mobility in water along with the absence of hydrogen-bond donor groups, play in providing systems with better protein resistance.

The use of the biocompatible aliphatic polyester moieties could be further explored in a linear form rather than a dendritic architecture to covalently functionalize surfaces and biomaterials. These neopentyl ester moieties, which are less susceptible than regular esters to acid or base hydrolysis, and can potentially be used as an alternative to PEG chains in order to overcome susceptibility to oxidation, which is known to be the major limitation of PEG chains as low fouling biomaterials.

Further investigation of the use of aliphatic polyester dendrons to promote cell adhesion and proliferation needs to be carried out by translating the chemistry developed in the present work to dendronize more biocompatible materials such as PDMS. Additional studies would focus on investigating various cell lines and comparing cells from a similar main source, i.e. human cells to human cells. This would provide better comparison of the responses of dendronized surfaces to various cell types originating from the same source. Moreover, direct comparative studies on the effect of aliphatic polyester dendrons to that of oligopeptides in promoting specific cell adhesion and proliferation would provide significant information on the potential use of these dendrons as alternatives to cell adhesion peptides.

Appendix I

Chapter 3: Protein Resistance of Surfaces Prepared by Chemisorption of Mono-Thiolated Poly(ethylene glycol) to Gold and Dendronization with Aliphatic Polyester Dendrons: Effect of Hydrophilic Dendrons

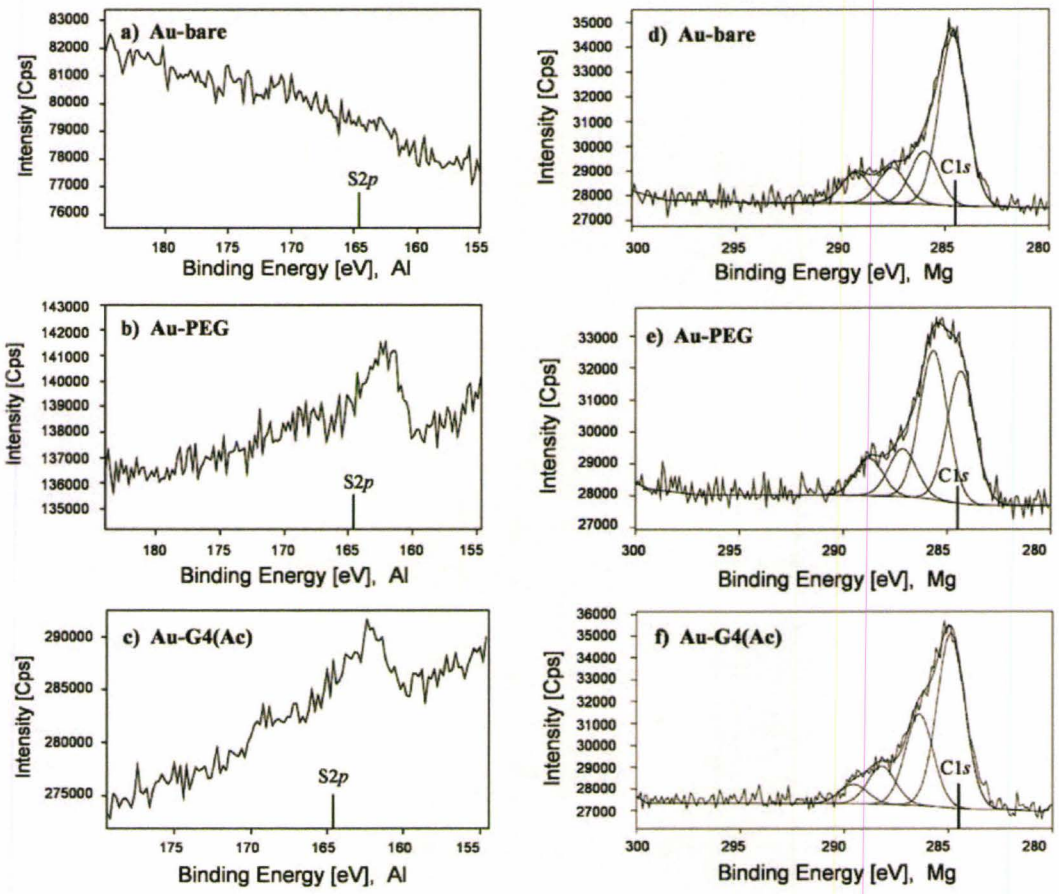

Figure 3.I.1. High-resolution S2*p* XPS data at 90° takeoff angle for: (a) Au-G1(Ac), (b) Au-G2(Ac), (c) Au-G3(Ac), and C1*s* data at 90° takeoff angle for: (d) Au-G1(Ac), (e) Au-G2(Ac), (f) Au-G3(Ac).

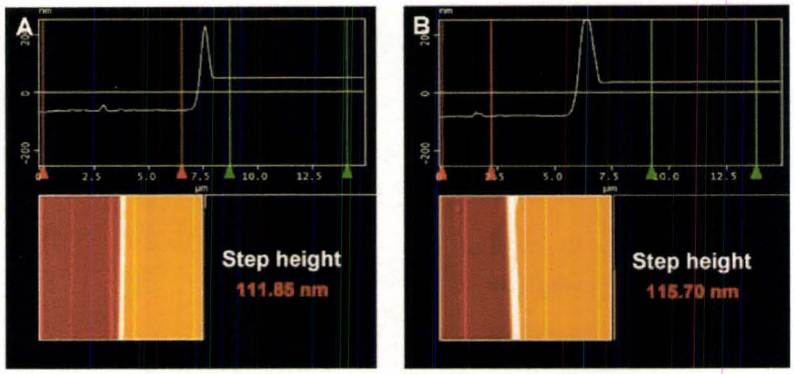

Figure 3.I.2. Film thickness measurement using Tapping Mode™ scratch-method AFM height analysis for **A**) Au-bare, and **B**) Au-PEG_{650}.

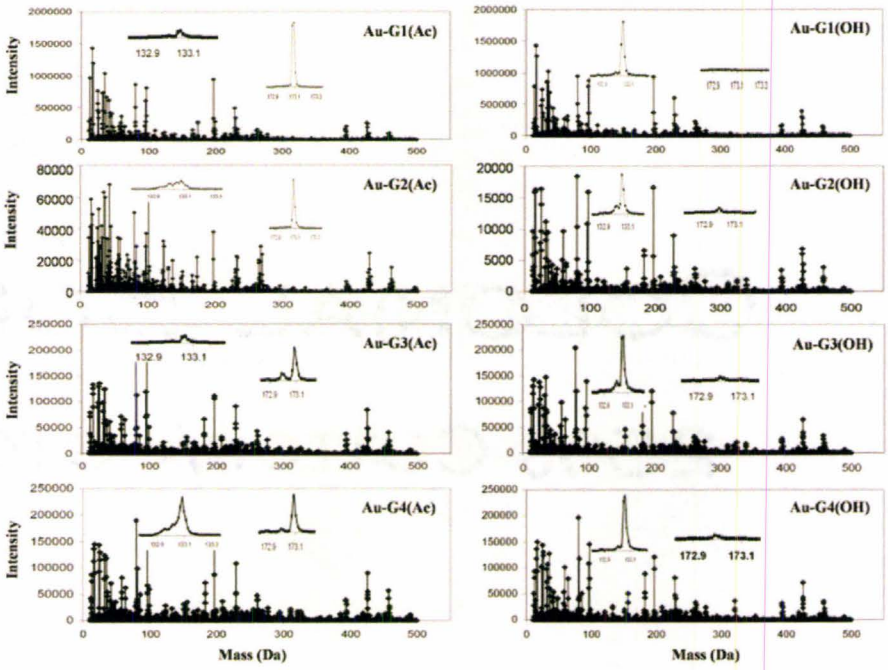

Figure 3.I.3. Normalized negative ion TOF-SIMS spectra of various surfaces, with insets showing signals at the mass ranges that correspond to the deprotected G1(OH) fragment ($C_5H_9O_4$) and the acetonide-protected fragment ($C_8H_{13}O_4$).

Chapter 4: Protein Resistance of PEG-Functionalized Dendronized Surfaces: Effect of PEG Molecular Weight and Dendron Generation

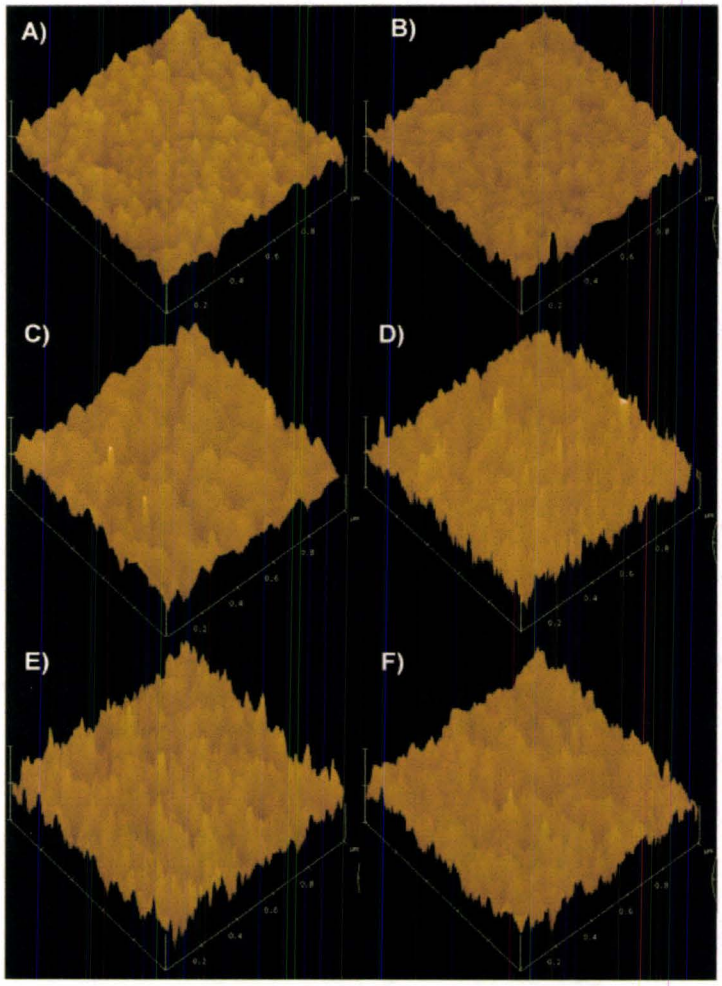

Figure 4.I.1. AFM height images of: a) Au-bare, b) Au-G1(OH), c) Au-G1-PEG_{350}, d) Au-G1-PEG_{750}, e) Au-G1-PEG_{2000}, f) Au-G1-PEG_{5000}. (Image size : 1 × 1 μm^2, height data scale: 10 nm).

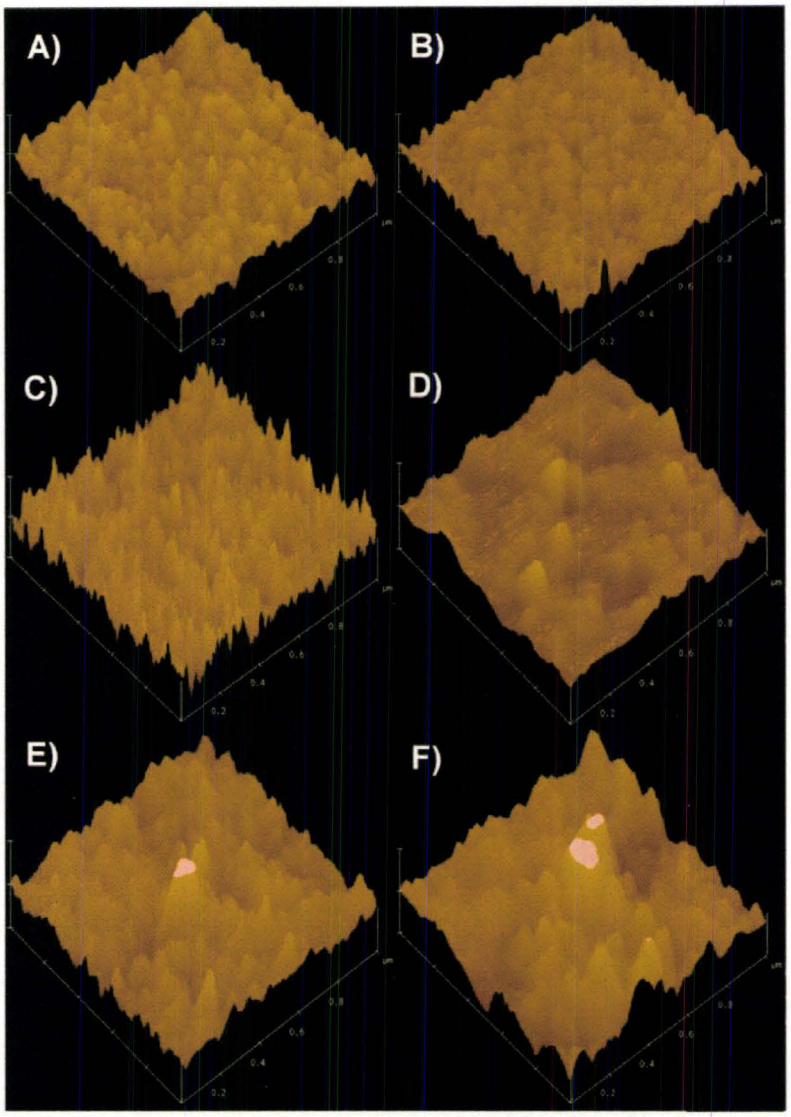

Figure 4.I.2. AFM 3D height images of: a) Au-bare, b) Au-PEG(G0), c) Au-G1-PEG_{2000}, d) Au-G2-PEG_{2000}, e) Au-G3-PEG_{2000}, f) Au-G4-PEG_{2000}. (Image size : 1 × 1 μm^2, height data scale: 10 nm).

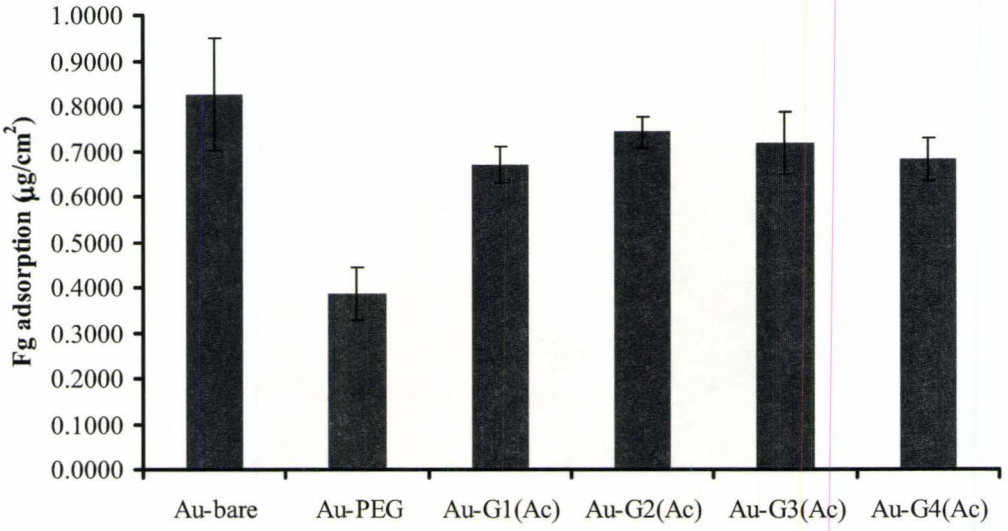

Figure 4.I.3. Fibrinogen adsorption from PBS buffer: effect of surface modification with PEG and dendronization with acetonide-protected aliphatic polyester dendrons G1-G4.

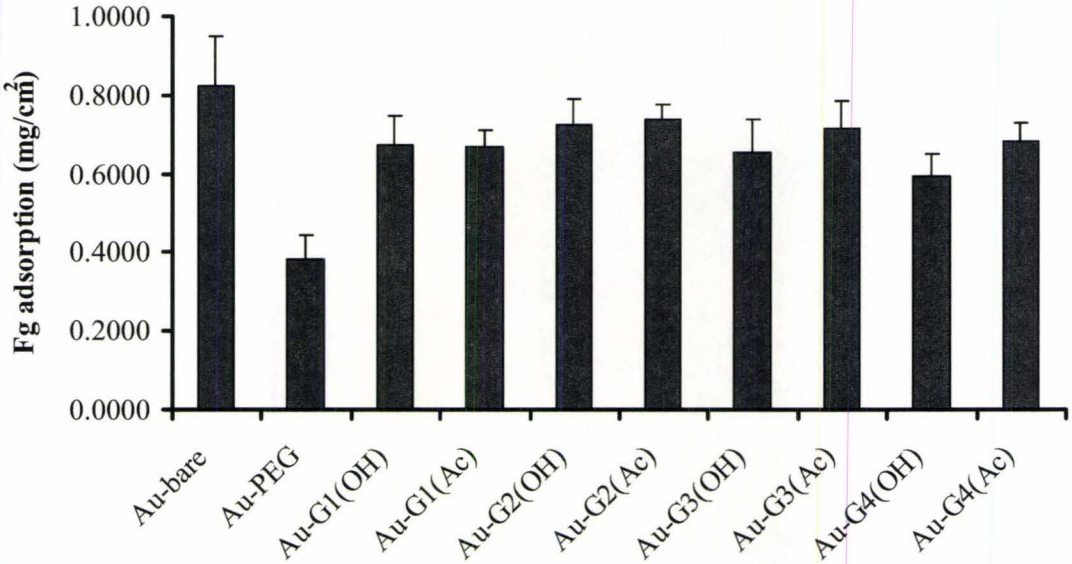

Figure 4.I.4. Fibrinogen adsorption from PBS buffer: comparison between acetonide-protected and deprotected aliphatic polyester dendrons G1-G4.

Chapter 5. Cell Adhesion and Proliferation on Dendronized Surfaces

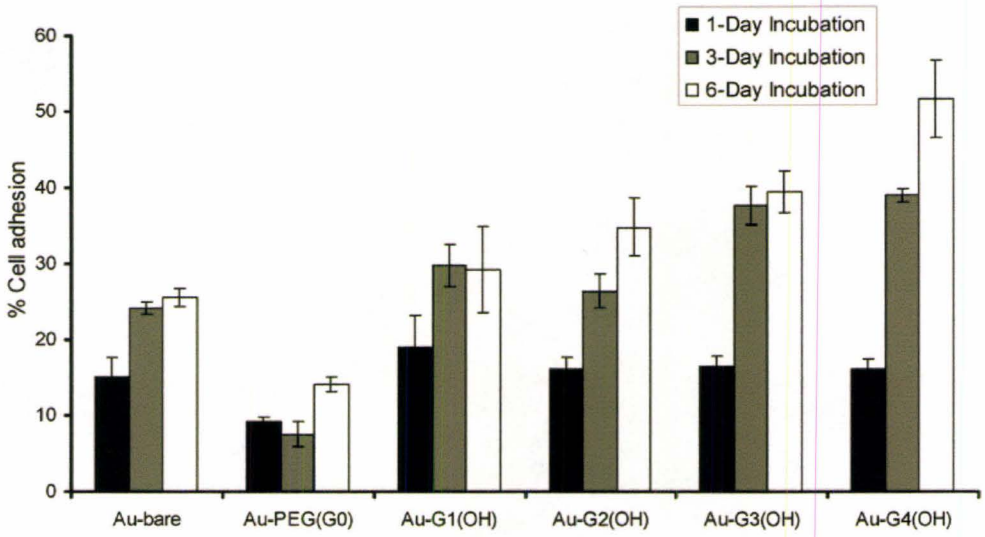

Figure. 5.I.1. Evaluation of % adhesion and proliferation of human corneal epithelial cells on various surfaces: Effect of hydrophilic dendrons.

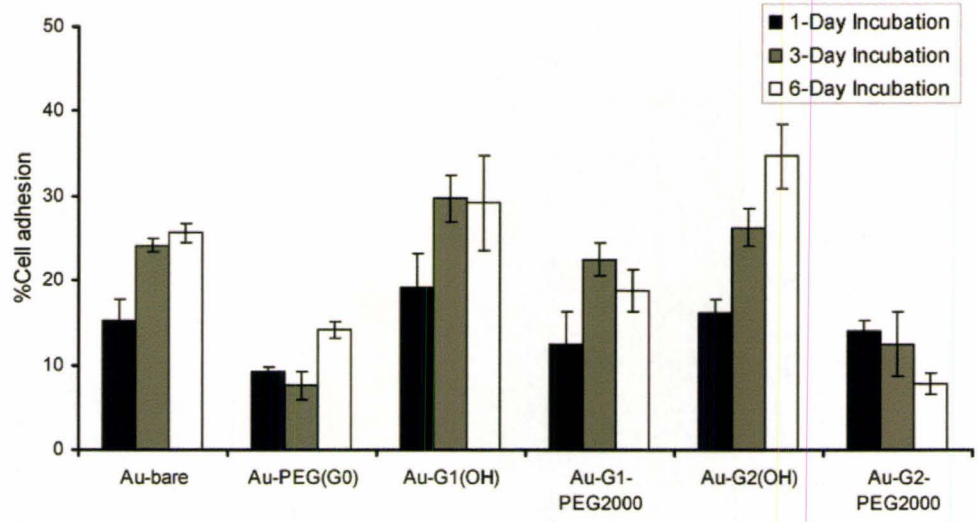

Figure. 5.I.2. Evaluation of % adhesion and proliferation of human corneal epithelial cells on various surfaces: Effect of PEGylation of G1 and G2 dendronized surfaces.

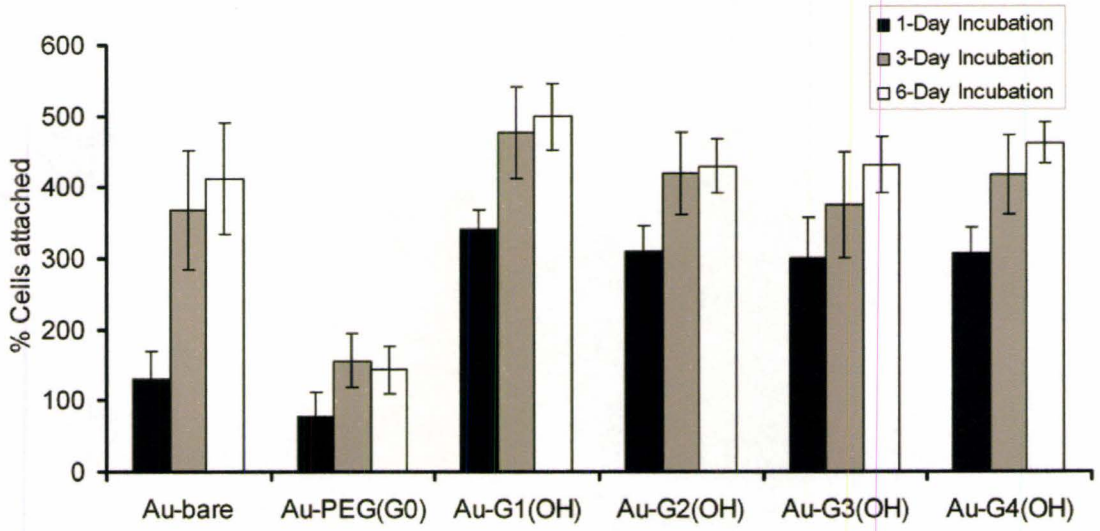

Figure. 5.I.3. Evaluation of % mouse 3T3 fibroblasts adhesion and proliferated on various surfaces: Effect of hydrophilic dendrons.

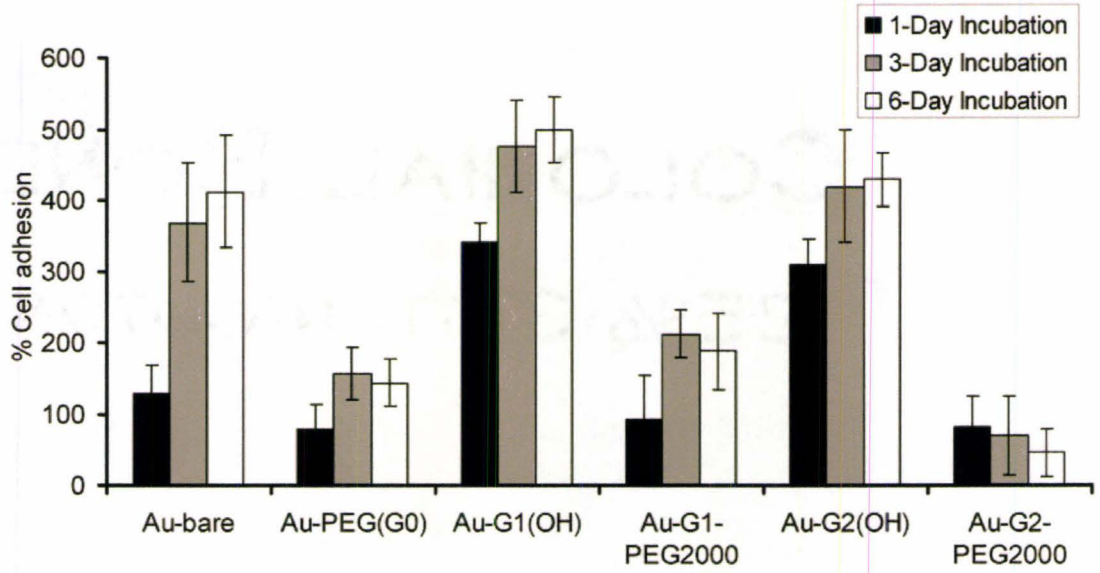

Figure. 5.I.4. Evaluation of % mouse 3T3 fibroblasts adhesion and proliferation on various surfaces: Effect of PEGylation of G1 and G2 dendronized surfaces.